UNIVERSITAT DE BARCELONA

Experimental and human studies on aging of adipose tissues: Role for Parkin

Alejandro Delgado Anglés

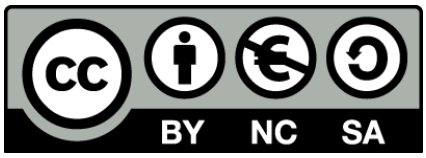

EXPERIMENTAL AND HUMAN STUDIES ON AGING OF ADIPOSE TISSUES: ROLE OF PARKIN

Alejandro Delgado Anglés

Doctoral Thesis

2021

UNIVERSITAT DE BARCELONA

Facultat de Biologia

Programa de Doctorat en Biomedicina

Departament de Bioquímica i Biomedicina Molecular

Grup de Metabolisme Molecular i Patologies associades

Experimental and human studies on aging of adipose tissues: role of Parkin

Memòria presentada per

Alejandro Delgado Anglés

per optar al grau de Doctor per la Universitat de Barcelona

Alejandro Delgado Anglés

Firma dels directors

Dr. Francesc Villarroya i Gombau
Director i tutor

Dr. Joan Villarroya Terrade
Codirector

Barcelona, 2021

UNIVERSITAT DE BARCELONA

Faculty of Biology

Biomedicine Doctorate Program

Dept. of Biochemistry and Molecular Biomedicine

Molecular Metabolism and Disease Laboratory

Experimental and human studies on aging of adipose tissues: role of Parkin

Doctoral Thesis

Alejandro Delgado Anglés

Barcelona

2021

Abstract

Brown and beige adipose tissues are mediators of adaptive energy expenditure in mammals, in contrast with the energy storage role of white fat. Mitochondrial activity, including uncoupled respiration, and the release of the so-called “batokines” in brown and beige adipocytes account for the majority of local and systemic adaptations to energy expenditure requirements mediated by these cells. One of these batokines is fibroblast growth factor 21 (FGF21), which has been recently proposed to be an antiaging hormone. Aging is associated with a decline in brown adipose tissue (BAT) activity and in browning of white adipose tissue (WAT). It has been proposed that the extent of BAT decline in aging may play a causative role in the enhanced propensity to age-associated metabolic conditions, and it has even been speculated that BAT reactivation may reverse them. On the other hand, aging is associated with increased amount of WAT. A loss of mitochondrial homeostasis by defective mitochondrial quality control as a result of decreased biogenesis but also to decreased degradation through mitophagy has been proposed as an underlying cause of aging in multiple tissues. Recently, Parkin has been identified as a key component of adipose tissue plasticity in response to thermogenic requirements, associated with the adaptive control of mitophagy. In the present study we investigated the impact of aging on adipose tissues in mice and humans with special focus on the status of the FGF21 system. We also tried to establish the role of Parkin in our mice model at distinct stages of aging. Parkin transcript and protein levels were up-regulated in relation to aging in mice adipose tissues, which may point to a compensatory homeostasis against diminished Parkin-independent mitophagy. Middle-aged wild-type mice presented an age-associated phenotype reminiscent of obesity and signs of BAT malfunction in middle-aged mice, which did not affect thermogenic response at this specific aging stage. Thus, our data would not support a massive effect of BAT in systemic derangements associated with aging. Parkin-KO mice were protected against age-associated obesity found in control animals. BAT activity does not seem to conduct the protection of Parkin-KO mice against aging-associated adiposity, as Parkin-KO mice do not present enhanced BAT- or browning-mediated energy expenditure. This phenomenon might rather be attributable to diminished food intake and risen energy expenditure-related processes in Parkin-KO mice. Our data denote that Parkin is possibly involved in the in the metabolic flexibility of lipid versus carbohydrate metabolism. FGF21 expression and its secretion in mice may be induced as stress hormone by mitochondrial dysfunctions in aged tissues. However, the chronic metabolic and stress-related disorders might elicit an FGF21 resistance, menacing healthy aging. Middle-aged mice lacking Parkin abolish increased levels of FGF21, which might be associated to the prevention of obesity occurring in those animals. In humans, serum FGF21 levels were increased in parallel with indicators of mildly deteriorated glucose homeostasis. FGF21-responsiveness machinery was not disrupted in subcutaneous adipose tissue from elderly individuals relative to those from young controls. Therefore, in contrast to what is observed in chronic metabolic pathologies or mice aging, high levels of FGF21 in healthy aging are not associated with repressed FGF21-responsiveness machinery in adipose tissue.

Contents

This doctoral thesis is organized according to current regulations regarding the format of “Classical thesis” established by the Faculty of Biology of the University of Barcelona. For this reason, it presents the following structure:

Index

Abbreviations list

Introduction

Objectives

Materials and Methods

Results

Discussion

Conclusions

Bibliography

Appendix

- Aging is associated with increased FGF21 levels but unaltered FGF21 responsiveness in adipose tissue.

Index

Abbreviations list

ATG	Autophagy-related protein
BAT	Brown adipose tissue
BMAT	Bone marrow adipose tissue
BMI	Body mass index
BNIP3	BCL2 interacting protein 3
C/EBPs	CCAAT-enhancer-binding proteins
cBMAT	Constitutive BMAT
cDNA	Complementary DNA
CREB	cAMP response element-binding
CXCL14	C-X-C motif chemokine ligand-14
DIO2	Iodothyronine 5'-deiodinase
DNA	Deoxyribonucleic acid
ELISA	Enzyme-linked immunosorbent assays
ER	Endoplasmic reticulum
ERK	Extracellular signal-regulated kinases
FGF21	Fibroblast growth factor-21
GDF15	Growth-and-differentiation factor-15
GLUT	Glucose transporter
GR	Glucocorticoid receptor
GTT	Glucose tolerance test
H&E	Hematoxylin and eosin
HFD	High fat diet
HSL	Hormone-sensitive lipase
iBAT	Interscapular brown adipose tissue
ITT	Insulin tolerance test
iWAT	Inguinal white adipose tissue
MAPK	Mitogen-activated protein kinases
mRNA	Messenger RNA
MSC	Mesenchymal stem cell
mtDNA	Mitochondrial DNA
NE	Noradrenaline
NEFA	Non-esterified free fatty acids
NIX	NIP3-like protein X
OXPHOS	Oxidative phosphorylation
PCR	Polymerase chain reaction
PD	Parkinson’s disease
PDH	Pyruvate dehydrogenase
PGC1α	PPARγ coactivator 1α
PINK1	PTEN-induced kinase 1
PPAR	Proliferator-activated receptor
PRDM16	PR domain containing 16
PUFA	Polyunsaturated fatty acids
PVDF	Polyvinylidene difluoride
qRT-PCR	Quantitative real-time PCR
rBMAT	Regulated BMAT
RNA	Ribonucleic acid
rRNA	Ribosomal RNA
RXR	Retinoid X receptor

s.e.m.	Standard error of the mean
SIRT	Sirtuin
SNS	Sympathetic nervous system
SVF	Stromal vascular fraction
T2DM	Type 2 diabetes mellitus
T3	Triiodothyronine
T4	Thyroxine
TCA	Tricarboxylic acid
TG	Triglyceride
TGFβ	Transforming growth factor beta
TH	Tyrosine hydroxylase
TZD	Thiazolidinedione
UCP1	Uncoupling protein 1
USP	Ubiquitin specific protease
WAT	White adipose tissue
WHO	World health organization
WNT	Wingless and Int1

Introduction

1. Obesity: The epidemic of the century

Even though COVID-19 is a new emerging pandemic that has affected global social welfare and economy due to its rapid transmission, progressivity and high case fatality rate; without doubt, obesity is the global epidemic of the 21st century: any other health issue affects so many people from so many countries in the world (Figure 1). According to the world health organization (WHO), in 2016, 39% of adults aged 18 years and over (39% of men and 40% of women) were overweight. Overall, about 13% of the world's adult population (11% of men and 15% of women) was obese in 2016[1]. Today, more people are obese than underweight worldwide. In addition, 65% of the world's population dwell in countries were overweight and obesity are responsible for more deaths than undernutrition[2]. Nowadays overweight and obesity are not only a problem in high-income countries, but these conditions are also dramatically on the rise in low- and middle-income countries, even in rural areas.

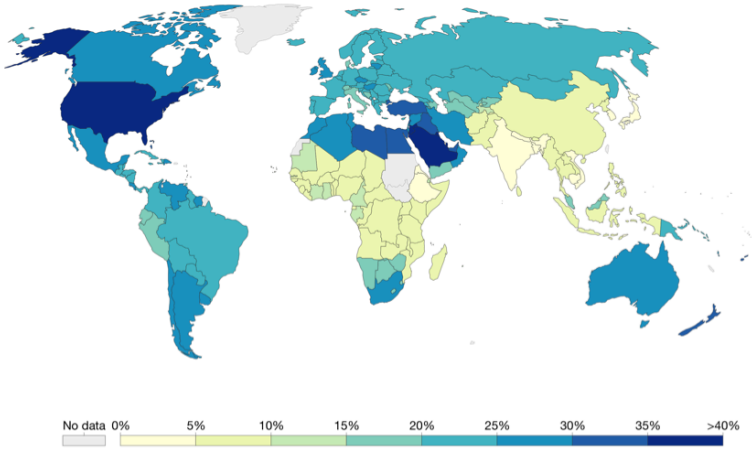

Figure 1. Share of adults that are obese (2016). Obesity is defined as having a body-mass index (BMI) equal to or greater than 30. BMI is a person's weight in kilograms divided by his or her height in metres squared. Adapted from https://ourworldindata.org/grapher/share-of-adults-defined-as-obese

According to the national health surveys, in Catalonia, 15% of the population was diagnosed with obesity and 35% were overweight. Data is also alarming in Spain, since 37% of the population is overweight, while there are a 17% of patients diagnosed with obesity. It has been estimated that if the current trend is sustained over time, 80% of men and 55% of women will have excess weight, that is obesity or overweight, by 2030.

Obesity -defined as excessive fat accumulation that may impair health- is a major cause of morbidity, disability and mortality as it increases the susceptibility to suffer from noncommunicable conditions such as hypertension, insulin resistance, dyslipidemia, metabolic syndrome, type 2 diabetes mellitus (T2DM) and cancer[3]. Obesity has been also described as an independent risk and prognostic factor for the disease severity and the requirement of advanced medical care in COVID-19[4].

The magnitude of the problem is immense and has tremendous repercussions for the health of people in an economic active age, but also in health systems and global macro-economy. It is crucial for the future to focus research and economic resources on the discovery of potential therapeutic targets for the treatment of obesity. Until now, many pharmacological treatments have been tested against obesity, but many have been discarded because they presented limited efficiency or they were highly invasive[2]. For example, some treatments targeted the central nervous system to regulate hunger sensation, but this is a very complex system as well as the neuronal network related to food intake. Feeding involves all our five senses, brain's pleasure center, learning and memory. Because of this complexity, many drugs targeting obesity have been withdrawn from the market. Although they certainly alleviated hunger, they provoked secondary effects such as anxiety or depression[5].

The main responsible organ for energy storage, the adipose tissue, has been in the spotlight to treat obesity and obesity-related conditions. Adipose tissue represents a promising alternative target for new therapeutic strategies and is currently receiving growing interest.

2. The adipose tissue

Adipose tissue had traditionally been conceived as an energy storage place to sustain organism's metabolic needs in periods of food scarcity. During the last decades, scientific research has revealed that adipose tissue is a complex and dynamic machinery able to coordinate energy balance and carry out endocrine functions. A healthy adipose tissue plays an important role in the regulation of physiological processes into the organism. For example, body temperature control, bone density or even reproduction[6]. However, its research has been usually prompted, especially in humans, by dysfunctions in itself: either for a lack of it (lipodystrophies) or, above all, for its excess (obesity).

Adipose tissue is mainly composed of adipocytes. These cells are highly specialized and essential to guarantee an energetic reservoir in form of lipid droplets (LD). Lipid droplets contain lipid molecules that are potentially toxic (lipotoxicity) and must be retained in safe and committed cellular containers[7]. Together with adipocytes, there are other cell types that comprise the highly heterogeneous stromal vascular fraction (SVF) of adipose tissue: nerve ends, adipose derived stem cells (ASCs), T regulatory cells, macrophages and other immune cells, endothelial cells and precursors, and preadipocytes in distinct differentiation status[8] (Figure 2). The last members mentioned, preadipocytes, are the ones that bring plasticity to the tissue due to their proliferation and differentiation capacity[9].

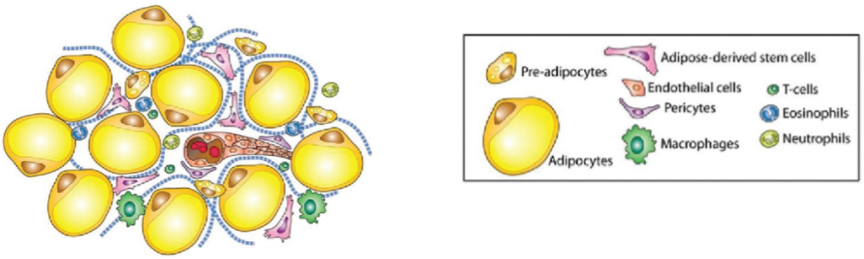

Figure 2. The cellular constituents of adipose tissue. Small representation of the AT cells population. Adapted from DOI:10.4103/jllr.jllr_1_17

2.1. Adipose tissues classification

In humans and other mammals, the adipose organ is structured in multiple depots. These deposits can be classified according to their functional and morphological phenotype in two main types: white adipose tissue (WAT) or brown adipose tissue (BAT)[10]. A third kind of adipose tissue has been recently described, the bone marrow adipose tissue (BMAT), which is yet not so well characterized as the others[11].

The adipocytes, anatomical subunits of these tissues, present a determinate morphology and phenotypic characteristics depending on the type of deposit to which they belong to and to the function that they develop. Adipocytes have been classically classified in different subtypes according to their chromatic appearance (white, brown or beige) (Figure 3A).

In WAT, white adipocytes store triglycerides (TG) as an energy source in a great lipid vesicle in the cytosol (unilocular morphology). When the organism requires the fuel stored, lipolysis is activated and TGs are hydrolyzed and non-esterified free fatty acids (NEFA) released to bloodstream, together with glycerol. This phenomenon occurs, for instance, during fasting periods.

On the other hand, in BAT, brown adipocytes, which are characterized by having lots of lipid droplets (multilocular morphology) and mitochondria, also store TGs but they use them as fuel to produce heat. The main function of brown adipocytes is to maintain body temperature by a mechanism known as non-shivering thermogenesis or adaptive thermogenesis. This phenomenon takes place because of the presence of uncoupling protein 1 (UCP1) in the inner mitochondrial membrane of these cells. This protein catalyzes there a proton mobilization, reducing the electrochemical gradient created by the electron transport chain and producing heat instead of ATP[12]. BAT is a very active metabolic tissue and it can exert great energy expenditure, as it contains mitochondria with a huge oxidative capacity.

Finally, it exists in humans and rodents a type of brown-like adipocytes with an inducible thermogenic capacity: beige adipocytes[13]. These adipocytes appear grouped in WAT depots when thermogenic stimuli are prolonged. This phenomenon is known as browning. That is because beige adipocytes share some features with classical brown adipocytes (Figure 3A,B). For example, they present multilocular lipid droplets, a high number of mitochondria and greater expression of UCP1. For this reason, they are also able to produce heat through uncoupled respiration. Beige adipocytes differentiation must be stimulated to promote thermogenesis. As a result of this, they are also termed as inducible adipocytes[14] (Figure 3C). It has been an intense research in order to characterize and differentiate beige adipocytes from classical brown adipocytes. First, some beige marker genes have been established in mice: *Tbx1*, *Tmem26*, *Tnfrsf9*, *Shox2*, *Cited1*; and others typical for classical brown: *Zic1*, *Lhx8*, *Eva1*, *Ebf3*, *Fbxo31*[13,15]. Besides, it has been proved that beige and classical brown adipocytes are originated from different cellular linages, as it will be explained later.

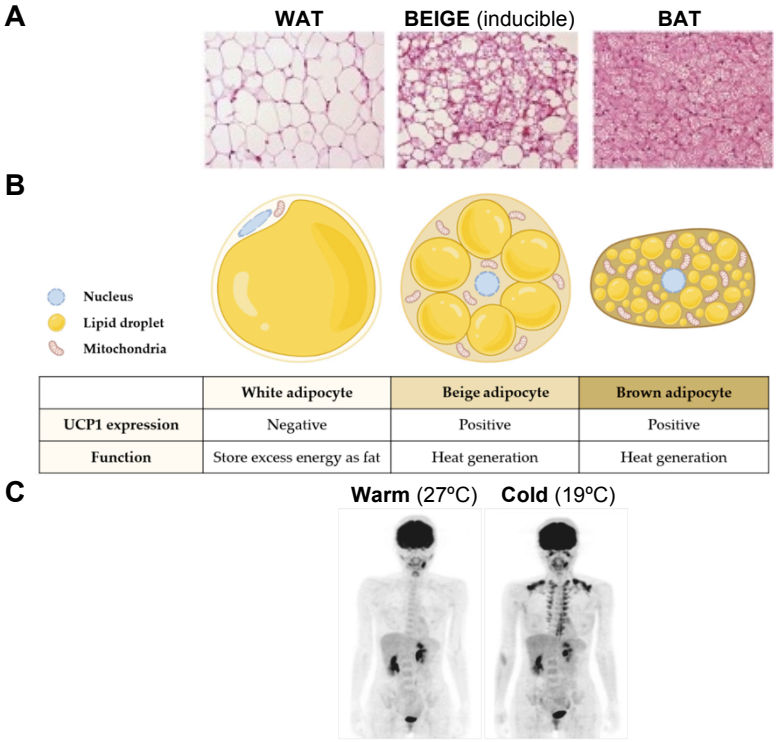

	White adipocyte	Beige adipocyte	Brown adipocyte
UCP1 expression	Negative	Positive	Positive
Function	Store excess energy as fat	Heat generation	Heat generation

Figure 3. (A) Optical microscopies of mice WAT, beige adipocytes and BAT ematoxylin and eosin stained. Adapted from DOI:10.1016/j.tcb.2016.01.004 **(B)** Scheme of the different types of adipocytes in the AT. Adapted from DOI:10.3390/antiox10020308 **(C)** Human brown adipose tissue detected by FDG-PET/CT scan. The FDG uptake into adipose tissues increases greatly after exposure to cold for 2 hours. Adapted from DOI:10.4093/dmj.2013.37.1.22

Two distinct types of adipocytes have been identified in BMAT: constitutive BMAT (cBMAT) is situated in the distal long bones and appears in the early postnatal period. These cells and white adipocytes phenotypically appear alike. cBMAT abundance is not affected by external insults. They present a huge and unique cytosolic LD. Nevertheless, BMAT function seems to be related to specifically to bone's energetic demands. Conversely regulated BMAT (rBMAT) is situated in the proximal regions of long bones. It develops after cBMAT, is mixed with hematopoietic cells and is modulated in various conditions. These two subtypes were recently shown to have different metabolic functions, with cBMAT being more resistant to lipolytic stimuli, and may have different repercussions on metabolic homeostasis[16]. BMAT -which constitutes over 10% of total fat mass in lean, healthy humans- has recently emerged as an active part of the bone marrow niche that exerts paracrine and endocrine functions thereby controlling osteogenesis and hematopoiesis[17]. It is known that BMAT positively correlates with age and diverse clinical conditions like T2DM or osteoporosis. In stark contrast to WAT, BMAT is also increased in caloric restriction and anorexia nervosa. These observations suggest that BMAT has systemic metabolic actions distinct to those of WAT and BAT[18]. Knowledge of BMAT formation and function is extremely limited, despite BMAT being identified over a century ago. This is partly due to the challenges inherent in studying a tissue so diffuse and difficult to access. It remains still unclear to what extent BMAT acts as a site of energy storage and release, how paracrine and endocrine actions of BMAT impact energy metabolism, the ability of BMAT to interact with bone cells, and the role of BMAT in hematopoiesis.

2.2. Adipose tissues distribution

The different fat depots composing the adipose organ are distributed along the body. Their anatomical disposition is closely related to the functions they perform and the organ's physiopathology[19,20]. In this fashion, mice fat depots can also be classified according to their location in subcutaneous or visceral depots (Table 1).

White Adipose Tissue (WAT)	
Subcutaneous WAT depots	
Posterior-subcutaneous	Located under the dermis in the area between the dorsal pelvis and the inguinal zone. It is subdivided in dorsolumbar, inguinal and gluteal.
Dorsal-subcutaneous	Located over the BAT, with which it is intrinsically united.
Anterior-subcutaneous	Located in the dorsoproximal area of the forelimbs, between the skin and the muscular fasciae.
Visceral WAT depots	
Perigonadal	Located surrounding sex glands, it is named epididymal in males and periovaric in females.
Retroperitoneal	Located in the dorsal area, it is encapsulated by a thin membrane that segregates it from kidney and perirenal BAT.
Cardiac	Located surrounding the heart, from the right ventricle to the apex, it is usually thin.
Mesenteric	Located in the mesentery surrounding the intestinal surface.
Omental	Located over the stomach surface in the abdominal cavity.
Brown Adipose Tissue (BAT)	
Interscapular	Located over scapulae in the shape of two symmetrical lobules. It is the biggest BAT deposit.
Cervical	Located under the cervical muscle fascicle in the inner part of the neck.
Subscapular	Located under scapulae, between the back musculature. It is also termed axillar BAT.
Periaortic	Located in the inner area of the thorax, in the mediastinum, surrounding the aorta.
Perirenal	Located surrounding a great portion of the renal hilum. It is in contact with the renal artery, renal vein and the ureter.

Table 1. Adipose tissue classification in mice according to their function and anatomical distribution. Adapted from DOI:10.1152/ajpendo.00249.2011.

Apart from the main deposits, other small clusters of adipose depots can be found disseminated through the organism. These are typically linked to certain organs like, for instance, clusters of adipose tissue in between muscle fibers or the aforementioned BMAT.

The distribution of adipose tissue in humans varies, in a certain way, from that presented in mice (Figure 4). There is also evidence of sexual dimorphism in both species[21,22]. In the first place, subcutaneous WAT is extended in a continuous manner under the dermis. However, there are some spots where it tends to accumulate in a preferential way; for example, the gluteo-femoral or abdominal subcutaneous areas. Secondly, visceral WAT can be subdivided in a variety of well-defined depots, as it is in mice: retroperitoneal, mesenteric, omental, pericardic and pararenal[23].

Regarding human BAT, this tissue has been classically considered to be limited to the first stages of life, during the neonatal period and childhood. It was assumed that BAT progressively disappeared when reaching adulthood[24]. It was only a decade ago when the clinical use of positron emission tomography (FDG-PET/CT scan), for detecting susceptible tumoral regions with a high glucose uptake, revealed the existence of active brown adipose tissue in adult humans[25,26] (Figure 3C). That which in a first place had been considered an artifact of the technique, ended up revealing metabolically active BAT depots and beige adipocytes[27-29]. By analyzing human BAT biopsies, it was detected that the different types of brown adipocytes (classic and inducible) coexisted in the same deposits during adulthood[30,31]. Active BAT inversely correlated with BMI and age in human subjects[32,33].

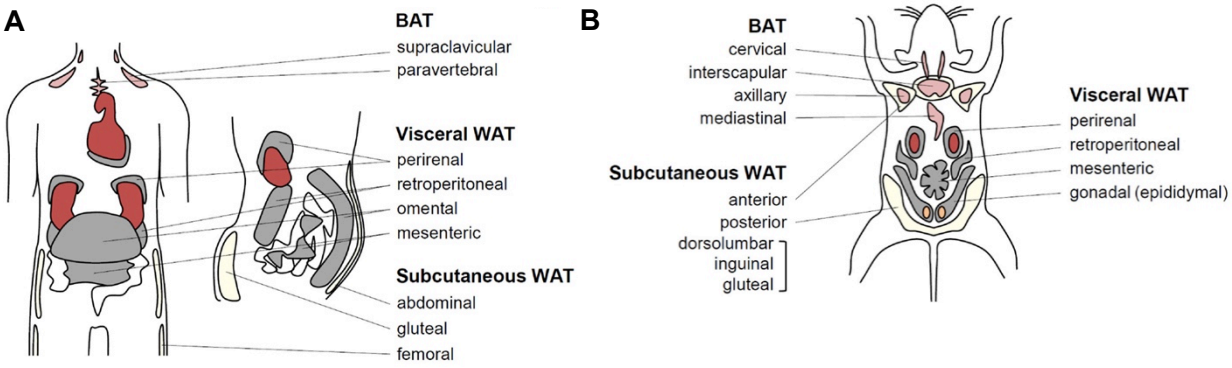

Figure 4. Scheme of adipose tissues main depots distribution in (A) humans and (B) mice. Adapted from DOI:10.3389/fendo.2016.00030

2.3. Adipocyte differentiation

Adipose tissue is originated in the mesoderm germ layer of the embryo. Adipocytes are formed from mesenchymal stem cells (MSCs) during a two-step process that is called adipogenesis. First, MSCs are committed to preadipocytes in the determination phase. Then, in the terminal differentiation, preadipocytes differentiate into mature adipocytes by acquiring the essential protein components to synthesize lipids and build up LD[34].
WAT and BAT are developed in different moments of the development of an organism. In most mammals, BAT is developed during the fetal period and activated just after birth. For example, in rodents' brown adipocytes mature rapidly during the first days of life[35,36]. By contrast, WAT appears at the middle of gestation in humans, whereas in mice it appears just after birth.

White and brown adipocytes arise from different precursor cells. It is generally considered that brown adipocyte precursors express myogenic factor 5 ($Myf5^+$) and paired-box7 ($Pax7^+$). They seem to be derived from the same population of stem cells than muscle cells. Meanwhile, white and beige adipocytes derive from $Myf5^-$ cells. However, the presence of white and brown adipocytes coming from $Myf5^+$ and $Myf5^-$ precursors, respectively, was recently reported[37,38]. Adipocytes from the dorsal and anterior regions may arise preferentially from $Myf5^+$ precursors, whereas the ones from the posterior and ventral areas may derive from $Myf5^-$ precursors. The anatomical position would be the most influential factor in the determination of the linage origin.

Adipocyte differentiation processes have been basically investigated from *in vitro* models. In the first step of these processes, there is a proliferation stoppage by a combo of secreted pro-adipogenic inputs. In this cocktail of factors there are proteins from the wingless and Int1 (WNT) family and transforming growth factor beta (TGFβ) superfamily. These stimuli are accompanied by physico-mechanical signals, like cell-cell interactions or the extracellular matrix rigidity and composition[34,39]. The combination of WNT and TGFβ factors can also favor other cell types, including osteoblasts (bone cells) or myocytes (muscle cells)[40,41]. In addition, some members of the TGFβ family known as bone morphogenetic proteins (BMPs), like BMP2 or BMP4, activate white adipocytes adipogenesis[42,43]. Other BMPs, like BMP7 or BMP9 promote brown adipocytes adipogenesis[44,45]. Some members of the WNT and TGFβ families, that control β-catenin pathway, like WNT10b or TGFβ, can act as adipogenesis inhibitors.

Once preadipocytes determination is accomplished, a series of transcriptional changes take place to differentiate into mature adipocytes. These terminal differentiation events are different for the different types of adipocytes.

2.3.1. White adipocytes differentiation

The key transcriptional factors that participate in the terminal differentiation of white adipocytes are peroxisome proliferator-activated receptor gamma (PPARγ) and CCAAT-enhancer-binding proteins (C/EBPs) α, β and δ.

At first, the presence of adipogenic factors induces the expression of C/EBPβ, in part through cAMP-PKA-CREB pathway[46], and of C/EBPδ[47]. These two members of the C/EBP family promote the expression of other transcription factors, such as glucocorticoid receptor (GR), retinoid X receptor (RXR). They also activate the master genes for the rest of the process, PPARγ and C/EBPα, beginning the second phase of terminal differentiation[48].

PPARγ and C/EBPα induction promote the expression of proteins that characterize the adipose phenotype like fatty acid synthase (FAS), glucose transporter type 4 (GLUT4), fatty acid binding protein 4 (FABP4/aP2), acetyl-CoA carboxylase (ACC), hormone-sensitive lipase (HSL) and some adipokines like adiponectin[49]. PPARγ binds DNA in heterodimer with RXR activating their target genes transcription[50]. Some transcriptional co-repressors, as receptor-interacting protein 140 (RIP140), regulate PPARγ activity during the process. RIP140 plays a role in the promotion of the white over the beige phenotype in WAT depots[51-53].

Adipogenesis can be pharmacologically modulated through molecules that regulate the master transcription factors mentioned before. These molecules are generally used in differentiation cocktails *in vitro*: 3-isobutyl-1-methylxanthine (IBMX), which raises intracellular cAMP, promotes C/EBPβ expression; dexamethasone is a glucocorticoid capable of inducing C/EBPs expression and indomethacin induces PPARγ expression. Moreover, insulin and insulin-like growth factor 1 (IGF1) also promote adipogenesis through the activation of cAMP response element-binding (CREB) and increasing glucose uptake to synthesize fatty acids[54,55].

2.3.2. Brown adipocytes differentiation

Noradrenaline or norepinephrine (NE) is one of the main extracellular inputs that activate the proliferation and differentiation of brown adipocytes. NE promotes proliferation through β_1 adrenergic receptors in preadipocytes and precursor cells. Once these cells are committed NE contributes to increase intracellular cAMP and activate C/EBPβ expression through CREB. It will be explained later how NE acts as the main thermogenic inducer in mature brown adipocytes through its interaction with β_3 adrenergic receptors[35].

Brown adipocytes arise generally from $Myf5^+$ precursors. Great part of the components in the transcriptional cascade for adipogenesis is shared between white and brown adipocytes, for instance PPARγ and C/EBPs. Nevertheless, C/EBPα induction takes place before C/EBPβ, which is fundamental for mitochondrial biogenesis and the acquisition of thermogenic capacity[56]. Thermogenic capacity is attained by UCP1 expression together with genes related to lipid metabolism and mitochondrial biogenesis. In this way, in contrast to white adipocytes, PPARγ co-activator 1α (PGC1α) and PR domain containing 16 (PRDM16) play an important role to obtain the thermogenic phenotype.

PRDM16 is preferentially expressed in BAT over WAT[57]. The lack of PRDM16 in brown preadipocytes promotes the myoblast linage and is a detriment to the thermogenic phenotype[58]. When PRDM16 is overexpressed in white preadipocytes or myoblast precursors instead, these cells acquire brown adipocyte traits and inhibit the expression of white adipocytes marker genes[59]. PRDM16 is also important in the maintenance of the thermogenic phenotype in mature adipocytes. Nonetheless, the loss of PRDM16 in mice has mild effects in the embryonic BAT development. Other proteins like PRDM3 might compensate that eventual loss[60].

One key step in PRDM16 action is its interaction with C/EBPβ, which induces PPARγ and PGC1α, triggering brown adipocytes transcriptional program[61]. Afterward, this factor interacts with the complex PPARγ-RXR and PPARα-RXR. Conversely to white adipocyte, PPARα expression coincides with the last phase of brown adipocyte differentiation. This is significant for the thermogenic phenotype, as it induces the expression of PGC1α and UCP1 in differentiated adipocytes[62-64].

PGC1α was originally identified as a PPARγ co-activator preferentially expressed in BAT over WAT and cold-inducible[65]. PGC1α is the gene product of *Ppargc1a*. It presents several isoforms due to alternative splicing. PGC1α1 is the most metabolically studied isoform in adipose tissues, liver and muscle[66]. Although PGC1α is expressed during the differentiation process, it is not essential for this process. Its absence can be replaced by the action PGC1β1. By contrast, the lack of PGC1α in mature brown adipocytes seriously impairs the thermogenic program display[67]. Some inhibitors of thermogenic program act by blocking PGC1α expression or activity, such as RIP140 or the retinoblastoma protein (Rb)[53,68].

In mature brown adipocytes, PGC1α expression is inducible by cold via p38MAPK and activating transcription factor 2 (ATF2)[69,70]. In brown and beige adipocytes, PGC1α induces UCP1, iodothyronine 5'-deiodinase (DIO2), respiratory chain and mitochondrial β-oxidation components transcription[65,71,72]. This is mediated by its interaction, among others, with PPARγ, PPARα and thyroid hormones receptors[63,73].

2.3.3. Beige adipocytes differentiation

Beige adipocytes appear grouped in WAT depots when thermogenic stimuli are sustained over time[74]. In order to explain the origin of these brown-like adipocytes, two different theories, non-mutually exclusive, coexist. The first one, argues that beige adipocytes can come from mature white adipocytes through trans-differentiation phenomena[75]. The second theory exposes that beige adipocytes are formed by differentiation of resident precursor cells in WAT depots (mainly Myf5^{-})[76].

In order to prove the theory of differentiation from specific precursors, various studies have been performed to determine the linages that potentially could differentiate in beige adipocytes. Some heterogeneous precursors populations in WAT with potential to differentiate in beige adipocytes *in vitro* have been isolated. However, these precursors required thermogenic inputs like β-adrenergic agonists or thiazolidinediones (TZD) to activate the thermogenic program[77]. For example, rosiglitazone, a TZD, activates PPARγ and induces browning and brown adipocyte differentiation through the induction of PGC1α expression[63]. Hence, beige phenotype is inducible; those resident precursor cells in WAT can perform either storage functions or energy expenditure[78]. Some marker genes reported in resident preadipocytes in WAT with capacity to differentiate into beige adipocytes are early B-cell factor 2 (EBF2), platelet-derived growth factor receptor α (PDGFRα), zinc finger protein 516 homolog (ZFP516), T-box transcription factor 15 (TBX15), together with PRDM16 and PGC1α[77,79,80]. Browning repressors have also been identified, like ZFP423[81].

It has recently been tried to establish a series of marker genes for differentiate beige from classical brown mature adipocytes. As we mentioned before, nowadays, the expression of *Tbx1*, *Tmem26*, *Tnfrsf9*, *Shox2*, *Cited1* is considered as a distinctive trait of beige adipocytes. Whereas classical brown adipocytes typically express *Zic1*, *Lhx8*, *Eva1*, *Ebf3* and *Fbxo31*[13,15]. Nevertheless, the settlement of these marker genes in mice and humans is still a matter of debate.

2.4. Adipose tissue function

As it was already pointed out, WAT and BAT carry out different and opposing functions: On the one hand, WAT stores energy; on the other hand, BAT is an energy expenditure regulator. Therefore, both types of fat deposits are involved in the energetic homeostasis and associated metabolic diseases[82]. Subcutaneous WAT also performs thermic insulating functions, contributing to body temperature management in a different way than BAT.

Certain adipose depots also accomplish structural functions with a protective mission of determinate regions. It can be found, for example, in the ocular globe embedding the orbital cavity or in the palm of the hand or the heels. These adipose depots, with a structural purpose, are distributed all along the organism and can also be affected by pathological conditions, like lipodystrophies.

2.4.1. WAT function

WAT is the main location for storing the body's energy. It works both, as an energy reservoir and as a buffer for excess energy consumed. WAT possesses great plasticity. This tissue can be tremendously expanded due to the phenomena of hypertrophy, that is increased adipocytes size, and hyperplasia, that is increased number of mature adipocytes. Other organs, like the liver and muscle are also capable of accumulating energy, especially by synthesizing glycogen molecules. However, the lipids in WAT are the main energetic substrate to sustain the body's metabolic needs in prolonged intervals of nutrient scarcity.

2.4.1.1 Triglycerides synthesis and storage

In feeding conditions, the lipids that are ingested are mainly triglycerides, some free fatty acids, cholesterol and other sterols. Lipids are transported in the bloodstream by chylomicrons (QM). In addition, the liver can transform excess carbohydrates into TGs through *de novo* lipogenesis and incorporate them into bloodstream through VLDL (very low-density lipoprotein). Both, QM and VLDL, distribute lipids throughout body. These lipids are captured by different tissues in the form of NEFA thanks to lipoprotein lipase (LPL) in the endothelial and adipose cells[83,84].

NEFA enter the cells mainly through specific transporters like CD36 and proteins of the family of fatty acid transporters (FATP)[83]. Once inside the cells, free fatty acids are esterified to acyl-CoA. Then, they are normally used as an oxidative energy substrate. However, in the adipose tissue, NEFAs can be re-esterified in TGs to be incorporated into LDs (Figure 5). In adipocytes, TGs are synthesized in the endoplasmic reticulum and accumulated in conglomerates until they are large enough to be cleaved, giving rise to the lipid droplet. Once cleaved, LDs are enclosed by a monolayer of phospholipids and cholesterol together with various anchored proteins, such as adipophilin, caveolin 1 or perilipin family proteins (PLIN). These are key proteins for the structure and regulation of LDs dynamics and formation-degradation processes[85]. In white adipocytes, LDs are merged into a large cytoplasmic lipid vesicle that ends up shifting the nucleus to the periphery during the differentiation process.

Lipogenesis is modulated by hormonal signals and growth factors. Under feeding conditions, insulin signaling induces *de novo* lipogenesis to manage excess carbohydrates. GLUT4 translocation is promoted into the cell membrane of adipocytes in order to promote glucose uptake[86]. Moreover, sterol regulatory element-binding protein 1 (SREBP-1) transcription is activated. This protein prompts the transcription of leptin and genes involved in the TGs synthesis, as FAS enzyme. In opposition, under fasting conditions, glucagon inhibits lipogenesis and activates lipolysis in WAT.

2.4.1.2 Lipolysis and energy mobilization

WAT lipolysis is activated whenever the body requires the mobilization of its energetic reservoirs. This metabolic pathway provides NEFAs to tissues that require energy. NEFAs are mainly consumed as a substrate for β-oxidation. Lipolysis is triggered by the decline in the insulin-glucagon ratio in fasting or an increase in catecholamine levels[87]. When lipolysis is initiated, hormone-sensitive lipase (HSL) and perilipin A are phosphorylated. As a result of its phosphorylation, HSL is translocated to the surface of LDs. Besides, perilipin A phosphorylation induce a conformational change that enables HSL and other lipases such as ATGL or MGL to access LDs. Consequently, TGs are hydrolyzed by adipose lipases resulting in NEFAs and glycerol[88,89] (Figure 5). Fatty acids generated by lipolysis can enter into mitochondria and be consumed by mitochondrial β-oxidation due to carnitine shuttle system and carnitine palmitoyl-transferase 1 (CPT1)[87].

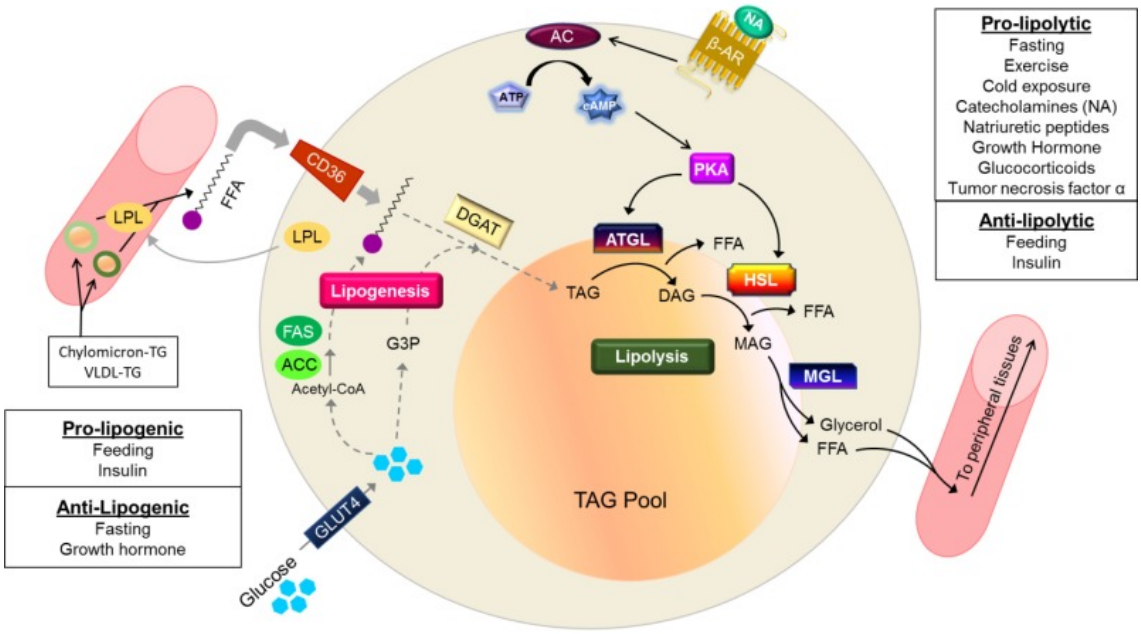

Figure 5. Summarized diagram of adipocytes' lipogenesis (left, gray arrows mark the pathway), **lipolysis** (right, marked by black arrows) and nutritional and hormonal cues that regulate both processes. Other abbreviations: glycerol 3 phosphate (G3P), diacylglycerol acyltransferase (DGAT), noradrenaline (NA), adenylyl cyclase (AC), protein kinase A (PKA), triglyceride (TAG), diglyceride (DAG); monoglyceride (MAG). Adapted from Bookshelf ID: NBK555602.

2.4.1.3 Adipokines, WAT as a secretory organ

Beyond its function as an energy storage organ, WAT is an endocrine organ that secretes hormones and cytokines of great importance in the regulation of multiple systemic functions. These secreted factors, denominated adipokines, can act at the autocrine, paracrine or endocrine level. The main adipokines are described below.

Leptin is an adipokine that informs the central nervous system about the nutritional status of the adipose tissue and regulates food intake[90]. Leptin signaling conveys several systemic responses coordinated from the hypothalamus. For instance: appetite control, lipolysis or thermogenesis. In contrast, the peripheral effects of leptin are related to improve insulin sensitivity and regulate the reproductive system. While leptin deficiency promotes a state of obesity, obesity itself has been described as a state of leptin resistance[91,92].

Adiponectin is the most abundantly expressed adipokine found in human serum at levels in the µg/mL range. Among other actions, adiponectin can activate the oxidation of fatty acids in the skeletal muscle, inhibit gluconeogenesis in the liver and inhibit lipolysis in WAT[93]. It promotes insulin sensitivity in peripheral tissues. Besides, it blocks the obesity-induced synthesis of pro-inflammatory cytokines and the infiltration of macrophages in adipose tissue[94]. However, adiponectin levels are reduced in situations of insulin resistance, in states of inflammation and in obesity[91,95].

Resistin is an adipokine secreted by WAT whose function is mainly related to glucose metabolism and inflammatory processes. In humans, resident immune system cells in WAT secrete resistin. In mice, it is produced by white adipocytes. In pathological conditions such as obesity, resistin promotes insulin resistance[96].

In addition to the most prominent adipokines described above, WAT secretes multiple regulatory molecules: adipsin, apelin, ometin, oncostatin M, retinol 4-binding protein (RBP4), vaspin, or visfatin. Besides, NEFAs from lipolysis can also act as signaling molecules.

Other than adipocytes, SVF and other WAT components also produce many secreted cytokines and chemokines. Anti-inflammatory cytokines secreted by these cells would have a role related to the maintenance of tissular homeostasis. Nevertheless, pro-inflammatory cytokines production is increased in response to stressors in the tissue microenvironment (i.e., oxidative stress, hypoxia, etc.). This changes lead to a state of chronic inflammation like in obesity and obesity-related conditions[97-99].

2.4.2. BAT function

BAT is the main place where adaptive thermogenesis takes place. This is an adaptive mechanism of heat production that contributes to the maintenance of body temperature. It is especially important in conditions of low environmental temperatures. The existence of BAT was first described in small mammals that carry out hibernation processes, which is why it was called the hibernation gland[100]. The presence of active BAT in humans was initially identified in newborns. This is because, unlike adults, newborns possess large amounts of BAT in the interscapular area. In adult humans, BAT and browning regions are distributed in a more scattered way than in newborns[24].
BAT is a highly innervated tissue and it is fundamental for its function. The nerve terminals of the noradrenergic neurons that come from the hypothalamus regulate the activation of thermogenesis[101]. BAT is also highly irrigated, since oxygen and metabolic substrates are extracted from the bloodstream and, simultaneously, the heat that is produced in it is transmitted through the blood to the rest of the body[35]. The browning process is accompanied by an increase in irrigation and innervation of WAT deposits in regions where beige adipocytes appear.

BAT plays an important role in regulating energy expenditure due to its high oxidative capacity. The activation of thermogenesis in BAT is a mechanism of protection against obesity and obesity-related conditions. Thermogenesis prevents the accumulation of fat by burning metabolic substrates[102]. One of the activating stimuli of thermogenesis is food consumption. This phenomenon is called diet-induced thermogenesis. It is partly controlled by postprandial activation of the sympathetic nervous system[103]. In obesity, the activity of TAM is systematically reduced[104].

2.4.2.1 UCP1 and the mechanics of heat production

Brown adipocytes are capable of inducing thermogenesis due to the expression of UCP1 (initially denominated thermogenin)[105]. The respiratory chain pumps protons into the mitochondrial intermembrane space, which creates a gradient whose electromotive force drives ATP synthase. The activation of UCP1 can short-circuit this gradient, dissipating the energy stored in the gradient as heat (Figure 6). In this way, the electron transport chain is uncoupled from ATP formation. In most cells, that do not express UCP1, the electrochemical gradient can only be dissipated by ATP synthase in order to generate ATP. UCP1 activation accelerates mitochondrial oxidation of energy substrates. Besides, its action prevents the accumulation of ATP, which would normally end up inhibiting mitochondrial catabolism. Although there are other members in the family of uncoupling proteins, UCP1 is the only one essential for thermogenesis[106,107].

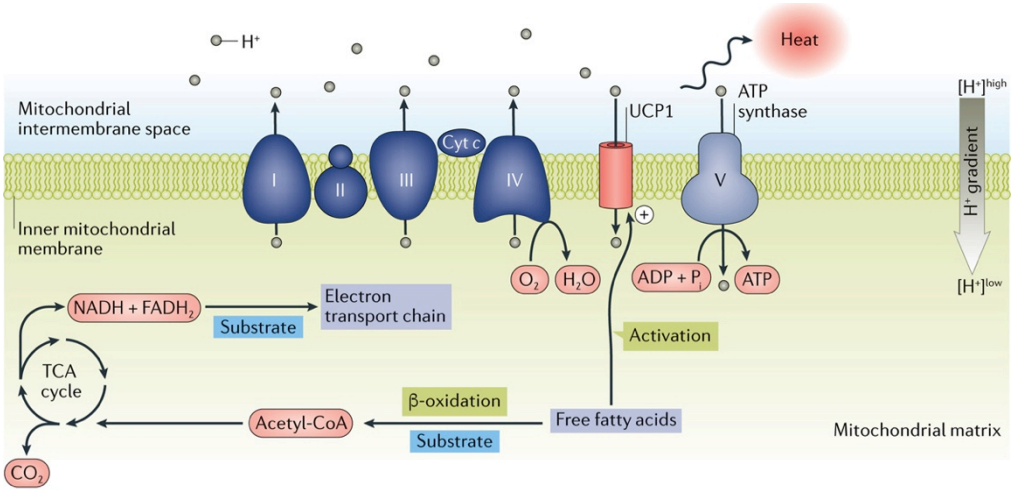

Figure 6. Mechanism of UCP1-mediated thermogenesis. Adapted from DOI:10.1038/nrendo.2017.132

2.4.2.2 Adaptive thermogenesis

The fundamental physiological stimulus that activates thermogenesis in brown adipocytes is the decrease in environmental temperature. In thermoneutral conditions the basal metabolism is sufficient to generate the heat needed to maintain body temperature. BAT is inactive in thermoneutrality and acquires some WAT characteristics, such as LD fusion and mitochondrial protein loss[108]. The thermoneutral zone range of temperatures varies according to the species. This is because the generation and dissipation of heat depends on the surface/volume ratio, the insulation capability and the basal metabolic rate. In adult mice, it is found around 30ºC[109].

When cold is perceived, the body triggers various adaptive responses that vary depending on the intensity and duration of the signal. Acute responses are mediated by an increase in sympathetic activity. These phenomena promote a rapid peripheral vasoconstriction, the production of muscle heat by tremor and the activation of thermogenesis in BAT accompanied by an increase in blood flow to this tissue[35,110]. At this point, the thermogenic capacity of BAT depends on the preexisting UCP1 levels. Under thermoneutral conditions UCP1 levels are very low. If the organism has been previously adapted to cold the thermogenic response will be faster, since it would have high basal levels of UCP1[109]. In the presence of prolonged cold stimuli, the synthesis of proteins of the thermogenic program and catabolic enzymes is activated in BAT. Moreover, new brown adipocytes are recruited (hyperplasia) and browning is induced in WAT depots.

2.5. BAT adaptive thermogenesis modulation

BAT activity is regulated at the central nervous system in the hypothalamus, specifically in the preoptic area and the ventromedial nucleus[101]. The hypothalamus controls the activity of the sympathetic nerve endings innervating adipose tissue. The perception of cold signals promotes the release of norepinephrine (NE) by these neurons and the activation of thermogenesis. It has recently been described that some adipose tissue resident immune cells may contribute to the thermogenic stimulus by secreting NE[111].

2.5.1. Noradrenergic regulation

NE, also called noradrenaline, is the major inducer of BAT activity through its interaction with adrenergic receptors in brown adipocytes. Although brown adipocytes express α and β-adrenergic receptors on their plasmatic membrane, β_3-adrenergic receptor is the one that is mostly expressed. These receptors are the main mediators of NE-induced thermogenic signaling.

β_1-adrenergic receptor is expressed in preadipocytes and is important for cold-induced BAT hyperplasia[35]. β-adrenergic receptors are G protein-coupled transmembrane receptors. In mature adipocytes, β_3-adrenergic receptors are generally coupled to G_s alpha subunit proteins. However, they can also signal through G_i protein alpha subunit by activation of the mitogen-activated protein kinases (MAPK) and extracellular signal-regulated kinases (ERK)[112].

During cold exposure, NE is released in the BAT. NE activates the β_3-adrenergic receptors, which in turn, promote the activation of adenylate cyclase through G_s-protein signaling. This is followed by a consequent increase of cAMP. Increased levels of cAMP mediate several signaling pathways. In brown adipocytes, the activation of thermogenesis takes place thanks to the activation of protein kinase A (PKA)[35,113].

Once activated, PKA triggers several signaling pathways: it activates lipolysis through the phosphorylation of perilipins and HSL; activates the MAPK, ERK1/2 and p38 pathways; and activates the thermogenic genetic program through cAMP response element-binding (CREB) and ATF2[70,114]. PKA can activate these transcription factors directly or via p38MAPK. CREB and ATF2 activate the transcription of genes containing the CRE response elements, such as UCP1 or PGC1α. Moreover, p38MAPK phosphorylates PGC1α, so that it can also act as a transcriptional co-activator of UCP1 through other DNA binding sites in the UCP1 promoter.

2.5.2. Endocrine and nutritional regulation

Although the main regulator of thermogenesis is the sympathetic nervous system, there are several non-adrenergic regulators of the thermogenic activity of BAT (Figure 7). These alternative activators of thermogenesis have a tremendous interest as potential treatments against obesity and have been at the focus of much research during the last years[115].

2.5.2.1 Thyroid hormones and the control of BAT activity

Brown adipocytes can produce triiodothyronine (T3) from thyroxine (T4) duet to the expression of the enzyme DIO2 which is induced by NE stimulus[116,117]. T3 is essential for thermogenic activation upon cold exposure. It acts synergistically with NE by increasing cAMP levels, inducing lipolysis and mitochondrial oxidation. In cell culture, T3 activates the transcription of thermogenic genes such as UCP1 through the thyroid hormone receptor (TR). At the systemic level, T3 regulates BAT activity indirectly through the hypothalamus, where it activates sympathetic activity[118].

2.5.2.2 FGF21-mediated regulation

Fibroblast growth factor-21 (FGF21) is an endocrine member of the FGF family that is mainly released by the liver. However, brown and beige adipocytes produce it too; they are a source and a target of this hormone[119]. FGF21 increases energy expenditure in adipose tissues by promoting lipolysis and glucose uptake. Experimental studies have demonstrated that FGF21 activates BAT and promotes the browning of WAT[120,121]. FGF21 signals through its interaction with their receptors (FGFRs) and the co-receptor β-klotho. In adipocytes, FGF21 promotes pathways that ultimately increase the expression PGC1α, UCP1 and GLUT4[120]. It has recently been described that FGF21 central effects may partly contribute to thermogenesis through the activation of sympathetic nervous system (SNS)[122]. FGF21 has powerful anti-diabetic and anti-obesity actions in rodent models[123], and there are also some indications of its healthy metabolic action in humans[124,125].

2.5.2.3 Gastrointestinal signaling in the control of BAT activity

The liver can modulate the activity of BAT through the secretion of bile acids. These, apart from enabling intestinal absorption of lipids, act as signaling molecules. Bile acids have direct actions on brown adipocytes as they bind to the G protein-coupled receptor TGR5, inducing the expression of DIO2[126]. In addition, bile acids can indirectly activate thermogenesis through their actions in the intestine. First, they stimulate the secretion of FGF15 (FGF19 in humans) by activating the farnesoid X receptor (FXR). Although the main function of FGF15 is the regulation of bile acid secretion in the liver, FGF15 can mildly stimulate BAT activity[127] and promote WAT browning through binding to FGFRs and β-klotho similarly to FGF21[128]. FGF15/19 signaling is required for thermogenic challenge-induced plasticity of WAT[129].

Moreover, bile acids induce intestinal secretion of glucagon-like peptide 1 (GLP-1), an intestinal-released incretin with anti-diabetic actions. In fact, pharmacological analogues of GLP-1, such as liraglutide, are used to treat T2DM and obesity. In mice, treatment with liraglutide increases thermogenesis and especially browning of WAT, but this is mainly due to central effects on the hypothalamus[130].

2.5.2.4 Myokine-mediated regulation of BAT activity

Muscle is also a recently recognized source of signaling molecules (myokines) that target BAT and the browning of WAT. It has been suggested that exercise-induced irisin, a myokine released by skeletal muscle, could serve to augment brown fat thermogenesis in concert with muscle derived FGF21 in humans[131]. BAIBA, a small molecule released by skeletal muscle, has also been shown to possess stimulating effects on the browning of WAT. Notably, BAIBA appears to act though PPARα, a nuclear receptor highly enriched in brown relative to white adipose cells[132]. Recently, musclin, a secreted factor highly homologous to natriuretic peptides, has been proposed to also act as a myokine to promote WAT browning[133].

In addition to skeletal muscle-derived myokines, the cardiac natriuretic peptides ANP and BNP, regulatory factors released by the heart (cardiomyokines) involved in the control of vascular system, have also been reported to act on BAT to promote thermogenic activation. Brown adipocytes contain natriuretic peptide receptors that, when activated, induce a cGMP-mediated intracellular cascade involving the activation of p38MAPK that regulates gene expression and induction of thermogenesis[134].

2.5.2.5 Dietary factors controlling BAT activity

There is long-standing evidence that diet may influence BAT activity and the browning of WAT. The identification of diet factors modulating AT thermogenic phenotype has great repercussions for food and pharmaceutical industries. For many years, BAT activity has been suspected to contribute to so-called "diet-induced thermogenesis", elicited according to the number of calories consumed and gross composition of diets. Besides, the composition of lipids and bioactive molecules present in the diet possess specific signaling properties that influence BAT activity and/or the browning of WAT. There is evidence that vitamin A derivatives, mainly retinoic acid, which participates in brown adipocytes' differentiation, activate the thermogenic program in BAT and induce the browning of WAT[135]. Retinoic acid induces UCP1 gene expression by its interaction with retinoic acid nuclear receptors (RAR). Consistent with this, there are reports that depletion of vitamin A in the diet impairs BAT activity in mice[136]. Other approaches, like dietary supplementation with nicotinamide, the amide form of vitamin B3 and a physiological precursor of nicotinamide adenine dinucleotide $(NAD)^+$, prevented body weight gain and adiposity in mice by boosting energy expenditure, with this being mainly attributed to enhanced thermogenic activity in BAT and browning WAT[137].

Another long-standing area of research on the potential effects of regulatory metabolites on BAT function relates to n-3 polyunsaturated fatty acids (PUFAs), reflecting the known beneficial effects of these fatty acids on adiposity and on the prevention and treatment of metabolic syndrome.

Experimental studies on the supplementation of fats in the diet with n-3 PUFAs have reported variable results in terms of their capacity to induce BAT activity and/or the browning of WAT[138]. Moreover, it has been found that not all n-3 PUFAs appear to have similar effects. For example, eicosapentaenoic acid included as a dietary supplement has a significant BAT-activating effect, whereas docosahexaenoic acid, does not[139]. GPR120, also known as FFAR4, is a G protein-coupled receptor for polyunsaturated fatty acids, has been identified as a promoter brown fat activation. GPR120 is induced by thermogenic activation and induces BAT activity and promotes the browning of white fat in mice by its interaction with n-3 PUFAs. GPR120 activation induces the release of FGF21 by brown and beige adipocytes, increasing blood FGF21 levels[140]. GPR120 also mediates the effects of n-3 PUFAs in brown and beige adipocyte differentiation.

Another compound of dietary origin that influences BAT activity and WAT browning is resveratrol. Resveratrol is a plant-derived polyphenol present in various foods characteristic of the Mediterranean diet, such as grapes or nuts. There is evidence that high doses of resveratrol in the diet induce BAT activity and promote WAT browning[141,142]. Resveratrol activates intracellular pathways involving AMP kinase, sirtuin 1 (SIRT1) and ultimately PGC1α and UCP1[143], which are key factors in the induction of thermogenic activity in brown adipocytes.

Among the dietary bioactive compounds that have most recently received attention for their potential role in regulating BAT activity are capsaicin and its analogues. Capsaicin is the component of hot chili peppers responsible for their pungency and is one of the most consumed spices in the world. Capsaicin and capsinoids are known to increase energy expenditure and decrease body fat in both rodents and humans[144]. These compounds mediate their effects through brown adipocytes recruitment and activation. Capsaicin and capsinoids act through binding to the vanilloid type 1 transient receptor potential channel TRPV1 in sensory neurons located in the tongue (capsaicin) and upper gastrointestinal tract (capsinoids). This selective activation of TRPV1 channels leads to the sympathetic activation of thermogenesis by the hypothalamus[145].

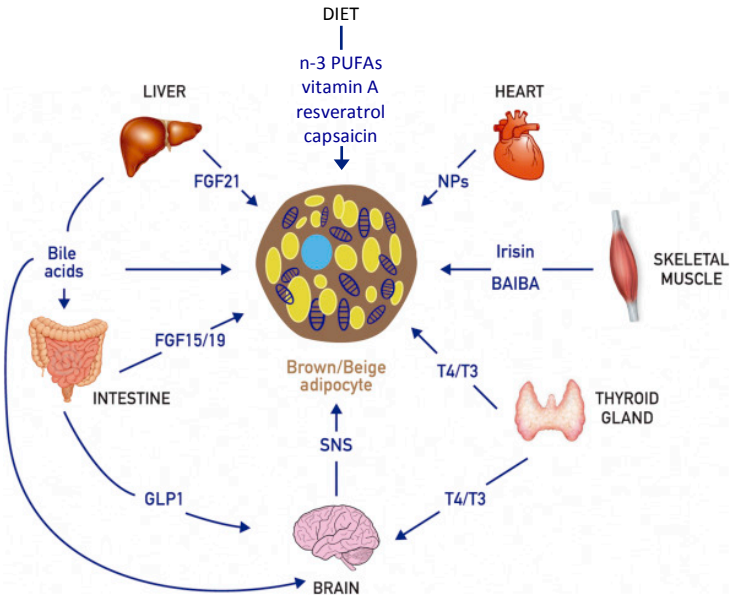

Figure 7. Scheme of the main endocrine and dietary factors that promote BAT thermogenesis. Adapted from DOI:10.1016/j.beem.2016.08.005.

2.5.2.6 Adaptive thermogenesis modulation through BAT batokines

In recent years, BAT has been recognized not only as a main site of non-shivering thermogenesis in mammals, but also as an endocrine organ. BAT secretes a myriad of regulatory factors (Figure 8). These so-called batokines exert local autocrine and paracrine effects, which may either be positive or negative, in the thermogenic function of brown adipocytes. Additionally, there is a growing recognition of the signaling molecules released by brown adipocytes that target sympathetic nerve endings, vascular cells and immune cells to promote the tissue remodeling associated with the adaptive BAT recruitment in response to thermogenic stimuli. Brown adipokines perform also endocrine actions targeting tissues and organs at a distance. The liver, heart, and skeletal muscle are the most commonly reported targets of batokines. The identification of the major brown adipokines and their roles is highly important for the discovery of novel candidates useful in formulating intervention strategies for metabolic diseases. Brown adipose tissue adipokines have been reviewed extensively by Villarroya et al.[146-148].

Multiple reports have indicated that the recruitment of alternatively activated macrophages to BAT and beige adipose tissue is positively associated with thermogenic activation[149]; however, the mechanisms by which macrophages intervene in BAT and/or beige adipose tissue activation remain controversial. The chemokine CXCL14 has been identified as a batokine that is released by brown adipocytes in response to noradrenergic stimulation and leads to the alternative activation and recruitment of macrophages[150]. Moreover, the CXCL14 released by BAT appears to influence the recruitment of M2 macrophages to subcutaneous WAT, thus promoting browning. This role of CXCL14 highlights the capacity of batokines to target immune cells. While CXCL14 accounts for the recruitment and activation of M2 macrophages, it does not appear to directly influence pro-inflammatory signaling in M1 polarized macrophages. However, the not long ago identified growth-and-differentiation factor-15 (GDF15), is secreted by brown adipocytes upon cold stimuli and exerts anti-inflammatory effects on M1 macrophages. GDF15 is a member of the TGFβ family that is widely recognized as a systemic marker of multiple pathologies, from cardiovascular disease to cancer[151]. The most representative role of GDF15 is its anorexigenic effect causing a reduction of body weight[152]. The GDNF family receptor α-like (GFRAL) has been later discovered as a receptor for GDF15 mediating the anorexigenic action, but is localized only in mice's hindbrain. Despite the restricted GFRAL expression in this brain region, there are numerous studies that cannot simply be explained by the anorexigenic action via GFRAL, including insulin sensitivity, lipolysis in adipose tissue, anti-inflammatory action, alleviation of hepatic steatosis, and muscle atrophy. It has been recently demonstrated that hepatic GDF15 is a biomarker of mitochondrial pathology together with FGF21 and both of them contribute to regulate systemic energy metabolism[153].

It appears that the secretome of thermogenically active brown adipocytes plays a key role in promoting the expansion of sympathetic nerve endings as a part of the recruitment of active BAT in response to environmental stimuli. NGF, NRG4, and S100b appear to be relevant components of the brown adipocyte secretome that mediate this action[154-156]. Importantly, it has been seen that NRG4 protects against diet-induced insulin resistance and hepatic steatosis through attenuation of hepatic lipogenesis, pointing the endocrine actions of batokines[157].

BAT activation is also autoregulated in a paracrine way. BMP8b, a member of the Bmp protein family, was identified as a brown adipokine released by brown adipocytes in response to noradrenergically mediated thermogenic stimulus[158]. BMP8b appears to be a brown adipocyte-secreted factor that promotes active brown and beige adipose tissue remodeling to increase thermogenic efficiency. This is achieved by directly and indirectly targeting innervation and vascularization, through the induction of brown adipocytes NRG4 secretion and angiogenic factors, respectively[159]. Importantly, not all batokines act in as thermogenic enhancers. It was recently identified that the kallikrein-kinin system is a relevant component of BAT thermogenic regulation that provides autoregulatory inhibitory signaling to BAT[160]. Other molecules secreted by BAT in response to cold have been proven to perform inhibitory actions over thermogenesis. This is the case of sLR11 or endocannabinoids. The function of these batokines may be to prevent tissue overactivation as a mechanism of tissue homeostasis.

A recent significant finding in assessing the endocrine role of BAT was the recognition of the capacity of BAT-released myostatin to affect skeletal muscle. Myostatin is a key molecule for the control of muscle growth. BAT is known to release myostatin, which has been proposed to play an autocrine role by negatively modulating BAT thermogenic activity[161]. It was found that the extent of BAT activation is reciprocally related to the release of myostatin[162].

FGF21 is among the first proposed endocrine signals acting as a batokine, given the strong release of FGF21 by BAT under conditions of thermogenic activation. The heart is one of the organs sensitive to FGF21 action, where it has a protective role against cardiac hypertrophy[163]. It was found that BAT-released FGF21 is essential to the prevention of hypertensive cardiac remodeling in mice[164]. Nevertheless, FGF21 does not account for all of the cardioprotective actions mediated by batokines. For instance, UCP1-null mice show exaggerated myocardial injury[165], but this is associated with an increase of BAT-released FGF21 in response to the UCP1 gene invalidation[166].

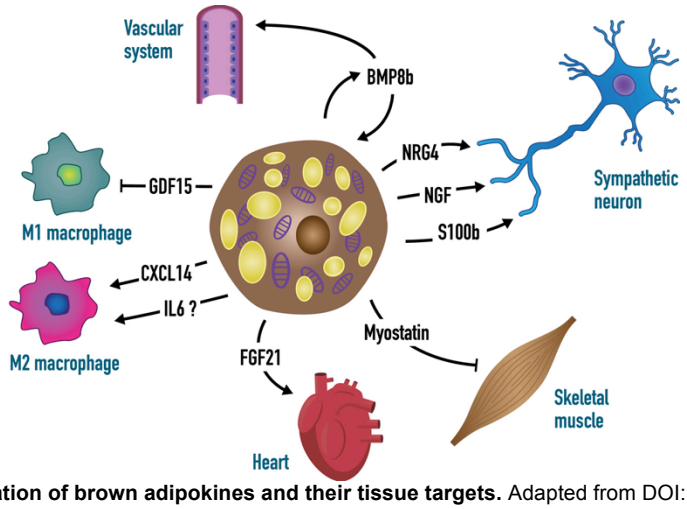

Figure 8. Representation of brown adipokines and their tissue targets. Adapted from DOI:10.1530/JOE-19-0295

3. Adipose tissue and aging

3.1. Aging and metabolism

The research into aging has been prompted by increased life expectancy and expansion of the elderly population in the years before the COVID-19 pandemic. The COVID-19 pandemic had a tremendous impact in the global population in drastic ways. In many countries, older people faced the most threats and challenges at this hard time. Although all age groups are at risk of contracting COVID-19, older people face significant risk of developing severe illness or dying if they contract the disease due to physiological changes that come with aging and potential underlying health conditions[167]. In fact, the Centers for Disease Control and Prevention states that 8 out of 10 COVID-19 deaths in the U.S. have been in adults 65 years old and older[168].

It is known that aging is the leading risk factor for a myriad of chronic diseases, such as cancer and diabetes, and to deterioration in physical function. Aging is a lifelong, creeping process of functional decline at organelle, cellular, tissue, and organism level. This progressive loss in physiological function leads to overt chronic disease, frailty and ultimately limits life. Some significant contributors to biological aging are known, among them cellular senescence, oxidative stress, and dysregulation of the energy homeostasis.

Several of those defective phenomena are also found in obesity, metabolic syndrome and associated metabolic diseases for which the prevalence is dramatically high and continues to rise consistently in Western and developing countries.

3.2. Aging in WAT

Upon obesity, some of the defects promoting aging such as elevated oxidative stress or premature accumulation of senescent cells have been found[169]. Obesity exacerbates aging-associated inflammation by impairing insulin responsiveness and contributes to the pathophysiology of diseases frequently observed in the elderly. For example, higher expression levels of SA-β-gal, p53, and cyclin-dependent kinase inhibitors, have been found in the adipose tissue of obese patients[170]. Another major process associated with aging in which the adipose organ emerges as an important player is dysregulation of the energy homeostasis. Of importance, key processes of adipose tissue physiology affect molecular pathways that regulate lifespan. For instance, in a mouse model of accelerated aging a SIRT1 reduction contributed to an aggravation of metabolic syndrome[171].

Additionally, various dietary and pharmacological interventions that extend health span and longevity also delay or prevent adipose tissue dysfunction. For example, metformin, an approved drug for the treatment of diabetes, appears to target many aging-promoting effects. Retrospective observational studies have linked metformin to a prolongation of human lifespan, reducing age-related diseases, improving cognitive function, and reducing the incidence of cancer[172].

Growing life expectancy has the potential to add some quality years to people in countries with increasing elderly populations. However, if those extra years in life are accompanied by excess adipose tissue and altered metabolic homeostasis, the extension in life may lead to a compromised health status because of age-associated conditions, such as chronic diseases, loss of physical function, and frailty. Consequently, maintenance of a lean phenotype, with a low adipose proportion in body composition, by caloric restriction, visceral fat removal or genetic modulation, prolongs healthspan.

It has been observed that weight increases with age. BMI peaks occur in people aged 50-59 years and adipose tissue reaches its peak between the ages of 60 and 79 years[173]. In the U.S., 38.5% of persons aged 60 and older were obese[174] and diabetes prevalence in adults over 65 years of age varies from 22% to 33%[175].

The characteristic rapidity and power to modulate systemic metabolism and inflammation of adipose tissue often vary by adipose depot and change with advancing age and health status.

At the organism level, at the onset of the aging process there is a characteristic redistribution of fat mass from subcutaneous to visceral fat deposits that provoke regional adiposity, dyslipidemia and the settlement of a low-grade inflammation milieu (Figure 9). Together, these changes are associated with metabolic abnormalities, particularly insulin resistance, with increased risk of metabolic conditions and cardiovascular disease[176,177]. Epidemiological evidence in middle-aged and older men or women reveals that chronic, sterile inflammation is at the basis of the interactions between obesity, insulin resistance, and diabetes in the context of aging in humans[178].
The origins of the alterations driving aging are diverse. Apart from the alterations in the cellularity and function of subcutaneous adipose tissue, hormonal variations during lifetime play also a role in both genders. In men, aging is accompanied by a decrease in the synthesis of testosterone and bioactive testosterone. These changes are associated with an expansion of the fat deposits in the trunk[179]. In women, after menopause, estrogen levels drop. Consequently, androgen hormones proportion increase predisposing a redistribution of lipids to the visceral compartments. These phenomena increase women's risk of cardiovascular disease, hypertension, and diabetes at an advanced age[180].

When approaching the senectitude, the aging process has proceeded and phenomena such as frailty and physical limitation appear on stage. Frailty is a geriatric syndrome related to an increase in the risk of adverse outcomes (i.e., falls, delirium and disability). The frailty phenotype includes declines in physical function and body composition, including unintentional weight loss or loss of muscle mass, muscle weakness, exhaustion or poor endurance, slow walking speed, and low physical activity, which result in reduced overall physiological reserve[181]. Consistent with that, in mice, adipocyte size decreases and fat loss occur when they enter the end of their life. Ectopic fat deposition due to adipose tissue dysfunction has been implicated in functional impairments into muscle in older adults (Figure 9). At the same time, these disturbances may limit functional ability important for mobility[182]. Another example by which lipoatrophy is related to aging has been observed in murine models. It has been reported a loss of subcutaneous WAT and concurrent accumulation of visceral WAT in the skin with age, promoting the appearance of aged skin. In this case, lipoatrophy takes place by the accumulation of macromolecular damage in dermal adipocytes. Dermal white adipose tissue is then replaced by fibrotic tissue and morphological and functional alterations in the skin appear[183].

3.2.1. Mechanisms of adipose tissue dysfunction in aging

At the cellular level, the function and relative amount of the diversity of cell types that comprise adipose tissue change throughout life. Age-related physiological changes occur in insulin-responsiveness, secretory profiles, and inflammatory status of adipose tissue, leading to adipose tissue dysfunction (Figure 9).

3.2.2. Cellular senescence

Aging impairs the ability to regenerate and to differentiate adipocyte stromal cells (ASCs), the precursors of mature adipocytes, which ultimately leads to the loss of the adipose organ function. It has also been seen that dysfunctional adipocyte-like cells that are smaller and less insulin responsive than fully differentiated adipocytes appear in white fat depots accompanying the decline with advancing age[184]. In addition, during aging ASCs exhaust their capacity to divide and they enter cellular senescence.

Cellular senescence is induced, among others, by telomere shortening[185]. It has been reported that the activation of p53 driven by telomere shortening, increased inflammation and insulin resistance in adipose tissue[170] (Figure 9). Senescent cells are progressively accumulated in adipose depots. Senescent cells normally show an aberrant secretome reminiscent of activated macrophages, also referred to as senescent-associated secretory phenotype (SASP). The SASP can adversely affect the local microenvironment in adipose tissue by promoting preadipocyte inflammatory processes, inhibiting differentiation, and driving immune cell infiltration, which induces generalized low-grade inflammation and reduces the functionality of the surrounding adipocytes[186].

Chronic low-grade inflammation is a hallmark of aging and is linked with the onset of diabetes and frailty. Given this fact, adipose tissue is believed to be a major contributor to systemic inflammation with advancing age. That is because, apart from SASP, aging exacerbates pro-inflammatory adipokines production in adipocytes that arises also from stress responses brought about by lipotoxicity, hypoxia, and/or replicative arrest[187,188]. The chronic low-grade inflammation in the absence of infection driven by endogenous signals that accompany aging has been originally termed "Inflammaging" by Claudio Franceschi[187]. The remodulation of the adipose organ secretome with increasing age ultimately endangers health, fitness status and promotes aging at organism levels. However, selective clearance of senescent cells by senolytic drugs or specific blockage of deleterious SASP components in aged animals extends their lifespan[190]. A common theme in most of these models of preservation and/or restoration of preadipocyte function in late life is that they are protected from low-grade inflammation, which undoubtedly plays a role in regulating the differentiation process.

These alterations in preadipocytes are particularly evident in subcutaneous depots, the major site of lipid storage in healthy mammals. Thus, these perturbations likely contribute to increased central adiposity and ectopic lipid accumulation that are often observed with advancing age[191].

The interventions with senolytic drugs could prevent the secondary effects of adipose tissue dysfunction, including lipid redistribution and metabolic perturbations, possibly despite increased adiposity[192].

3.2.3. Macromolecular damage

The adipose organ is also susceptible to the progressive accumulation of damaged macromolecules, such as DNA and proteins. It has been observed in various progeroid syndromes an increased rhythm in the processes of aging and adipose tissue redistribution due to alterations in different elements of DNA repair pathways[193]. There are also some environmental factors promoting DNA damage such as UVA irradiation. All these cellular disruptors participate in the functional decline of the adipose organ with age as they induce a loss of the proliferative potential of ASCs and induce the senescent phenotype of those cells. Thus, strategies to restore repairing enzymes and block macromolecular damage of ASCs may be protective to maintain a lasting state of health at old age[194].

3.2.4. Mitochondrial function

During the process of aging, it has been reported a repression in mitochondrial enzyme expression from old mice in adipose tissue[195]. In the same way, it has also been published that the mitochondrial function of the human WAT, measured by oxygen consumption of the tissue, is diminished in both obesity and aging[196]. Some hypotheses claim that the alterations in mitochondrial function in association to aging could be mediated by lipotoxicity or changes in the mitochondrial phosphoproteome. However, little is known about the underlying mechanisms that may participate in these phenomena and their interconnections. Mitochondrial dysfunction is known to be also a trigger of cellular senescence[197].

3.2.5. Altered adipokines/cytokines

Finally, the aging process alters adipose tissue bioactive mediators' secretion and endocrine function. The age-associated cellular senescence, local tissular inflammation, androgenic hormones and stress pathways promote changes in the huge amount of adipokines produced by adipose tissue (Figure 9). As a rule, practically all adipokines levels among aged individuals rise its levels in comparison with younger subjects with the same body fat as indicated below. However, the reallocation and excessive amount of fat within the visceral depots induces pro-inflammatory adipokines over anti-inflammatory mediators[198].

Leptin levels correlate with total fat mass throughout the life course and age does not appear to have an independent effect on leptin and adiposity in men or women[199]. Therefore, the increased levels of circulating leptin in older adults are primarily due to increased fat mass in comparison with younger adults. In addition, it remains to be seen if leptin responsiveness is diminished with increasing age due to impaired hypothalamic leptin receptor signaling, that is linearly correlated with total body fat and BMI[200].

Age does not appear to affect resistin levels independent of fat mass. Nonetheless, elevated levels of this adipokine are associated with an increased risk of cardiovascular disease in elderly men and women and insulin resistance in patients with a history of coronary intervention[201,202].

The synthesis of classical pro-inflammatory cytokines such as CCL2, IL1B, IL6, IL12, IL18 and TNFα, that are associated with the M1 classically activated macrophage phenotype, is favored by aging due to either increased adipose tissue mass and adipose tissue dysfunction[203,204].

Adiponectin plays a protective role against a bunch of obesity-induced conditions, like insulin resistance, cardiovascular disease, fatty liver, depression and some types of cancer[94]. Serum adiponectin levels are elevated with age, fasting, treatment with glucocorticoids, and conditions that enhance the expansion of bone marrow adipose tissue[205-207]. In contrast, lower levels of adiponectin are associated with obesity, cigarette smoking, and oxidative stress[208,209]. Centenarians have higher levels of adiponectin and this may be associated with longevity. While elevated adiponectin may be associated with improved metabolic status in the elderly, it has also been associated with reduced physical functioning[210]. Serum adiponectin levels are higher in women than in men.

Although the mechanisms underlying adipose tissue dysfunction are multifactorial, the consequences basically converge in secretion an accumulation of senescent cells, and an increase in pro-inflammatory cytokines. These processes synergistically promote chronic sterile inflammation, insulin resistance, and lipid redistribution away from subcutaneous adipose tissue. Which in turn, are consolidated predictors of impaired physical function and frailty onset. Thus, adipose tissue dysfunction may be a fundamental contributor to the elevated risk of chronic disease, disability, and adverse health outcomes with advancing age. These intimate links convert adipose tissue in an attractive entity to target therapies in order to combat age-related diseases and disability as a single entity in contrast to targeting individual conditions one-at-a-time.

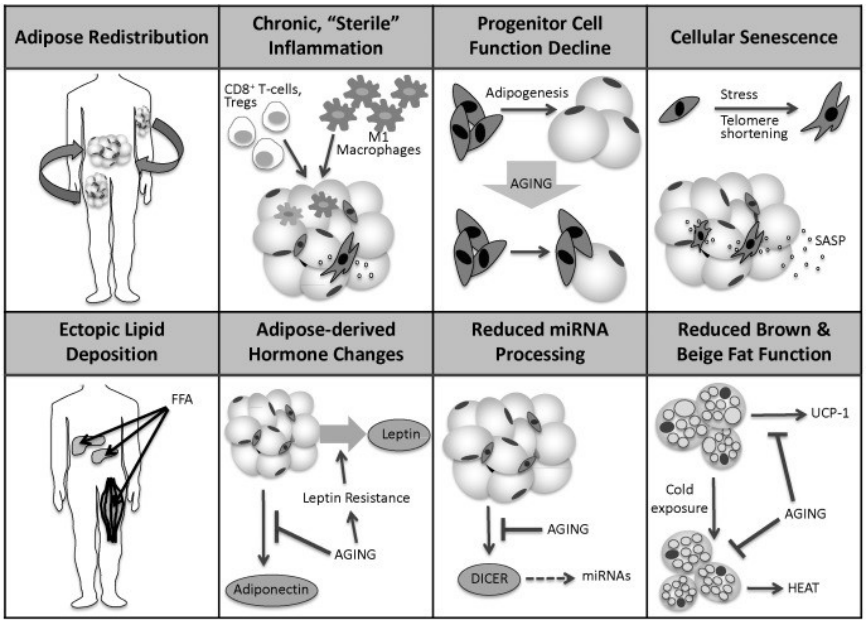

Figure 9. Adipose tissue changes with aging. Adapted from DOI:10.1016/j.exger.2016.02.013

3.3. Aging in BAT

As stated above, the activation of brown and beige adipose tissues increases energy expenditure and has been postulated to counteract the development of obesity and adipose tissue dysfunction. In humans, BAT undergoes different modulations throughout life (Figure 10). This tissue is originated during gestation to allow newborns, who lack the ability to shiver, to cope with temperature changes in their environment. Then, infants still maintain active BAT in their supraclavicular depots[211]. In adolescents, metabolically active BAT is detected only in about half of them after cold exposition. However, evidence suggests that BAT activity increased in adolescent population in parallel with sexual maturation and musculoskeletal development[212]. The growth of BAT and skeletal muscle appears to be a synchronized at that age, which is not strange, as both tissues arise from a related linage. Nevertheless, in rodent models and humans, the amount of detectable BAT declines with advancing age, in parallel with the capacity of activation of beige adipocytes in WAT through adrenergic stimuli (Figure 9). In a greater detail, it has been observed in BAT that the proliferation capacity and UCP1 expression are prevented in response to cold stimulus, together with an infiltration with white-like adipocytes in the tissue[213,214].

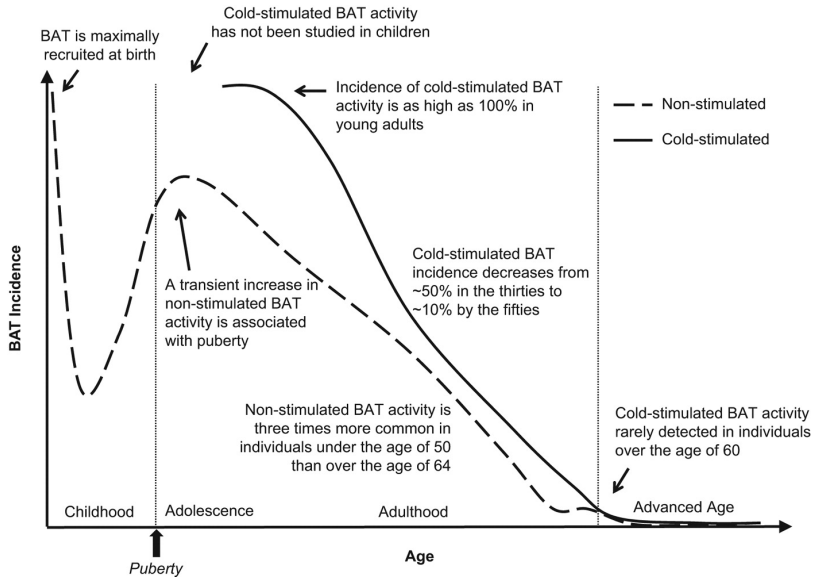

Figure 10. Human BAT presence and involution in association with advancing age. Metabolically active BAT incidence (y-axis) in the neck region of humans as a function of age (x-axis). Adapted from DOI: 10.3109/07853890.2014.914807

In aging, the first BAT depots to be lost are the peripheral ones, such as the interscapular compartment. Deeper depots, as perivascular or perirenal ones, decline later in life. The loss of BAT may plateau around the sixth decade of life and further decrease in the senectitude, as cold-stimulated BAT is rarely detected over the age of sixty[215] (Figure 10). This fact may be determinant to explain why the elder population worsens their tolerance to cold and their ability to control body temperature.

In a similar way, the consensus concerning beige adipocytes is that there is a progressive bias to a white adipocyte phenotype, which impedes browning in aged mice and older humans[216]. A loss of UCP1 in rats' subcutaneous WAT depots is also observed in association with aging. Therefore, it seems that many forms of BAT, if not all, potentially suffer a transition towards a WAT phenotype with advancing age both in human and rodents.

In summary, aging is one of the most relevant determinants of BAT activity and it is associated with a ubiquitous decline of BAT activity throughout life.

3.3.1. Mechanisms underlying BAT declines with advancing age

The potential mechanisms by which brown adipose tissue activity shows a regression with age include a reduction in sympathetic nerve output and mitochondrial function, changes in the expression of some key regulatory proteins, alterations in brown adipogenic progenitors' function and differences in endocrine signaling and the batokines secretion profile in association with aging.

3.3.2. Sympathetic nervous system

The SNS has a tremendous impact on brown adipose tissue regulation as BAT is activated and recruited to generate heat by the SNS. In a study by Bahler et al. sympathetic nerve activity and brown adipose tissue recruitment and activity were lower in lean elderly men of 50–60 years old vs. lean young men aged 20–28 years[217]. Therefore, a reduction in sympathetic drive involves a decline in brown adipose tissue with aging. This phenomenon may also contribute to explain why older humans present difficulties to regulate their temperature appropriately when exposed to cold.

3.3.3. Mitochondrial functionality and loss of stemness

On a different note, brown adipocytes rely on mitochondrial function for maintaining their unique metabolism. We have seen in WAT that the function of those organelles is compromised during aging. Two of the most promising interventions focused on reversing this problem in WAT in obesity are calorie restriction and treatment using PPARγ agonists. Interestingly, both may be related to BAT, as they regulate or enhance its functionality, respectively[218,219]. In BAT, some known mitochondrial functionality disruptors are the accumulation of mitochondrial DNA mutations and a reduction in biogenesis and oxidative phosphorylation[220]. These changes potentially result in dysfunctional brown stem cells, diminished regenerative potential of BAT depots and gathering dysfunctional brown adipocytes with aging.

3.3.4. Brown adipogenic progenitors' function

Age-related dysfunctional regeneration and reduction of classical brown and beige tissues could be due to a defective ability to proliferate and differentiate from inducible WAT or due to a loss of CD137/TMEM 26^{+} progenitors, the ones that show a greater ability to differentiate into beige cells[221].

One of the proposed participants in this loss of potential beige adipocytes is SIRT1, an important target in adipose tissue biology. This protein drives the browning of adipose tissue by promoting the interaction between PPARgamma and PRDM16, a potent inducer of beige adipose-specific genes[222]. SIRT1 has also been described to be an important repressor of senescent pathways in precursor cells. During aging there is a reduction in SIRT1 levels. This fact mediates the loss of stemness in beige and brown adipose tissues linages[223].

3.3.5. Remodeling in endocrine signaling and batokines relative levels

Changes in the somatotropic and gonadotropic axes may have an impact on BAT mass and/or activity. It has recently observed that sexual hormones are related to an increase in BAT activity and function[224]. Meanwhile, glucocorticoids are known to provoke negative effects in this tissue. For example, dexamethasone reduces the catecholamine-induced expression of UCP1[225]. Aging is accompanied by a decrement in the levels of gonadotropic hormones and a relative increase in glucocorticoid activity, which may participate in the reduction of BAT activity that comes with advancing age.

Moreover, thyroid hormones are positive regulators of thermogenesis in BAT and WAT. It has been seen in mice that the aging process is associated with a reduction in the production of bioactive T3 due to a loss of DIO2[224,226].

Additionally, recent data purpose ghrelin signaling as an actor in thermogenic regulation across aging[227]. This signaling system is composed by growth hormone secretagogue receptor (GHS-R), ghrelin and obestatin, which are both derived from the same preproghrelin gene. In brown adipose tissue, ghrelin represses the expression of UCP1 while obestatin increases it. Plasma ghrelin and GHS-R expression in BAT increase with advancing age. In contrast, plasma obestatin remains stable. Thus, the pathway is deviated towards thermogenic repression in aged individuals.

Another piece of data supports that fibroblast growth factor 21 (FGF21), a potent activator of thermogenesis and browning in WAT, which is produced by the liver and adipose tissues, may play a role in aging. It has been observed that sustained increases in FGF21 levels, attained by transgenic overexpression of FGF21, extend the lifespan of mice[228], suggesting that FGF21 is a pro-longevity hormone. Moreover, circulating FGF21 levels in humans increase with age from 5 to 80 years in healthy individuals independently of body composition[229]. In contrast, low levels of FGF21 are related to healthy aging in centenarians[230]. In addition, endurance exercise in elderly individuals reduces FGF21 levels[231]. To explore the role of FGF21 in relation to aging of adipose tissues has been one of the objectives in this thesis (see below).

As in WAT the inflammaging phenomenon, by which pro-inflammatory cytokines relative abundance increases in general with age also impacts BAT activity. Even though it has been observed that brown and beige adipose tissues are less prone to suffer inflammation by immune cells infiltration, the permanent and constant influence of inflammatory mediators and the infiltration of immune cells associated with aging may ultimately impact in BAT thermogenic activity through an impairment in insulin sensitivity and a reduction glucose uptake[232].

Finally, age may affect the production of batokines (brown adipose tissue adipokines) that are known to regulate precursor cell adipocyte commitment, differentiation, and factors that promote thermogenesis. Brown adipose tissue adipokines have been introduced in the section 2.5.2.6 of this introduction. They have also been reviewed extensively by Villarroya et al.[146-148].

In conclusion, BAT is postulated as a promising candidate organ to treat obesity, but possibly also to slow the process of aging. Some nutritional and pharmacological approaches have been explored in order to maintain BAT and beige mass and sensitivity during aging[233]. However, any therapeutical targeting of BAT activity and/or mass will first require a clear understanding of the mechanisms involved in potentiating BAT activity before human intervention.

4. Autophagy

Autophagy or “self-eating” is a catabolic process for eliminating macromolecules and damaged organelles by a highly regulated lysosomal pathway. Autophagy in the most general sense involves the formation of the phagophore membrane and maturation of a double membrane structure, the autophagosome. Autophagosomes engulf nucleic acids, proteins, damaged organelles and cytoplasmic structures. The fusion of the autophagosome with the lysosome hydrolyzes and degrades the autophagosome and cargo contained within[234]. Importantly, autophagy serves as an integral quality control mechanism by recycling cellular constituents for energy consumption and cellular rejuvenation under basal and stress conditions. Macroautophagy, herein referred to as autophagy, is among the most common and frequently studied forms of autophagy next to microautophagy and chaperone-mediated autophagy[235] (Figure 11).

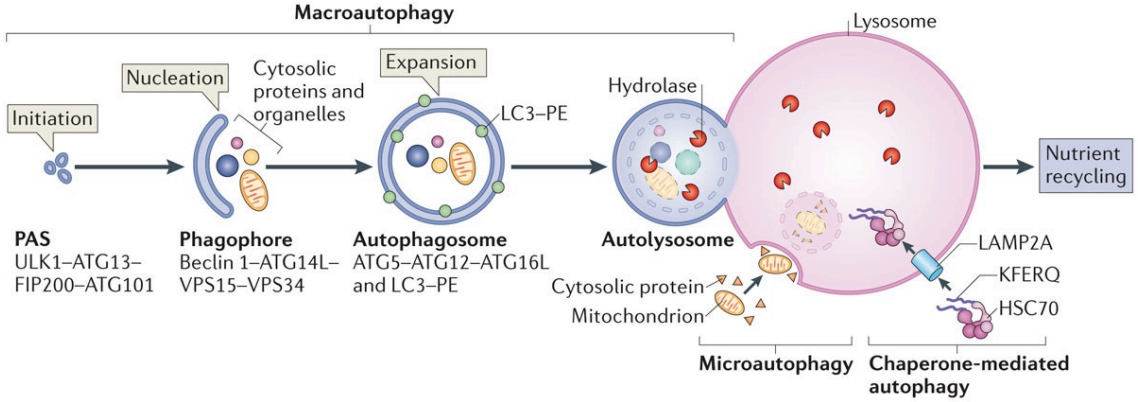

Figure 11. Scheme of the three different types autophagy: macroautophagy, microautophagy and chaperone-mediated autophagy. In macroautophagy, initiation begins with the formation of the phagophore assembly site (PAS). This is mediated by the UNC51-like kinase (ULK) complex, which consists of ULK1 (or ULK2), autophagy-related protein 13 (ATG13), FAK family kinase interacting protein of 200 kDa (FIP200) and ATG101. Further nucleation requires the class III PI3K complex, which is composed of the vacuolar protein sorting 34 (VPS34) PI3K, along with its regulatory subunits ATG14L, VPS15 and beclin 1. Phagophore membrane elongation and autophagosome completion requires two ubiquitin-like conjugation pathways. The first produces the ATG5–ATG12 conjugate, which forms a multimeric complex with ATG16L; ATG7 and ATG10 mediate this process. The second results in the conjugation of phosphatidylethanolamine (PE) to LC3 (the microtubule-associated protein 1 light chain 3) via ATG4. PE-conjugated LC3 (LC3–PE) is required for the expansion of autophagic membranes, their ability to recognize autophagic cargoes and the fusion of autophagosomes with lysosomes. The resulting autophagosome fuses with endocytic and lysosomal compartments, ultimately leading to formation of the autolysosome. In microautophagy, substrates are directly engulfed at the boundary of the lysosomal membrane. In chaperone-mediated autophagy, substrates with the pentapeptide motif KFERQ are selectively recognized by the heat shock cognate 70 kDa protein (HSC70) chaperone and translocated to lysosomes in a LAMP2A-dependent manner. In all three processes, the autophagic cargo is degraded via lysosomal hydrolases. Adapted from DOI:10.1038/nrm4024

Autophagy plays a housekeeping role in preserving cellular homeostasis and cell survival. However, autophagy is rapidly activated to face cellular stress; including nutrient deprivation, hypoxia, invasive pathogens or even protein aggregates[236]. The inability to effectively remove damaged organelles and proteins can trigger ER stress and programmed cell death. Similarly, massive induction of autophagy can also trigger cell death. Hence, too little or too much autophagy can be either adaptive and promote survival or maladaptive and promote cell death. There are strict regulatory mechanisms that allow the induction of the process when necessary and maintain basal levels when not.

Autophagy has been considered a generic degradation system. Nonetheless, several mechanisms have been recently described by which autophagosomes are formed specifically around certain structures, in what is called selective autophagy. There are different types of selective autophagy according to the degradation substrate such as mitophagy (mitochondria), pexophagy (peroxisomes), reticulophagy (endoplasmic reticulum), aggrephagy (protein aggregates), glycophagy (glycogen) or lipophagy (lipids)[237]. The different substrates of selective autophagy are recognized thanks to the interaction with proteins that tag them as degradation targets: the autophagic receptors.

4.1. Autophagic receptors

For a given element to be recognized for being selectively degraded it must, first, be labeled as a degradation target and then, interact with proteins that initiate the autophagosome formation. Ubiquitination plays a key role in selective autophagy signaling. Degradation targets are often ubiquitinated in order to be recognized by autophagic receptors. Most receptors contain ubiquitin-binding domains and LC3 interacting regions.

Several receptors capable of inducing autophagic degradation of protein aggregates have been described, such as sequestosome-1 (p62/SQSTM1), the neighbor of BRCA1 gene 1 (NBR1), optineurin, or histone deacetylase 6 (HDAC6). In addition to these protein aggregates, selective autophagy plays an important role in the degradation of damaged organelles or those that are no longer required by the cell. This is the case of mitochondria and mitochondrial degradation. The main receptors involved in mitophagy are: p62/SQSTM1, optineurin, the BCL2/adenovirus E1B 19 kDa protein-interacting protein 3 (BNIP3), the NIP3-like protein X (NIX), and the FUN14 domain-containing protein 1 (FUNDC1)[238].

4.2. Autophagy in adipose tissues

Both beige adipose tissue and BAT show marked plasticity in response to environmental stimuli, making them unique among mammalian tissues. It is becoming increasingly clear that autophagic processes are relevant as a remodeling mechanism. Autophagy can modulate the intracellular protein and organelle composition to contribute to BAT and beige adipose tissue plasticity.

The first evidence for the involvement of autophagy in adipocyte biology showed that this process is progressively induced during white adipocyte differentiation to facilitate its correct progression. This was first corroborated *in vitro* using mouse embryonic fibroblasts or 3T3-L1 cells deficient for ATG7 or ATG5[239,240]. These cells exhibited impaired lipid accumulation during differentiation and enhanced apoptosis compared with wild-type cells. Later studies in 3T3-L1 cells revealed that during adipogenesis, autophagy is involved in inducing PPARγ and C/EBPα, which are downstream of C/EBPβ. C/EBPβ activates transcription of the autophagy-related protein ATG4B, which is required for the autophagic degradation of transcriptional repressors of *Pparg* and *Cebpa*[241].

Specific deletion of Atg7 in Myf5-expressing cells (affecting brown/beige precursor cells but not white preadipocytes) alters BAT development, especially during the later stages of embryogenesis and after birth[242].

In adult mice, impaired autophagy in fat mass (e.g., via adipose-specific deletion of Atg7) was found to enhance the amount of beige adipocyte and β-oxidation rate in BAT, subsequently reducing the body fat content[243]. Hence, adipose tissue-specific deficiency of autophagy was found to promote a healthy metabolic profile in mice. In this sense, pro-browning drugs such as mineralocorticoid receptor antagonists (i.e., spironolactone) have been reported to be associated with impaired autophagic activity in adipocytes[244]. Overall, these findings indicate that the loss of autophagy may have a different qualitative impact on brown and beige adipogenesis depending on the developmental status of mice.

Autophagy therefore functions to regulate body lipid accumulation by controlling adipocyte differentiation and determining the balance between white and brown fat.

5. Mitophagy and Parkin

Mitochondria are double-membrane-bound subcellular compartments that function in fundamental processes such as ATP production, phospholipid biosynthesis/transport, calcium signaling, and iron homeostasis[245]. These organelles act as platforms for key events including apoptosis, innate immune response, and cell differentiation[246-248].

Since mitochondria generate reactive oxygen species (ROS) from the electron transport chain, they are constantly challenged with oxidative stress that ultimately may lead to their structural and functional failure[249]. Therefore, cells need sophisticated systems for maintaining mitochondrial fitness. Mitochondrial quality control relies on diverse pathways: ROS scavenging, DNA repair, and protein refolding/degradation[250]. Moreover, mitochondrial fusion and fission play key roles in mitochondrial quality control. While fusion promotes content mixing between healthy and partially dysfunctional mitochondria, fission separates damaged mitochondrial components from the mitochondrial pool[251].

The selective removal of superfluous or dysfunctional mitochondria, named mitophagy, is a crucial mechanism conserved from yeast to humans that regulates mitochondrial quality and quantity control. Mitophagy-mediated elimination of mitochondria plays an important role in many processes including early embryonic development, cell differentiation, inflammation, and apoptosis. Recent advances in analyzing mitophagy *in vivo* also reveal high rates of steady-state mitochondrial turnover in diverse cell types, highlighting the intracellular housekeeping role of mitophagy. Defects in mitophagy are associated with various pathological conditions such as neurodegeneration, heart failure, cancer, and aging, further underscoring its biological relevance[252]. Mitophagy is promoted via specific mitochondrial outer membrane receptors, or ubiquitin molecules conjugated to proteins on the mitochondrial surface leading to the formation of autophagosomes surrounding mitochondria. These mechanisms often act reciprocally as regulators of mitochondrial homeostasis. The PTEN-induced kinase 1 (PINK1)/Parkin-mediated mitophagy system, the main mediator of depolarization-induced and the first mitophagic pathway identified, is an example of these mechanisms.

5.1. Cellular Parkin function: mitophagy

Parkin and PINK1 are proteins involved in familial Parkinson's disease (PD), a neurodegenerative disorder with motor symptoms linked to the loss of dopaminergic neurons[253,254].

Parkin is an E3 ubiquitin ligase generally found in the cytosol. In 2008, a key study revealed that loss of the mitochondrial membrane potential triggers the recruitment of Parkin to mitochondria[255]. Parkin attaches poly Ub chains to outer mitochondrial membrane (OMM) proteins in a non-selective manner[256]. Thus, promoting the recruitment of autophagic receptors such as p62/SQSTM1 and NIX and the degradation of damaged mitochondria through autophagy. Parkin translocation to mitochondria is mediated by PINK1, a serine/threonine ubiquitin kinase that acts as a sensor of mitochondrial damage[257].

Under normal circumstances, when mitochondria are healthy, PINK1 levels are very low. This is because, once synthesized, PINK1 is continuously imported through the translocase of the outer membrane (TOM) complex and is processed by the presenilin-associated rhomboid-like protein (PARL). Then, PINK is released into the cytosol through the N-end rule pathway to undergo proteasomal degradation[258] (Figure 12).

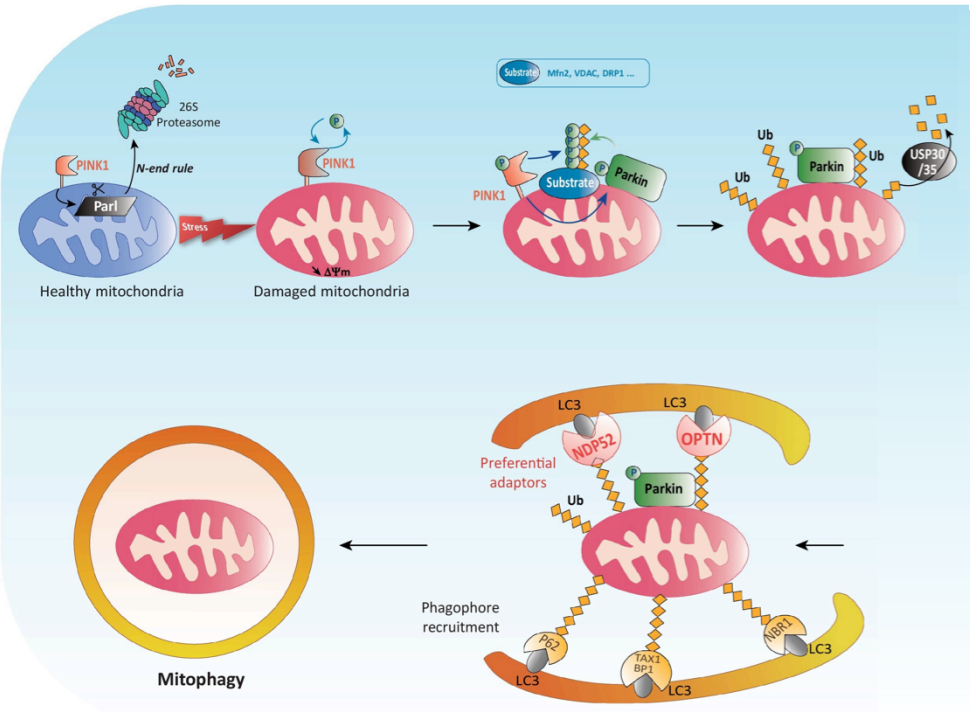

Figure 12. Scheme showing the different steps of Parkin/PINK1 dependent mitophagy. Abbreviations: transmembrane potential (ΔΨm); mitofusin 2 (Mfn2); voltage-dependent anion-selective channel protein (VDAC); dynamin-1-like protein (DRP1); ubiquitin specific peptidase 30/35 (USP30/35); optineurin (OPTN), calcium binding and coiled-coil domain 2 (NDP52); tax1 binding protein 1 (TAX1BP1) and next to BRCA1 gene 1 protein (NBR1)

Following a stress, damaged mitochondria lose their transmembrane potential. Thereby PINK1 is stabilized at the OMM as the translocation system is interrupted and PINK1 can no longer be cleaved by PARL. Thus, PINK1 can autophosphorylate itself, phosphorylate ubiquitin, poly-ubiquitin chains and Parkin in order to recruit and activate Parkin at the damaged mitochondria. Intriguingly, the poly-phosphorylated ubiquitin chain of OMM proteins functions as a receptor for activated Parkin, thereby massively increasing the amount of OMM proteins polyubiquitylated. Therefore, when this cycle is activated, OMM proteins are explosively ubiquitylated. Because PINK1 and Parkin amplify the ubiquitin signal via a positive-feedback loop, the low substrate specificity of Parkin mentioned above may facilitate this amplification process[259].

Ubiquitylation is a reversible process as ubiquitin specific proteases (USPs) can remove ubiquitin from ubiquitylated substrates. USP8, USP15, and USP30/35 regulate PINK1/Parkin-mediated mitophagy positively and negatively[252]. To counteract Parkin activity, USP15 and USP30/35 deubiquitylate mitochondrial substrates. However, PINK1-mediated ubiquitin phosphorylation impedes these enzymes activities. USP8 detaches ubiquitin from autoubiquitylated Parkin, acting as a positive regulator that promotes Parkin mitochondrial targeting and accelerates mitophagy. These enzymes add a new layer of complexity to the ubiquitin-mediated mitophagy. Nonetheless, their contribution remains poorly understood.

Most of the studies reporting PINK1/Parkin-mediated mitophagy of damaged mitochondria were obtained from experiments using cultured cells (e.g., Parkin-expressing HeLa cells). There is much less evidence for PINK1/Parkin-mediated mitophagy *in vivo*. In genetic studies using *Drosophila*, it is controversial whether PINK1/Parkin-catalyzed ubiquitylation induces mitophagy or not. One study reported that age-dependent rise in mitophagy activity is abrogated in PINK1- or Parkin-deficient flies[260], whereas another work showed that any substantial impact on basal mitophagy was observed in pink1 or parkin-KO flies[261]. In a similar way, mice lacking either parkin or PINK1 only show a mild phenotype due to minor changes in mitochondrial morphology and quality control[262,263], suggesting that the Parkin/PINK1 pathway is not accountable for all mitophagic processes induced. To reconcile these conflicting findings, we must introduce the notion that, in mammals, several pathways can trigger removal of damaged/superfluous mitochondria, including other ubiquitin ligases and receptor-mediated mitophagy. These could compensate for PINK1/Parkin-mediated mitophagy and function redundantly when the PINK1/Parkin function is inhibited. Since mammalian cells contain many mitochondria that are heterogeneous (e.g., membrane potential, respiratory activity, and oxidative damage), they may have needed to additionally evolve diverse ubiquitin-mediated pathways that establish selectivity toward dysfunctional mitochondria versus healthy mitochondria, acting as a quality management system.

5.2. Parkin and aging

Autophagy has been suggested to be a convergent mechanism whose activity prevents aging and declines with age[264]. Similarly, the activity of mitophagy in specific brain regions decreases during aging, as indicated by an *in vivo* study using transgenic mice expressing mt-Keima[265]. On the other hand, a study using *Drosophila* expressing mt-Keima reveals that mitophagic activity increases in aged flight muscles[260], raising the possibility that age-related changes in mitophagy vary in some species and/or tissues. mt-Keima is a fluorescence-based imaging tool for monitoring mitophagy *in vitro* and *in vivo*. The accumulation of excess mitochondrial DNA (mtDNA) mutations is one of the underlying factors in mammalian aging[266], implying that mitophagy may function to eliminate mitochondria with mutated mtDNA and prevent aging.

PINK1/Parkin-mediated mitophagy in aging have extensively been studied in short lived model organisms like *Drosophila* and *C. elegans*. In *Drosophila* Parkin-KO flies are viable but they present aberrant muscles and defects in locomotor functions[267]. These flies show significantly reduced longevity compared with wild-type flies. Ubiquitous overexpression of Parkin in flies leads to lifespan extension, likely via modulating intracellular proteostasis and mitochondrial dynamics[268]. Similarly, PINK1 mutant flies also display shortened lifespan and myopathology[269]. In *C. elegans*, disruption of mitophagy contributes to progressive accumulation of damaged mitochondria and decreased cellular functions during aging. The *daf-2* insulin/IGF-1 receptor mutant, a model of extended lifespan, show up-regulated mitophagy and knockdown of mitophagy regulators shortens their lifespan. These data suggest that mitophagy is critical for lifespan extension of the *daf-2*[270].

In mice, one of the most studied targets of Parkin-mediated mitophagy is the heart. The conditional cardiac-specific deletion of Parkin was not detrimental and failed to trigger any of the anticipated abnormalities associated with a mitochondrial clearance defect, Parkin role as a mediator of mitochondrial clearance in cardiac myocytes has been called into question. This could reflect that alternative cardiac mitochondrial quality control mechanisms have the capacity to compensate for the loss of Parkin as BNIP3 or NIX receptor-mediated mitophagy[271]. However, Parkin-mediated mitophagy has been identified to have a prominent role for the metabolic switch in myocardial metabolism between the fetal and adult heart (i.e., carbohydrates in fetal heart compared to fatty acid metabolism in the adult myocardium)[272]. In addition, evidence suggests that Parkin-mediated mitophagy acts primarily as a defensive mechanism in response to cardiac stress or mitochondrial injury[273].

As stated above, the accumulation of damaged mitochondria has been identified as one underlying cause of neuronal death in the pathogenesis of PD[274]. However, genetic mouse models of human PD, harboring mutations in PARK2 or PINK1 exhibit defects in mitophagy but fail to recapitulate or phenocopy the neurological defects typical of PD patients. Again, it has been purposed that redundant systems in mitophagy likely compensate for Parkin deficiency in mice. In addition, despite deficiencies in mitophagy arising from mutations in PINK1 or Parkin, development of PD in human involves abnormalities beyond defects in mitophagy. For example, it has been seen that aged Parkin knockout mice exhibit motor dysfunction and dopaminergic neuronal loss at their end-stage, when they surpass two years of life[275]. Similarly, mitophagy deficient mice models showed glial dysfunction and reduced neuroprotection during aging[276].

In this PhD thesis our goal has been to explore the role of Parkin and Parkin-mediated autophagy in the aging of brown and white adipose tissues.

5.3. Parkin and metabolism

Multiple Parkin functions have been described beyond the functions related to the degradation of mitochondria. For instance, it has been related to cell cycle control, mitochondrial biogenesis or energy metabolism[277,278]. Parkin ubiquitination promotes the degradation of a transcriptional inhibitor of PGC1α, the Parkin interacting substrate (PARIS), thereby inducing mitochondrial biogenesis[279]. In fact, *in vitro* studies had previously linked Parkin activity to mitochondrial biogenesis through interaction with mitochondrial transcription factor A (TFAM)[280].

5.3.1. Parkin and glucose metabolism

Parkin can regulate enzymes in glucose metabolism through its ubiquitin-ligase activity. Parkin can perform protective functions against the Warburg effect, thus acting as a tumor suppressor protein[281].

The Warburg effect is a switch to aerobic glycolysis. It is characteristic of many solid tumors and essential for tumor progression. Under aerobic conditions, cells normally transform pyruvate from glycolysis into acetyl-CoA thanks to the enzyme pyruvate dehydrogenase (PDH). Acetyl-CoA then follows the tricarboxylic acid (TCA) cycle to generate ATP via oxidative phosphorylation. In contrast, in conditions of low oxygen availability, pyruvate is preferentially transformed in lactate (lactic fermentation). The Warburg effect is a variant in glucose metabolism by which cells in aerobic conditions use glycolysis as the major route for obtaining ATP. Aerobic glycolysis produces ATP very inefficiently in comparison to oxidative phosphorylation. Tumor cells compensate that by increasing glucose uptake. The glucose captured is partly derived to obtain ATP from aerobic glycolysis, whereas most of it is used in anabolic pathways (synthesis of nucleotides and macromolecules) in order to support tumor growth.

Several studies have shown that Parkin ablation leads to increased glycolysis and lactate production, promoting increased glucose uptake and reducing oxygen consumption in some cell types[279,282]. These effects are in part due to a reduction in PDH enzyme expression and activity, so that the amount of acetyl-CoA supplied into the TCA cycle is altered.

Parkin can also regulate glycolysis by controlling pyruvate production. Parkin ubiquitinates the pyruvate kinase 1/2 (PKM1/2) enzyme. This enzyme catalyzes the transformation from phosphoenolpyruvate to pyruvate, the last step of glycolysis, being one of the limiting factors in the process. Ubiquitination of PKM1/2 reduces its activity, decreasing overall glycolytic flow[283]. In addition to regulating glucose metabolism at the cellular level, the lack of Parkin has been shown to affect systemic glucose levels as it appears to be important for proper insulin production by pancreatic cells in rodent models[284].

5.3.1. Parkin and lipid metabolism

Parkin has recently emerged as a new regulator of lipid metabolism due to its interaction with the CD36 lipid transporter. In a study, mainly focused on the liver, it was observed that Parkin could promote the stabilization of CD36 and increase its expression. This fact is particularly relevant in obesity[283]. Moreover, it has also been published that Parkin-deficient mice may have problems with intestinal lipid absorption[285].

Parkin has also been found to be involved in adipogenesis and this finding was first explored after reports of reduced weight gain in Parkin-KO mice as compared to WT controls across lifespan[263,282,]. Upon a high fat diet (HFD), Parkin-KO mice were resistant to weight gain, fat accumulation, and displayed glucose intolerance and insulin resistance[285].

5.3.2. Parkin in the adaptive activation and inactivation of BAT

Reduced body fat in Parkin-KO mice on a HFD was also associated with smaller lipid droplet size, lower circulating leptin levels, and overactivated brown adipose tissue (BAT)[287]. Thermogenesis in BAT causes a repression of autophagy genes, decreasing mitophagy in BAT[288]. Selective β_3-adrenergic receptor agonist treatment also leads to a reduction in Parkin levels[289]. Using a mitophagy reporter mouse, mt-Keima, Parkin-mediated mitophagy was found to modulate the beige-to-white fat transition after removal of a selective β_3-adrenergic receptor agonist, while Parkin-KO mice retained their BAT activated after removal of the stimulus[290]. The repression of Parkin after thermogenesis and the retention of BAT after thermogenesis in Parkin-KO mice verified these previous findings[287].

Objectives

The global objectives established for the current PhD thesis were to find out the impact of aging on adipose tissues and to establish the role of Parkin in this process. The specific objectives are detailed below:

1. To determine the evolution of cellular and molecular features of brown and white adipose tissues, and related systemic metabolic and endocrine parameters, at three stages of aging in mice, representative of adulthood, middle aging and advanced aging.

2. To characterize the alterations caused by genetic invalidation of Parkin in mice across these aging stages in systemic metabolism, cellular and molecular features of adipose tissues, and on the FGF21 system.

3. To analyze the alterations in gene expression and metabolic/endocrine parameters in adipose tissue from healthy elderly individuals, with special focus on the status of the FGF21 system.

Materials and Methods

Part 1. Experimental studies related to Parkin in animal models during aging

Mouse studies

Animals were housed at 22°C under a 12-h light cycle (lights on, 08.00 am to 08.00 pm) with 50% ± 5% relative humidity with free access to water and. Mice were fed a standard commercial rodent diet (2018 Teklad, Envigo) with an energetic density of 3.1 kcal/g and relative frequency of 24% protein, 58% carbohydrates and 18% lipids obtained per each kcal consumed. Male mice were studied at 5 months old (adult), 15 months old (middle age) and 23 months old (advanced age). After sacrifice, interscapular brown adipose tissue (iBAT), inguinal white adipose tissue (iWAT), epididymal adipose tissue (eWAT), liver, heart and tibia were dissected. Glucose tolerance tests (GTT) were performed in mice the morning after overnight fast by intraperitoneally administration of 2.5 mg glucose/g body weight. The insulin tolerance test (ITT) was performed in the evening after a short fast (2 h); mice were injected intraperitoneally with 0.75 IU/kg insulin (Actrapid, Novo Nordisk). Glucose levels were measured (see below) using blood samples collected from the tail vein.

Mice were injected subcutaneously into the interscapular region over the BAT depot with 1 mg/kg CL316243, and their surface temperature was recorded as indicated below.

The volume of consumed oxygen, the volume of produced carbon dioxide and the respiratory quotient were determined on an Oxylet system (Harvard Apparatus) before and after i.p. injection of 10 mg/kg CL316,243 and analyzed with Oxylet Metabolism 3.0 software (Harvard Apparatus).

All experiments were performed in accordance with European Community Council Directive 86/609/EEC, and the experiments and numbers of animals to be used were approved by the Institutional Animal Care and Use Committee of the University of Barcelona.

Details and development of Parkin-KO mice colony

Parkin-KO (B6.129S4-Park2tm1Shn/J) mice were obtained from Jackson Laboratories, and wild-type littermates were used as controls. The Jackson Laboratory donating investigator of this mutant strain of mice originally targeted a designed vector to replace most of exon 3 of the endogenous Parkin gene with the in-frame EGFP coding sequence followed by translation and transcription termination sequences and a PGK-Neo^R cassette. These mice model the most common mutation in human autosomal recessive juvenile Parkinsonism patients. Homozygous mice are viable and fertile, and exhibit grossly normal brain morphology. Reverse-transcription polymerase chain reaction shows that exon 2 splices to exon 4, skipping exon 3 entirely, resulting in a frame shift and a premature stop codon in exon 5. Although Parkin-EGFP truncated transcripts are present, it is unlikely that functional Parkin fragments can be produced from these truncated transcripts. Moreover, Western blot analysis using an antibody specific to C-terminal sequences indicates the absence of full-length gene product[291].

DNA purification and genotyping of Parkin-KO mice colony

Mice were genotyped using DNA purified from ear clippings subjected to fast hot-alkaline lysis. The mouse nucleotide primer sequences (5'-3') of wild-type sense (GCAGAATTACAGCAGTTACCTGG, corresponding to a sequence maintained in wild-type mice), wild-type antisense (CCTACACAGAACTGTGACCTGG) and mutant (ATGTTGCCGTCCTCCTTGAAGTCG, corresponding to a sequence of the PGK-Neo^R cassette inserted in the KO mice) were used to perform the separate polymerase chain reaction (PCR) amplification. All primers were synthesized (Sigma-Aldrich) and stocked in PCR-quality water to a final concentration of 1000 pmol/mL.

The general PCR amplification conditions were as follows: 1.25 U RedTaq DNA polymerase (Sigma-Aldrich), 1X buffer provided, 25 mmol/L $MgCL_2$, 17 mmol/L dNTPs (Invitrogen), 25 µmol of each primer, nuclease-free water enough to generate 25 µL total reaction volume and 1 µL DNA. The PCR thermocycle profile was: an initial single 3 min step at 94ºC, 35 cycles of three steps consisting of 30 sec denaturation, 1 min annealing and 1 min extension at 94ºC, 60ºC and 72ºC, respectively, and a final 4 min extension step at 72ºC. The products of PCR were resolved in 2% agarose gels prepared in 1X Tris-acetate-EDTA buffer and visualized using GelRed (Biosalab) as in Figure 13.

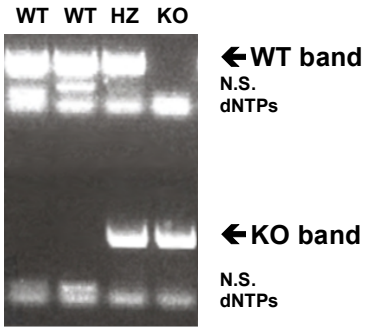

Figure 13. Representative genotyping PCR of wild-type, heterozygous and Parkin-KO mice using DNA obtained from ear clips. WT: wild-type; HZ: heterozygote; KO: Parkin knock-out; N.S.: Not specific; dNTPs: deoxynucleotide triphosphates

Analytical procedures in blood and plasma samples

Glucose and triglyceride levels were measured using Accutrend Technology (Roche Diagnostics). FGF21 and GDF15 levels were quantified with enzyme-linked immunosorbent assays (ELISA) (RD291108200R, BioVendor and MGD150, R&D Systems, respectively). Insulin, adipokines, and cytokines were quantified using a Multiplex system (MADKMAG-HK, Merck Millipore).

Thermography imaging

Surface temperatures were monitored every 2 minutes for 20 minutes using a T335 infrared digital thermography camera (FLIR Systems), which features a thermal sensitivity of 0.1°C and an image resolution of 640 × 480 pixels. Environmental parameters (relative humidity, room temperature, and reflected apparent temperature) were measured *in situ* and set in the camera as parametrical inputs for each experiment. Mice were shaved and allowed to recover for 2 days. Then, infrared pictures of non-anesthetized animals were taken from a distance of 30 cm. The images were analyzed using the FLIR QuickReport software (FLIR Systems), which allowed us to normalize temperature ranges and quantify temperature values arising from the isotherms. Maximal temperature values obtained from the interscapular area were compared between genotypes.

Optical and electron microscopy

For hematoxylin and eosin (H&E) staining, tissue samples were fixed overnight in 4% paraformaldehyde and paraffin-embedded and processed in the microtome. Tissue sections of 4 μm thickness were mounted onto glass slides, dewaxed, rehydrated, stained with H&E, then dehydrated again in a graded ethanol/xylene series and sealed with DPX and a coverslip, according to the standard procedures. Finally, samples were observed under an optical microscope.

For electron microscopic analysis, tissue samples were fixed in 2.5% glutaraldehyde and 2% paraformaldehyde in 0.1 M phosphate buffer (pH 7.4) and post-fixed in 1% osmium tetroxide and 0.8% FeCNK in phosphate buffer. After dehydration in a graded acetone series, tissue samples were embedded in Spurr resin. Ultrathin sections were stained with uranyl acetate and lead citrate and examined with a Jeol 1010 transmission electron microscope (Izasa Scientific). The sample management and preparation from post-fixation was performed with the support of professionals in the Electron Microscopy center in the Scientific and Technological Centers of the University of Barcelona (CCiTUB).

Mitochondrial DNA quantification

DNA was prepared from iBAT, iWAT and liver using a proteinase K plus phenol/chloroform-based method. Relative mtDNA was quantified using quantitative real-time polymerase chain reaction (qRT-PCR) and employing TaqMan (Applied Biosystems) probes for mt-*Cytb* (Supplemental Table 1). Data were referred to nuclear DNA abundance as estimated by quantitative PCR of the intronless *Cebpa* gene, as already reported[292].

Analysis of adipose tissue cellularity

The analysis of adipocytes size was performed in sections of inguinal adipose tissue. Digital images were captured using an Olympus DP70 digital camera (Olympus) attached to a brightfield light microscopy (Nikon Eclipse 90i Upright Microscope). The digital images were stored in an uncompressed file format (tiff) for further analysis. At least 4 fields of view were analyzed for each sample; n= 3 samples per genotype per timepoint. All the images were acquired under the same conditions at 200×magnification. The adipocytes' sizes were measured using the open-source image software program Fiji[293], a distribution of ImageJ, with the semi-automated plug-in Adiposoft[294], and were manually reviewed.

Respiratory chain activities

The activities of respiratory Complex I and Complex IV were determined in iBAT extracts using enzyme specific assay kits (ab109721, Abcam and ab109911, Abcam, respectively). iBAT samples for assays were prepared by homogenization with ice cold PBS. In these colorimetric assays, capture antibodies specific for Complex I or Complex IV were pre-coated in the microplate wells. Samples are added and Complex I enzyme activity is determined by following the oxidation of NADH to NAD^+ and the simultaneous reduction of a dye which leads to increased absorbance at OD=450 nm. Complex IV activity is determined by following the oxidation of reduced cytochrome c by the absorbance change at 550 nm.

RNA isolation and quantitative real-time PCR

RNA was extracted from adipose tissues and liver using a NucleoSpin RNA column kit (Macherey-Nagel) and from heart's left ventricles using Tripure (Roche). Reverse transcription of 0.5 µg of total RNA in a total reaction volume of 20 µL was performed using a high-capacity complementary DNA (cDNA) kit. Samples were systematically checked for no-amplification in the absence of reverse transcriptase. qRT-PCR was performed using the appropriate TaqMan probes (Supplemental Table 1); each 25 µL reaction mixture contained 1 µL cDNA, 12.5 µL TaqMan Universal PCR Master Mix (Thermo Fisher Scientific) and 250 nM probes. The cDNA level of each gene of interest was normalized to that of a housekeeping reference gene (*Ppia* mRNA) for adipose tissues and liver; (18S rRNA) was used as an endogenous reference gene for heart's gene expression analyses. The comparative CT ($2^{-\Delta Ct}$) method was applied for normalization, according to the manufacturer's instructions. Main results were checked using 18S rRNA or *Ppia* mRNA as a second independent housekeeping gene. A transcript was considered not detectable for CT ≥40.

Western blotting

Tissue extracts were prepared by homogenization in a buffer consisting of 20 mM Tris-HCl (pH 7.4), 1 mM EDTA, 1 mM EGTA, 1% Triton X-100, a protease inhibitor cocktail (Roche Diagnostics), 2 mM sodium orthovanadate, and 10 mM β-glycerophosphate. The total protein content was measured using a Pierce™ BCA Protein Assay Kit (Fisher Scientific). Equal amounts of protein were separated by sodium dodecylsulfate-polyacrylamide gel electrophoresis (SDS-PAGE) on 12% or 15% gradient gels and electrotransferred onto Immobilon-P PVDF (polyvinylidene difluoride) membranes (GE Healthcare). The membranes were incubated with primary antibodies specific for Parkin (2132, Cell Signaling Technology), UCP1 (ab10983, Abcam), total OXPHOS rodent WB Antibody Cocktail (ab110413, Abcam), VDAC (529536, Merck (Calbiochem)), β-klotho (sc-74343, Santa Cruz) and tyrosine hydroxylase (ab152, Merck Millipore), and then with horseradish peroxidase (HRP)-conjugated anti-mouse IgG (170-6516, Bio-Rad) or anti-rabbit IgG (sc-2004, Santa Cruz), as appropriate. 1:1000 and 1:8000 dilutions were systematically employed for primary and secondary antibodies incubations, respectively. Signals were detected using a chemiluminescence-HRP substrate (WBKLS0100, Merk). Membranes were stained with Ponceau to normalize the amount of protein loaded Densitometry analyses of digitalized images were performed using the Fiji software (ImageJ). Images were processed using Adobe Photoshop CS6 (Adobe Systems); brightness and contrast adjustments were applied uniformly across the entire image.

Statistical analysis

Statistical significance was assessed using the two-tailed unpaired Student's t-test, one-way ANOVA or two-way ANOVA followed by Tukey's *post hoc* test, all of which were applied using GraphPad statistical software (GraphPad Software). Analysis of discrepancies among standard deviation in experimental groups was assessed with the F-test. Welch's correction was applied whenever unequal variances were detected. Exact numbers of replicates are shown at each figure legend. Outliers were detected and removed prior to significance analyses using Grubbs' test. Statistical significance was set with an α-value of $P<0.05$, and the underlying assumptions for validity were assessed for all tests. Data are expressed as means ± standard error of the mean (s.e.m.).

Part 2. Experimental studies related to FGF21 and adipose tissue in aging

Cohort study and demographic data

The study was approved by the ethics committee of Hospital de la Santa Creu i Sant Pau, Barcelona. A total of 28 healthy individuals over 70 years old and 35 healthy controls were enrolled in this cross-sectional study. To consider an old patient healthy, no evidence of any chronic disease had to be present, including inflammatory diseases, cardiovascular disease, hepatitis, liver insufficiency, fever of undetermined origin, diabetes mellitus, and cancer. Only arterial hypertension and antihypertensive therapy were allowed. Exclusion criteria also included BMI > 30 kg/m^2, anticoagulant treatment, oral antidiabetic therapy, and hormonal treatment. All patients provided informed written consent. Demographics, body composition and metabolic markers are shown in Table 3 (see Results Part 2).

BMI was calculated, and waist circumference was measured to the nearest millimeter using anatomical landmarks, as defined by the Third National Health and Nutrition Evaluation Survey. Whole-body, dual-energy X-ray absorptiometry (DEXA) scans (HologicQDR-4500A; Hologic, Inc., Waltham, MA, USA) were conducted by a single operator and used to determine body fat content. Plasma and serum were obtained from blood drawn from seated patients after a 12-hour overnight fast and at least 15 minutes after the placement of a peripheral intravenous catheter. All lipid measurements were performed using a Hitachi 911 system (Roche Diagnostic Systems, Basel, Switzerland). Insulin resistance was estimated by the homeostasis model assessment method (HOMA-IR). Laboratory procedures have been described elsewhere[295].

Systemic parameter detection

Serum FGF21 and FGF19 levels were determined in duplicate for each sample using ELISA specific for human FGF21 and FGF19 (Biovendor, Czech Republic). Serum FGF21 and FGF19 data distribution was skewed and was thus log-transformed before analysis.

Circulating TNFα and MCP-1 levels in serum were measured using an antibody-linked, fluorescently labeled microsphere bead-based multiplex analysis system (Linco Research/Millipore, Billerica, MA, USA) and quantified using Luminex100ISv2 equipment.

Biopsy samples and protein measurement

Biopsy samples of subcutaneous fat from abdominal area from lean healthy controls (n=10) and healthy elderly individuals (n=13) were collected from patients through a small surgical biopsy performed by an 8 mm punch under local anesthesia with mepivacaine. Tissue samples were immediately frozen and stored at -80°C.

RNA preparation and quantification of transcripts by qRT-PCR

RNA isolation from adipose tissue samples and qRT-PCR procedures were as in Materials and Methods, Part 1. The primer pair probes specific for humans *β-Klotho* (Hs00545621_m1), *ATG4A* (Hs00364702_m1), *ATG4D* (Hs00262792_m1), *BNIP3* (Hs00969291_m1) *FGFR1* (Hs00222484_m1), *GARBAP* (Hs00740588_mH), *MCP-1* (Hs00234140_m1) *Parkin* (Hs01038325_m1), *TNFα* (Hs00174128_m1) and 18S rRNA (Hs99999901) were used. Controls with no RNA, primers, or RT were included in each set of experiments. Each sample was run in duplicate, and the mean value of the duplicate was used to calculate the mRNA levels for the genes of interest. Expression levels of gene transcripts were considered negligible when, under the standard RT-PCR conditions, cycle threshold was > 40. Values were normalized to that of the reference control (18S ribosomal RNA) using the comparative $2^{-\Delta CT}$ method, following the manufacturer's instructions. Parallel calculations performed using the reference gene *PPIA* (Hs99999904) yielded essentially the same results.

Detection of specific proteins

Adipose tissue samples were homogenized and processed for Western blotting as in Materials and Methods, Part 1. After electrotransference onto Immobilon-P PVDF membranes (GE Healthcare), proteins were probed using antibody directed against β-Klotho (ab106794, Abcam), Phospho-ERK1/2 and total ERK1/2 (9101 and 9102, Cell Signaling Technology, respectively). Goat anti-rabbit HRP-conjugated antibody (sc-2004, Santa Cruz) and ECL reagents (WBKLS0100, Merk) were used to detect the immunoreactive signals. Membranes were stained with Coomassie blue (Sigma-Aldrich) to normalize the amount of protein loaded. Multi-Gauge software (Fujifilm) was used for densitometric analyses. Four individual samples for each group were analyzed.

Study of adipose tissue explants

Adult young (5-month-old) and aged (15-month-old) C57BL/6 mice (Harlan Laboratories) were sacrificed. Blood was obtained and subcutaneous (inguinal) adipose tissue explants were obtained and incubated in Dulbecco's modified Eagle Medium, 1.5 g/L glucose for 15 or 30 min in the presence (or absence) of 30 nM FGF21. The remaining tissue was frozen for further analysis. The following gene transcripts were measured in frozen tissues and explants, using qRT-PCR as for human samples (see above), but using the mouse-specific TaqMan probes: *Fgfr1* (Mm00438930_m1), *β-klotho* (Mm00473122_m1), *Egr1* (Mm00656724_m1) and *c-Fos* (Mm00487425_m1). P-ERK and ERK levels were determined as above, using mouse/human cross-reactive antibodies (9101 and 9102, Cell Signaling Technology, respectively).

Statistical analysis

Data was expressed as means ± s.e.m, frequencies or percentages relative to healthy controls (defined as 100%). The normality of parameter distributions was determined using a Kolmogorov-Smirnov analysis and data were normalized by log-transformation when needed. Two-tailed unpaired Student's t-test was used for comparisons of parametric data. Correlation analysis was used to determine the linear relationships of anthropometric, metabolic, and other variables with quantitative serum FGF21. Statistical analyses were performed using the Statistical Package for Social Sciences version 17.0 (SPSS) and SAS version 9.1.3 software (SAS Institute Inc.). P-values < 0.05 were considered significant.

Results

Part 1. Experimental studies related to Parkin in animal models during aging

1. Parkin expression is up-regulated in brown and white adipose tissue during aging

Parkin mRNA expression levels (*Park2* gene) were significantly increased in BAT and iWAT from 15 months old mice relative to young, 5 months old, mice. When 23 months old, Parkin mRNA levels declined back to the levels found in 5-month-old mice in both adipose depots (Figure 14A). The relative abundance of Parkin protein levels in BAT and iWAT across aging changed in the same way as for transcript levels: a significant increase in Parkin protein abundance occurred in BAT and iWAT from 15-month-old mice and this was followed by a decline at 23 months of age, in which Parkin protein levels became intermediate between levels in 5- and 15-month-old mice (Figure 14B,C).

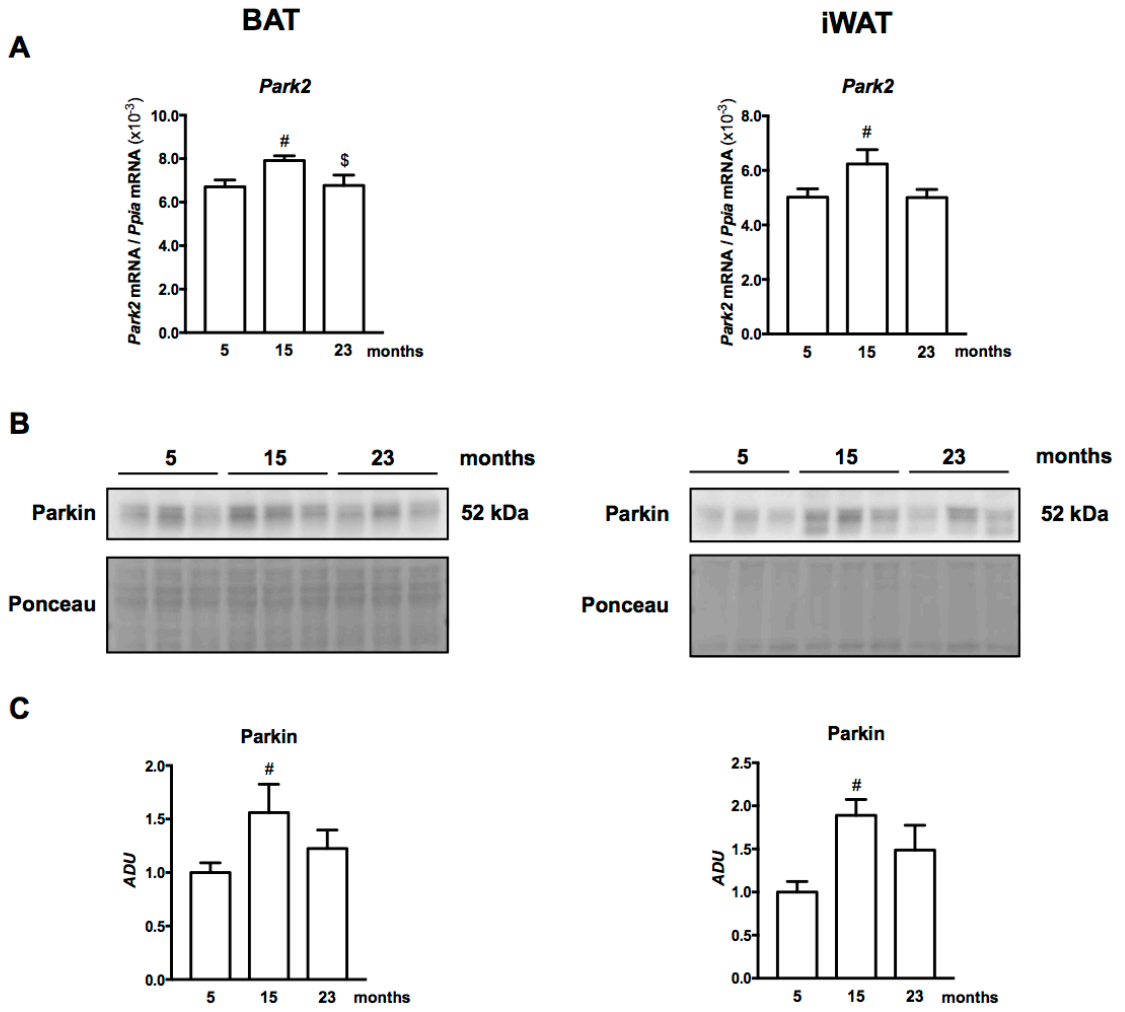

Figure 11. Parkin expression in adipose tissues from WT mice during aging. (A) Relative transcript levels of Parkin (Park2) gene in BAT and iWAT from WT mice at 5, 15 and 23 months old (n=8). **(B)** Immunodetection and **(C)** quantification of Parkin protein in brown (BAT) and inguinal white (iWAT) adipose tissues from WT mice at 5, 15 and 23 months old (n=3). The bars represent means ± s.e.m. Two-tailed unpaired Student's t-test (#p<0.05, 15 months vs. 5 months; $p<0.05, 15 months vs. 23 months).

2. Altered systemic metabolic parameters and adiposity during aging in Parkin-KO mice

The effect of the Parkin gene invalidation across aging was determined. Adult Parkin-KO mice (5 months old) did not show significant differences in body weight, food intake and adiposity relative to wild-type controls (Table 2). Similarly, glycemia, insulinemia and triglyceridemia (Figure 15) and glucose tolerance (Table 2) were also unaltered.

	5 months		15 months		23 months		ANOVA	
	WT	KO	WT	KO	WT	KO	Age	Genotype
Body weight (g)	30,3± 0,7	27,4± 0,6	42,8 ± 1,0#	**34,7 ± 0,8*#**	36,6 ± 0,9#$	**32,8 ± 0,8*#**	#↑	*↓
Food intake (kcal/day)	10,7 ± 0,2	9,78 ± 0,2	10,2 ± 0,3	**8,35 ± 0,3*#**	10,4 ± 0,3	**8,62 ± 0,2*#**	#	*↓
iBAT (mg)	84,7± 4,9	59,2± 2,0	154 ± 14#	**100 ± 9,4*#**	80,6 ± 7,2$	75,6± 5,9	#↑	*↓
BAT protein (%)	7,81 ± 0,3	**11,6 ± 0,7***	7,76 ± 0,8	8,74 ± 0,3#	8,27 ± 0,6	7,91± 0,5#	#	*
BAT protein/iBAT (mg)	7,81 ± 0,2	5,89 ± 0,4	14,4 ± 3,7#	**7,36 ± 0,5***	7,43 ± 0,9$	6,73 ± 0,6	#↑	*↓
iWAT (mg)	209± 29	193± 32	1162 ± 108#	**686 ± 86*#**	396 ± 68$	381 ± 70$	#↑	*↓
iWAT protein (%)	2,13 ± 0,4	2,05 ± 0,3	1,85 ± 0,7	1,69 ± 0,2	1,67 ± 0,3	2,02 ± 0,2	-	-
iWAT protein/iWAT (mg)	5,64 ± 0,3	5,71 ± 0,7	20,3 ± 4,7#	**8,58 ± 0,3***	5,44 ± 1,6$	5,96 ± 0,5	#	*
Liver (mg)	1328± 30	1116± 49	1819± 96#	**1336± 107***	1636± 65	1449± 44	#↑	*↓
Tibia length (mm)	17,8± 0,2	17,8± 0,3	18,4± 0,1#	18,5± 0,1#	18,6± 0,1#	18,5± 0,1#	#↑	-
iBAT/TL (mg/mm)	4,72 ± 0,3	3,33 ± 0,1	8,41± 0,8#	**5,42± 0,5*#**	4,33± 0,4$	4,08 ± 0,3	#↑	*↓
iWAT/TL (mg/mm)	15,9 ± 1,2	13,2 ± 1,6	63,2± 5,8#	**37,1± 4,6*#**	21,2± 3,6$	20,6± 3,8$	#↑	*↓
eWAT/TL (mg/mm)	31,1 ± 3,4	27,8 ± 2,2	86,9± 3,9#	69,6± 5,7#	56,1 ± 7,5#$	42,7± 4,8$	#↑	*↓
Liver/TL (mg/mm)	74,7 ± 1,4	62,7 ± 2,1	99,1 ± 5,3#	**72,4 ± 5,8***	87,8 ± 3,4	78,3 ± 2,4	#↑	*↓
GTT (AUCx10^3)	21,2± 0,7	26,4± 0,7	57,9± 7,2#	67,3± 4,4#	47,6 ± 11#	62,7 ± 9,3#	#↑	-
ITT (AUCx10^3)	5,78± 0,1	5,87 ± 0,7	9,70 ± 0,4#	**7,34 ± 0,3***	5,03 ± 0,4$	5,15 ± 0,4$	#	*↓

Table 2. Metabolic effects of Parkin gene invalidation throughout aging. Morphometric parameters, tissue weight and circulating levels of metabolites in WT and Parkin-KO mice with advancing age (n=8). Data are means ±s.e.m. Two-way ANOVA with Tukey's *post hoc* test. Statistical significances between genotypes are highlighted in bold. When the sense of changes (age or genotype) is concordant among the different groups, up-(↑) or down-(↓) regulation is indicated (*p<0.05, WT vs. Parkin-KO; #p<0.05, 15 months or 23 months vs. 5 months; $p<0.05, 15 months vs. 23 months). Food intake was recorded for 15 days. iBAT: interscapular brown adipose tissue; iWAT: inguinal white adipose tissue; eWAT: epididymal white adipose tissue; TL: tibia length; GTT: glucose tolerance test; AUC: area under the curve; ITT: insulin tolerance test.

In contrast, in aged mice (15 months old), the lack of Parkin resulted in profound alterations in adiposity and systemic metabolic parameters. The increased adiposity associated with aging found in 15 months wild-type mice compared with 5 months old wild-type mice, evidenced by massive increase in the size of all adipose depots (Table 2) did not occur in Parkin-KO mice. Thus, 15-month-old Parkin-KO mice showed reduced body weight associated with reduced weight of adipose depots and liver with no signs of altered growth (unchanged tibia length) (Table 2).

The induction of iBAT and iWAT mass in 15-month-old Parkin-KO mice relative to wild-type involved the structural, potentially active portion of the tissue, as it also occurred for total protein iBAT and iWAT amounts (Table 2). In 23-month-old mice the iBAT and iWAT mass was decreased to levels similar to those found in 5-month-old mice.

Regarding food intake, it was unaltered in association with aging in wild-type mice. However, food intake was significantly reduced in 15- and 23-month-old Parkin-KO mice compared with 5 months old Parkin-KO mice. Aged Parkin-KO mice ate significantly less than their wild-type counterparts (Table 2). Nonetheless, this difference in food consumption may not attain to explain the huge variations in body weight among 15 months old Parkin-KO and wild-type mice. In this context, metabolic energy efficiency would shed some light. Considering that the increase in body weight in wild-type mice from 5 to 15 moths is 12,5 g in 10 months (i.e, 300 days), we would obtain a body weight increase rate of 0,04 g/day. The ratio between this and food intake results in the estimated metabolic energy efficiency, in this case 4 mg of weight gain per kcal consumed. The same calculations for the same period in Parkin-KO mice result in a metabolic energy efficiency of 2,5 mg/kcal. These differences in metabolic energy efficiency report that other metabolic inputs, apart from food consumption and possibly related to altered energy expenditure, may contribute to the differences found in body weight and adiposity between aged wild-type and Parkin-KO mice.

Wild-type mice at 15 months of age had higher blood glucose and plasma insulin (Figure 15) as well as reduced glucose tolerance and insulin responsiveness (Table 2) relative to the younger 5-month-old wild-type mice, in accordance with previous reports indicating a deterioration of glucose/insulin homeostasis in aged mice[296-298]. Glycemia and insulinemia were significantly reduced in 15-month-old Parkin-KO mice relative to wild-type mice at the same age (Figure 15). These changes were no associated with significantly altered glucose tolerance whereas insulin sensitivity according to the insulin tolerance test, was somewhat improved in 15-month-old Parkin-KO mice (Table 2).

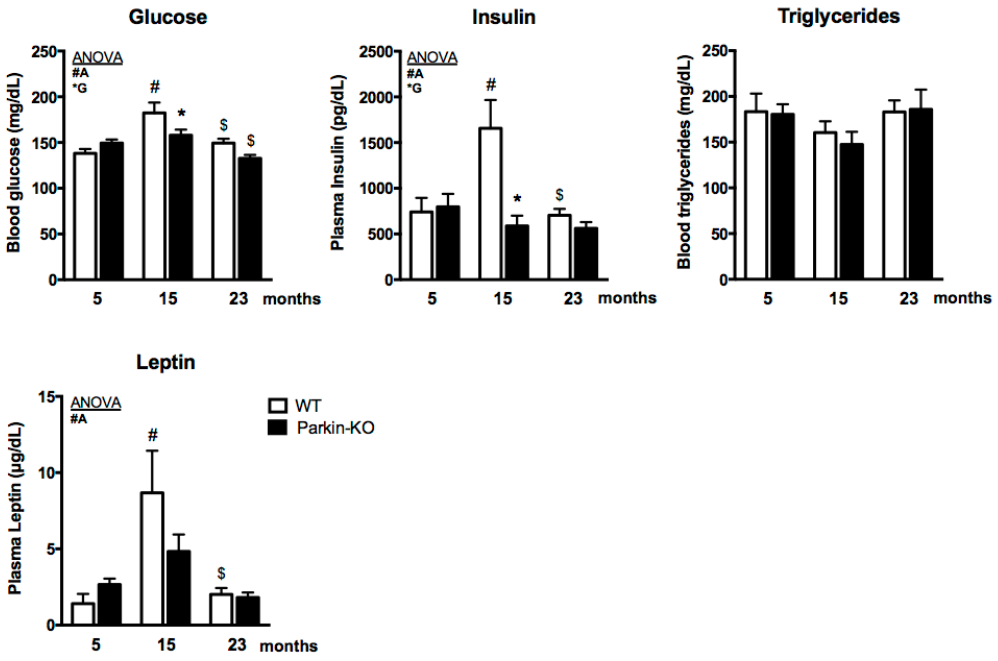

Figure 15. Circulating parameters in WT and Parkin-KO mice during aging (n=6 WT, n=7 Parkin-KO). The bars represent means ± s.e.m. Two-way ANOVA with Tukey's *post hoc* test (*G: genotype factor p<0.05; *p<0.05, WT vs. Parkin-KO; #A: age factor p<0.05; #p<0.05, 15 months vs. 5 months; $p<0.05, 15 months vs. 23 months).

The assessment of hormonal factors related to adiposity and energy balance revealed that 15-month-old Parkin-KO mice did not show the age-associated increase in leptin levels found in wild-type mice at that age, which was indeed consistent with the reduced acquisition of adiposity mentioned above. In 23-month-old wild-type mice, leptin levels were lowered relative to 15-month-old mice and attained similar levels to 5-month-old mice (Figure 15), consistently with the regression of white adipose tissue amounts found in mice at this advanced age (Table 2). Lack of Parkin did not affect leptin levels in 23-month-old mice.

3. Changes in BAT morphology and function in Parkin-KO mice across aging

In light of the changes found in iBAT for Parkin-KO mice relative to wild-type littermates (especially in 15-month-old aged mice) regarding tissue mass, we explored further iBAT. Figure 16A show representative picture of iBAT appearance across aging in wild-type mice and Parkin-KO mice at the three ages studied. Reduced mass of iBAT was apparent in Parkin-KO iBAT depots. No signs of loss of "brown color" intensity were found in association with aging, indicating that changes in size were not associated to "whitening" (fat accumulation) of the BAT depot. Besides protein portion followed the same pattern of changes across aging (Table 2). Figure 16B shows optic microscopy pictures evidencing no major changes in cellular fat droplet accumulation between Parkin-KO and wild-type mice at the distinct age stages analyzed, including 15-month-old mice, which showed the maximal difference in iBAT size.

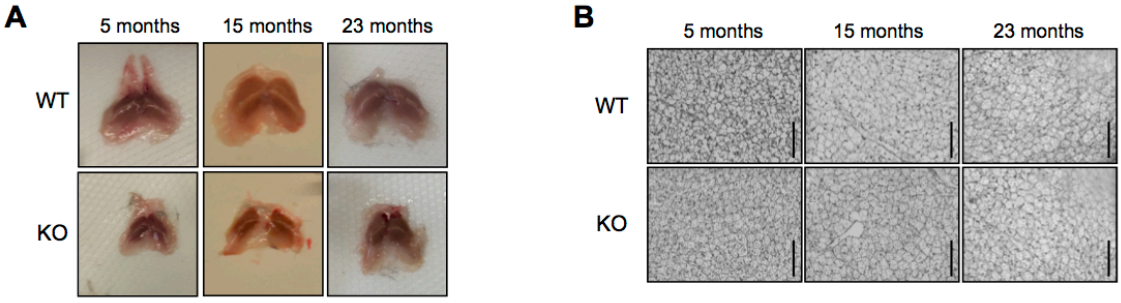

Figure 12. Morphology of interscapular BAT from WT and Parkin-KO mice during aging. (A) Representative images of the brown fat depots. **(B)** Representative optical microscopy images of H&E-stained BAT (200X) from WT and Parkin-KO mice. Scale bars, 100μm.

We analyzed functional parameters related to energetic metabolism and BAT function in 15 months old Parkin-KO mice versus wild-type mice, the time when morphological changes in iBAT between wild-type and Parkin-KO mice were more prominent.

In basal conditions, oxygen consumption trended to decrease in association with increasing age in wild-type mice. 15-month-old Parkin-KO mice did not show that trend and basal oxygen consumption was slightly increased in comparison to wild-type mice at 15 months of age. In fact, energy expenditure, calculated indirectly from oxygen consumption data, was significantly higher in Parkin-KO mice at 15 months old when compared with wild-type controls at the same age (Figure 17A). The basal respiratory quotient was not significantly affected by aging or the animals' genotype in our experiment. This parameter indicated that macronutrients were being metabolized in a balanced way, but slightly deviated towards carbohydrates metabolism (Figure 17A).

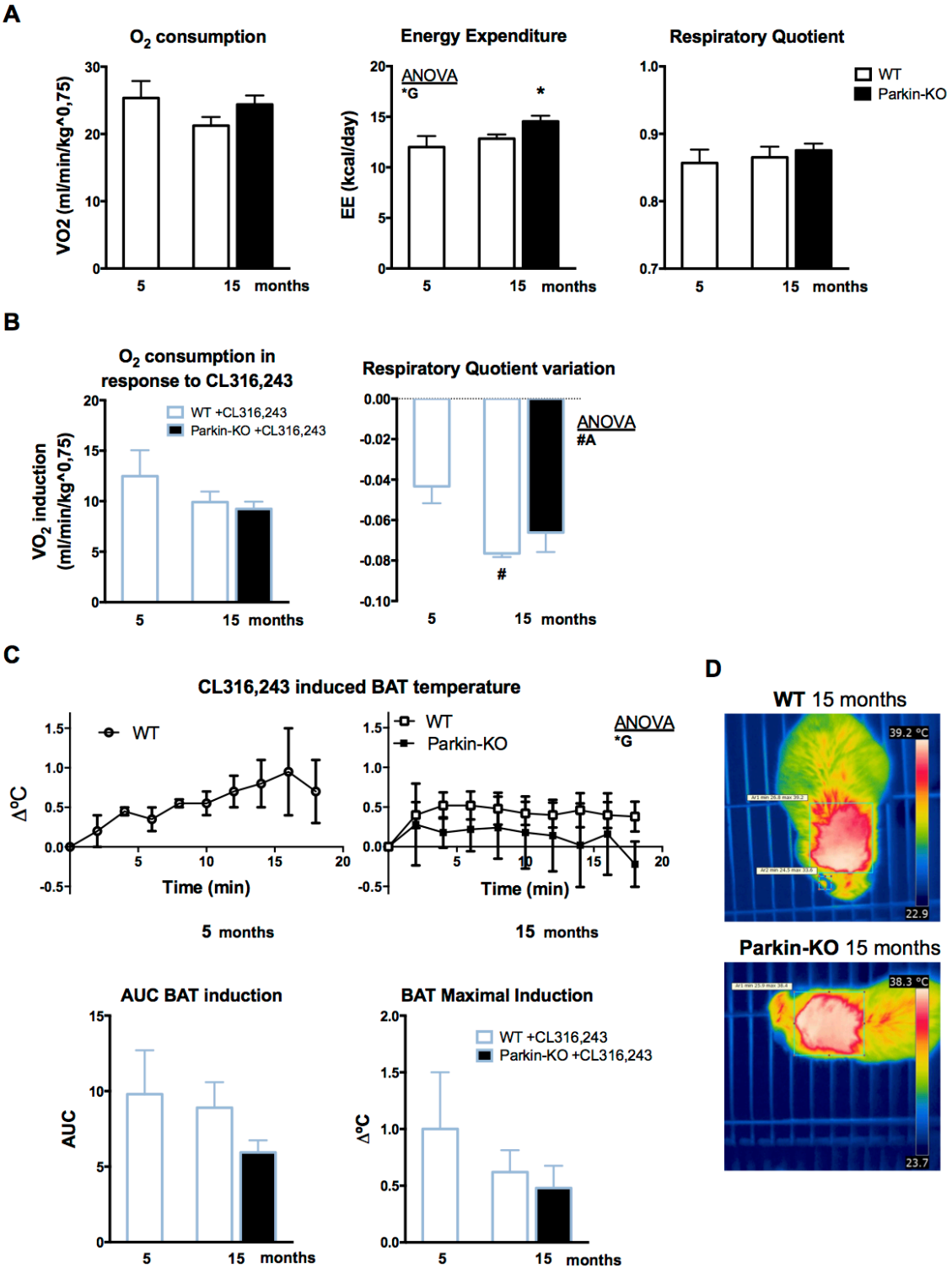

Figure 13. Functional parameters related to energetic metabolism and BAT activity in WT and Parkin-KO mice in aged mice. (A) Oxygen consumption (left), energy expenditure (center) and respiratory quotient variation (right). EE: Energy expenditure. **(B)** Oxygen consumption induction (left) and respiratory quotient variation (right) in response to β_3-adrenergic agonist CL316,243 injection in 15-month-old WT and Parkin-KO mice and 5-month-old WT reference values. **(C)** Temperature induction at the interscapular BAT depot in response to β_3-adrenergic agonist CL316,243 injection in 15-month-old WT and Parkin-KO mice and 5-month-old WT reference values. The area under de curve (AUC) and the maximal temperature induction are represented below (n=5). The bars represent means ± s.e.m. One-way ANOVA with Tukey's *post hoc* test (*G: genotype factor $p<0.05$; *$p<0.05$, WT vs. Parkin-KO; #A: age factor $p<0.05$; #$p<0.05$, 15 months vs. 5 months). **(D)** Representative thermographic images of WT and Parkin-KO 15-month-old mice 4 min after subcutaneous injection of CL316,243 in the area of iBAT.

Regarding BAT activity-related parameters, oxygen consumption in response to the β_3-adrenergic stimulation (CL316,243), a surrogate indicator of the capacity of brown/beige adipose tissue associated non-shivering thermogenesis[299] trended to be reduced due to aging (higher rates in 5-month-old wild-type mice relative to 15-month-old mice). However, it was not significantly different in 15 months old Parkin-KO mice relative to age-matched wild-type mice (Figure 17B). CL injection caused a reduction in respiratory quotient, consistent with the preferential usage of lipids for oxidation in response to β_3-adrenergic activation (Figure 17B); such effect was enhanced in aged mice (15-month-old relative to 5-month-old) and such age-associated effect took place in a more moderate manner in 15-month-old Parkin-KO mice relative to 15-month-old wild-type mice.

As a second approach, we determined the local increase in skin temperature at the interscapular region of mice, a surrogate indicator of thermogenic activity of iBAT[160,300], in response to CL injection. Figure 17D shows representative pictures of infrared thermography images used in these assays. Figure 17C shows the profile of local temperature changes throughout the 20 min after CL injection and the maximum temperature peak values attained. Whereas peak values of temperature induction were lower in 15-month-old mice relative to 5-month-old mice, the AUC and overall profile of values across the time-course of temperature induction in response to CL were not affected by aging. However, the profile of temperature induction in response to CL was significantly reduced in 15-month-old Parkin-KO mice relative to age-matched wild type mice.

4. Effects of aging and Parkin gene ablation on gene expression in iBAT

Next, we determined the expression of genes encoding distinct processes relevant to iBAT function.

The expression of genes encoding specific components of the thermogenic program (*Ucp1*, *Dio2*, *Pgc1α*) was progressively down-regulated in iBAT in association with aging as remarked by the ANOVA analysis. Parkin ablation resulted in a trend to more intense lowering at some aging states but not in adult, 5-month-old mice (Figure 18).

The expression of genes encoding components of lipid metabolism was distinctly affected by aging with especially marked changes in 23-month-old mice. According to ANOVA analysis, a significant down-regulation of expression of *Mcad* (medium chain acyl-CoA dehydrogenase, key enzyme of fatty acid oxidation) associated with aging takes place. In contrast, the expression of *Acaca* (Acetyl CoA carboxylase-alpha) and *Scd1* (Stearoyl-CoA Desaturase), involved in fatty acid synthesis, are found to be significantly up-regulated in association with aging, which is basically due to an intense induction in 23-month-old mice. In Parkin-KO mice, differences in gene expression were found only at 23 months of age: up-regulation of *Scd1* mRNA expression and down-regulation of *Acaca*. No changes due to aging or Parkin gene invalidation were found for other lipid synthesis (*Fas*, fatty acid synthase; *Sreb*, sterol regulatory element-binding protein-1) and general adipogenesis (*Pparγ*) related genes (Figure 18).

Next, we determined the mRNA levels of genes whose expression is indicative of distinct extents of infiltration of immune cells polarized to synthetize type I (pro-inflammatory) cytokines or type II (remodeling, non-inflammatory) cytokines, which are known to affect BAT thermogenic activation. Among genes encoding type I cytokines, no major changes were found due to aging. For instance, a trend to increased expression of tumor necrosis factor-alpha (*Tnfa*) expression in iBAT from 23-month-old mice, with no effects due to Parkin gene ablation (Figure 18). For Type II cytokine pathway, an irregular pattern of regulation of gene expression in iBAT associated with aging was found. The genetic expression of *Mrc1* (macrophage mannose receptor 1) and *Clec10a* (C-type lectin domain family 10 member A), marker genes of type II macrophages and other non-inflammatory cells, was progressively down-regulated in iBAT in association with aging as remarked by the ANOVA analysis. This reduction was especially marked for *Clec10a*, whose expression resulted practically negligible in iBAT from 23-month-old mice relative to 5-month-old mice. None of these changes were affected differentially in Parkin-KO mice. *Arg1* (arginase-1) gene expression, another type II marker gene, trended to be higher in 15-month-old mice relative to 5-month-old mice. In 23-month-old mice its expression was reduced, in a more pronounced way in wild-type mice (Figure 18).

We also analyzed the expression of genes indicative of oxidative (*Sod2*, superoxide dismutase 2; *Cat*, catalase), endoplasmic reticulum (ER) (*Hspa5*, heat shock 70 kDa protein 5) stress, or both (*Ddit3*, DNA damage-inducible transcript 3). Most of these genes trended to be less expressed in aging iBAT with no significant differences in Parkin-KO mice at any age studied. Except for *Ddit3* expression, that was increased in 23-month-old Parkin-KO mice (Figure 18).

Finally, considering the known role of Parkin in the mitophagic pathway, expression of genes encoding components of autophagy machinery for which evidence of transcriptional regulation has been shown previously[286] was determined. No relevant changes either in association with overall aging or Parkin-KO genotype was found, apart from a trend to down-regulation of *Lc3b* and *Pi3kc3* increased expression in iBAT from 15-month-old mice (Figure 18).

Thermogenic activity

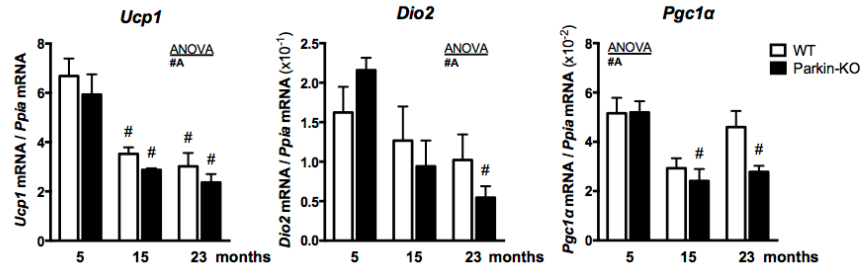

Glucose and lipid metabolism

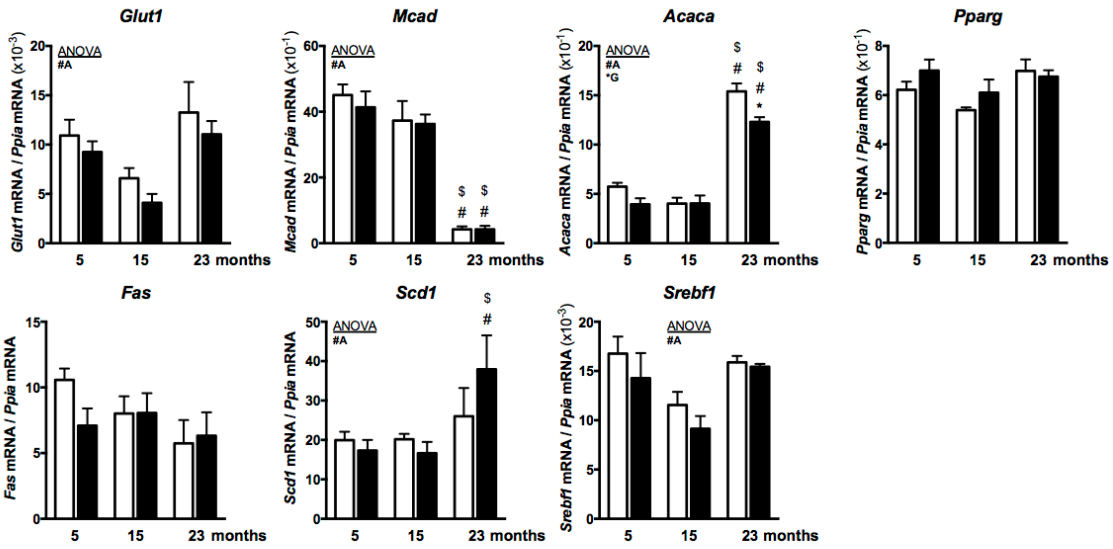

Type I cytokines

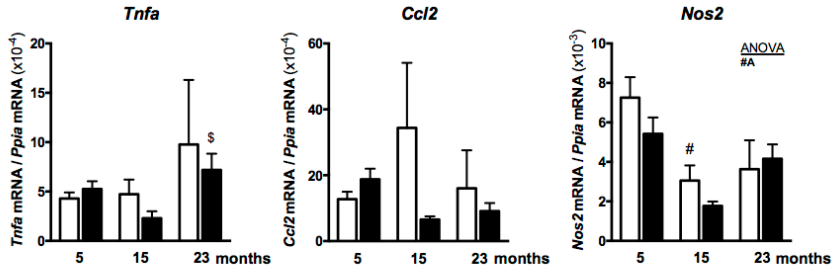

Type II cytokines

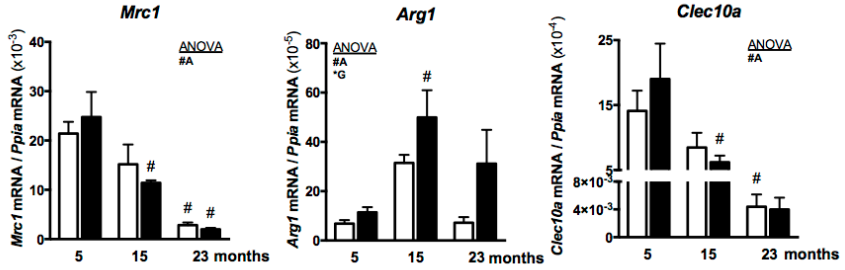

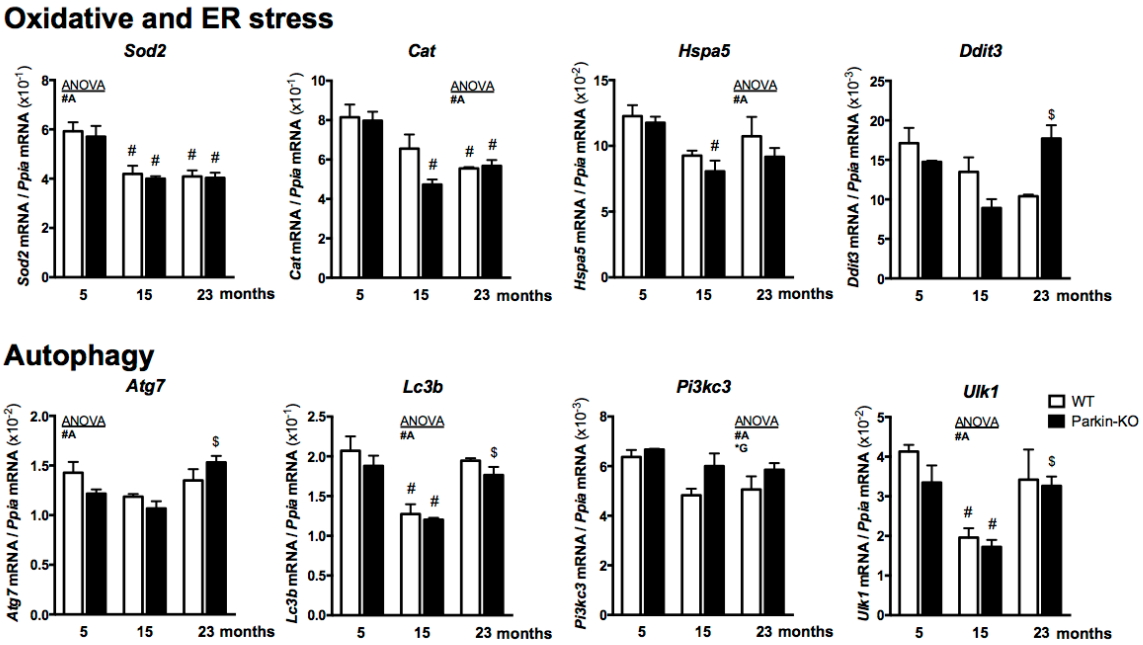

Figure 14. mRNA relative expression levels of genes related to different key metabolic pathways in interscapular brown adipose tissue from WT and Parkin-KO mice at 5, 15 and 23 months old (n=8). The bars represent means ± s.e.m. Two-way ANOVA with Tukey's *post hoc* test. (*G: genotype factor p<0.05; *p<0.05, WT vs. Parkin-KO; #A: age factor p<0.05; #p<0.05, 15 months or 23 months vs. 5 months; $p<0.05, 15 months vs. 23 months).

Considering the known relevance of sympathetic innervation in the control of BAT activity, we determined the levels of tyrosine hydroxylase (TH) in the tissue, an indicator of the relative abundance of sympathetic nerve endings[301]. TH levels declined in BAT from 15-month-old and 23-month-old mice relative to younger 5-month-old mice (Figure 19). That happened similarly in BAT from Parkin-KO mice.

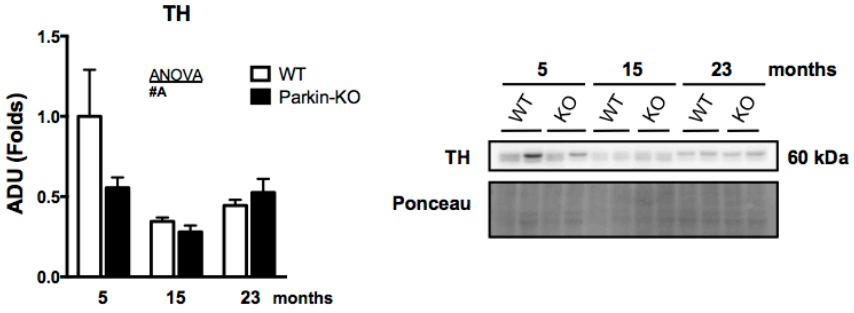

Figure 15. Tyrosine hydroxylase expression in BAT from WT and Parkin-KO mice during aging. Quantification (left) and representative immunoblot (right) for tyrosine hydroxylase (TH) in BAT from WT and Parkin-KO mice at 5, 15 and 23 months old. Ponceau staining was used as the loading control (n=3). The bars represent means ± s.e.m. Two-way ANOVA with Tukey's *post hoc* test. (#A: age factor p<0.05).

5. Electron microscopy analysis of the cellular alterations in iBAT associated with aging and Parkin gene invalidation

Figure 20 shows representative EM pictures of iBAT at the three ages studied. Morphological features of mitochondrial ultrastructure revealed a progressive alteration in mitochondria cristae distribution and size in association with aging (yellow arrowheads in the figure), these alterations being particularly intense in iBAT from 23-month-old mice, in which profound loss of internal cristae structures is found at some mitochondria. No apparent differential appearance in relation to these alterations was observed in iBAT from Parkin-KO mice.

Figure 21 depicts enlarged EM pictures focused to show morphological structures compatible with autophagy-related events. Blue arrowheads show autophagosome structures. Some of them showed a content indicative of mitochondria structures, indicating mitophagic events. Such structures were found similarly at pictures corresponding to iBAT from all the ages studied regardless of a wild-type or Parkin-KO genotype. Thus, no obvious effect at this level of analysis could be found in relation to autophagy and mitophagy events due to aging and Parkin gene deletion conditions.

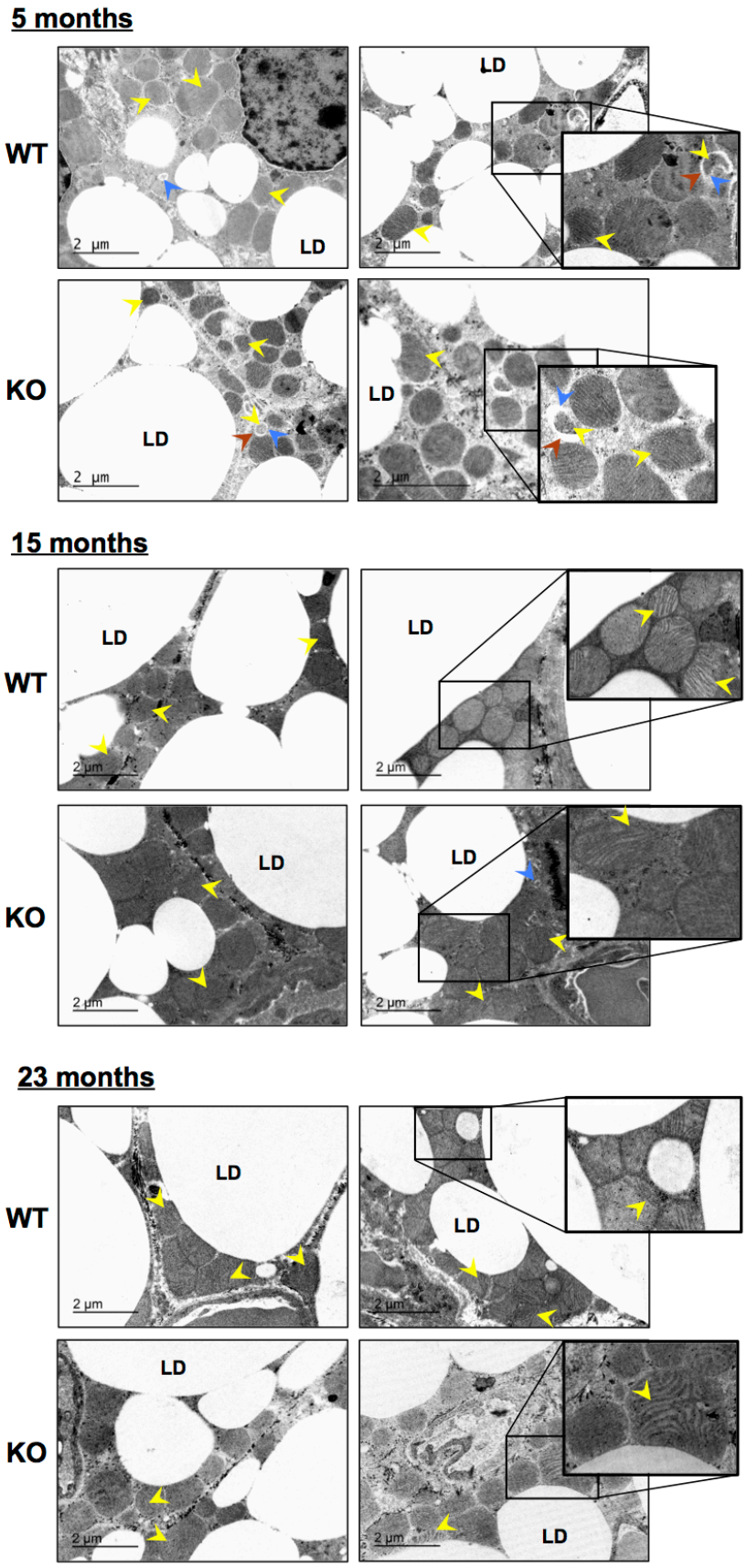

Figure 20. Representative electron microscopic pictures of brown adipose tissue showing mitochondrial integrity and lipid droplets from WT and Parkin-KO mice during aging. Yellow arrowheads indicate mitochondrial cristae, blue arrowheads indicate double-membrane autophagosomes, and red arrowheads indicate structures compatible with mitochondria-derived vesicles. LD: lipid droplet. Scale bars are indicated in every picture.

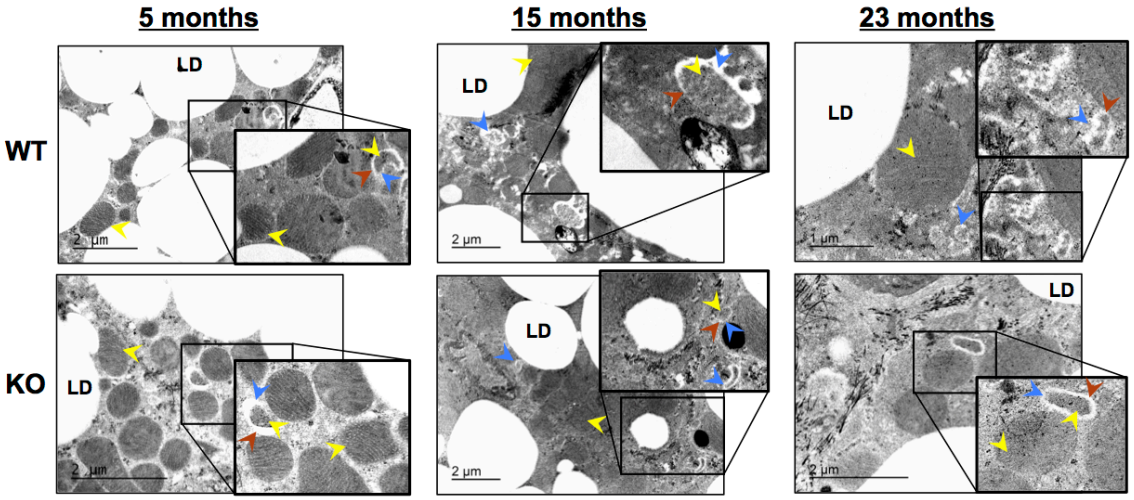

Figure 21. Representative electron microscopic pictures of autophagic and mitophagic events in brown adipose tissue from WT and Parkin-KO mice during aging. Yellow arrowheads indicate mitochondrial cristae, blue arrowheads indicate double-membrane autophagosomes, and red arrowheads indicate structures compatible with mitochondria-derived vesicles. LD: lipid droplet. Scale bars are indicated in every picture.

6. Mitochondrial dysfunction in BAT in association with aging and effects of Parkin gene deletion

Some parameters indicatives of mitochondrial function were determined in BAT. Relative abundance of mtDNA was reduced in iBAT from 15-month-old and 23-month-old relative to 5-month-old wild-type mice (Figure 22A). A dramatic increase in mtDNA abundance was found in iBAT from Parkin-KO mice, especially marked in 15-month-old mice.

The relative abundance of the mtDNA-binding protein TFAM in BAT followed a distinct pattern: it trended to be up-regulated in association with aging whereas no marked difference was found between Parkin-KO mice and wild-type mice at any age (Figure 22B). The relative abundance of VDAC (mitochondrial voltage dependent carrier, porin), often used as biomarker of mitochondrial mass, was unaltered in BAT in relation to age or Parkin gene deletion (Figure 22B).

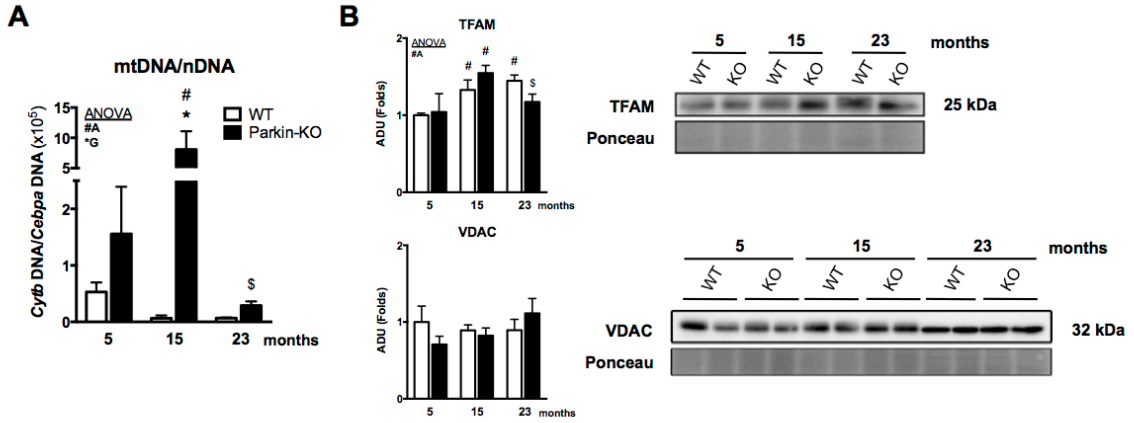

Figure 16. Mitochondrial DNA and mitochondrial mass-related parameters in brown adipose tissue from WT and Parkin-KO mice during aging. (A) Mitochondrial DNA (mtDNA) content in BAT relative to nuclear DNA (nDNA) (n=5 WT, n=6 Parkin-KO). **(B)** Quantification (left) and representative immunoblot (right) for TFAM and VDAC in BAT. Ponceau staining was used as the loading control (n=3). The bars represent means ± s.e.m. Two-way ANOVA with Tukey's post hoc test. (*G: genotype factor $p<0.05$; *$p<0.05$, WT vs. Parkin-KO; #A: age factor $p<0.05$; #$p<0.05$, 15 months or 23 months vs. 5 months; \$$p<0.05$, 15 months vs. 23 months).

The relative abundance of *Cox1* mRNA, corresponding to the mtDNA gene encoding for cytochrome c oxidase subunit 1, was also down-regulated in BAT in association with aging, and it was significantly increased in iBAT from Parkin-KO mice at 15 months and 23 months of age (Figure 23A). The relative abundance of the transcript for *Cox7a1* (mitochondrial cytochrome c oxidase subunit 7a1), encoded by the nuclear genome, in BAT was also reduced with aging mice but no difference was found between wild-type and Parkin-KO mice at any age (Figure 23A).

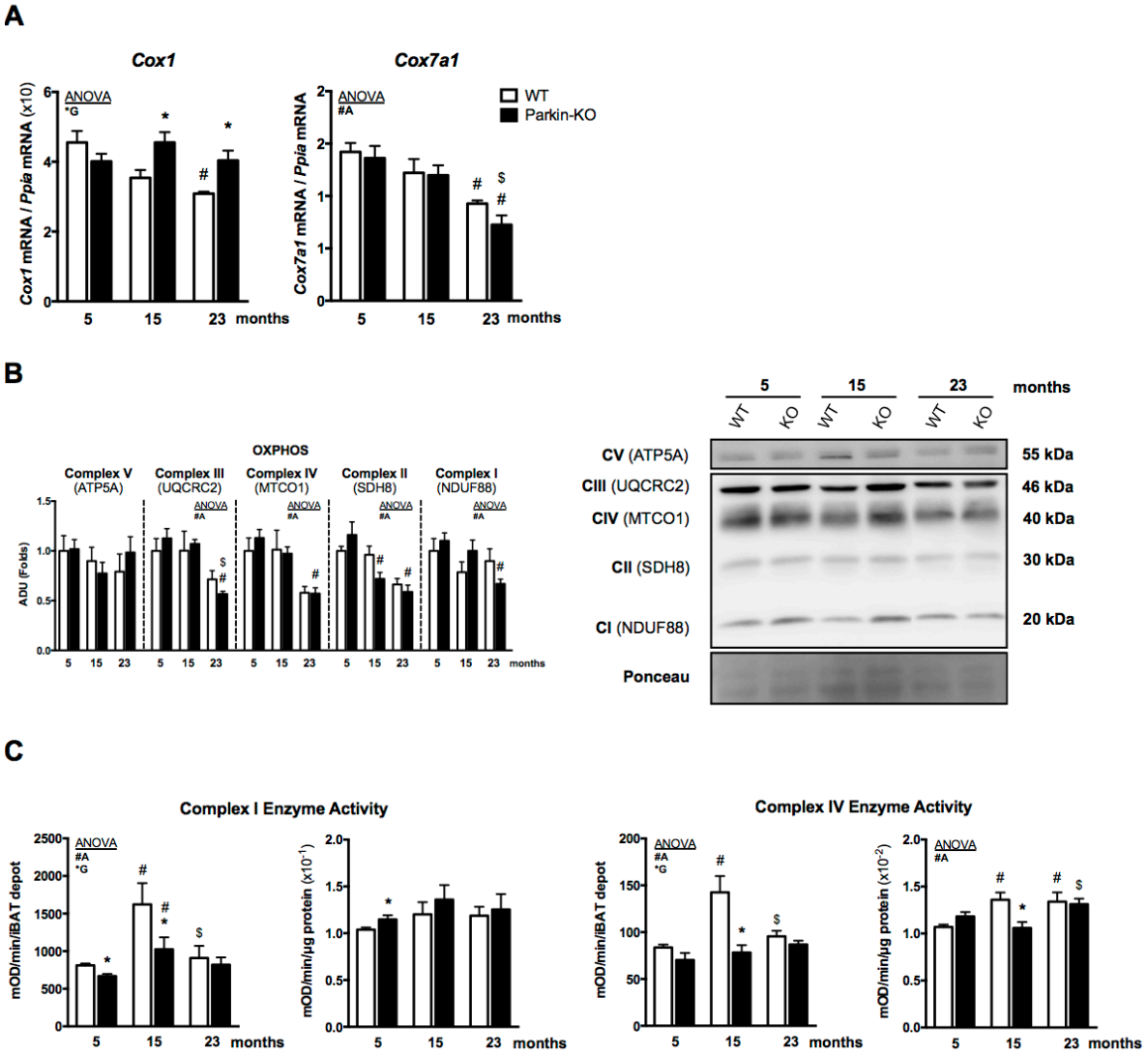

Figure 17. Mitochondrial activity-related parameters in brown adipose tissue from WT and Parkin-KO mice during aging. (A) Relative transcript levels of gens of BAT from WT and Parkin-KO mice at 5, 15 and 23 months old (n=8). **(B)** Quantification (left) and representative immunoblot (right) for the indicated OXPHOS protein subunits in BAT (n=4). **(C)** Complex I and Complex IV specific enzymatic activity (right) and per total iBAT deposit (left) (n=6). The bars represent means ± s.e.m. Two-way ANOVA with Tukey's post hoc test. (*G: genotype factor p<0.05; *p<0.05, WT vs. Parkin-KO; #A: age factor p<0.05; #p<0.05, 15 months or 23 months vs. 5 months; $p<0.05, 15 months vs. 23 months).

The pattern of relative abundance of proteins corresponding to subunits of the complexes of respiratory chain/oxidative phosphorylation (OXPHOS) system was determined. Data revealed minor changes and only a significant trend of reduced abundance of SDH8 (succinate dehydrogenase subunit 8, from Complex II), UQCRC2 (Cytochrome b-c1 complex subunit 2, from Complex III) and MTCO1 (cytochrome oxidase subunit I, from Complex IV) in iBAT from 23-month-old mice was found (Figure 23B). No significant differences in abundance of any of these proteins were found in the comparison of iBAT from Parkin-KO versus wild-type mice at any age.

Finally, we assessed the enzymatic activity of mitochondrial respiratory complexes (Figure 23C). The relative activity of the Complex I (NADH dehydrogenase) in iBAT was essentially unaltered in relation to aging and Parkin gene invalidation. Calculation of total activity per iBAT in wild-type mice revealed increased activity in 15-month-old mice and a further decline in 23-month-old mice as well as a decrease in Parkin-KO mice at 5 months and 15 months of age, although these changes were basically attributable to the trophic changes in iBAT tissue described previously. For Complex IV (cytochrome c oxidase) specific activity, a mild increase in activity was found in BAT from 15-month-old and 23-month-old mice relative to 5-month-old mice (Figure 23C). We also found a significant reduction in BAT from Parkin-KO mice versus wild-type controls at 15 months of age. The calculation of total Complex IV activity per tissue indicated also a significant reduction in Parkin-KO mice at 15 months of age.

7. Changes on morphology and gene expression in inguinal WAT in Parkin-KO mice across aging

Considering the capacity of WAT to acquire beige (brown-like) cellular and functional features (browning process), our study was expanded to the analysis of inguinal WAT, a representative subcutaneous WAT depot particularly susceptible to browning.

Figure 24A shows representative pictures showing, in wild-type mice, the enlargement of the iWAT depot in 15-month-old mice and further reduction in 23-month-old mice. The reduced size of inguinal WAT depots in Parkin-KO mice, especially marked in 15-month-old Parkin-KO mice, is also shown. Optical microscopy images, as shown in Figure 24B, evidenced that, in wild-type mice, white adipocytes were hypertrophied in iWAT from 15-month-old mice but not in 23-month-old mice. No such hypertrophy was evident in iWAT from 15-month-old Parkin-KO mice.

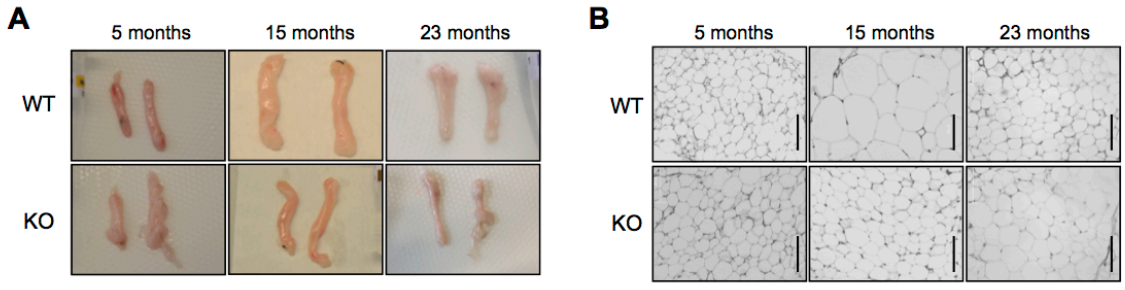

Figure 18. Morphology of inguinal WAT from WT and Parkin-KO mice during aging. (A) Representative images of the inguinal fat depots. **(B)** Representative optical microscopy images of H&E-stained iWAT (200X) from WT and Parkin-KO mice. Scale bars, 100µm.

Quantitative assessment of adipocyte size distribution confirmed the shift of adipocyte size towards larger values in 15-month-old mice relative to 5-month-old mice iWAT and the reversal of this phenomenon in 23-month-old mice. A much less intensity of these alterations was found when analyzed in Parkin-KO mice, in which there was a progressive aging-associated increase in adipocyte size (Figure 25A,B).

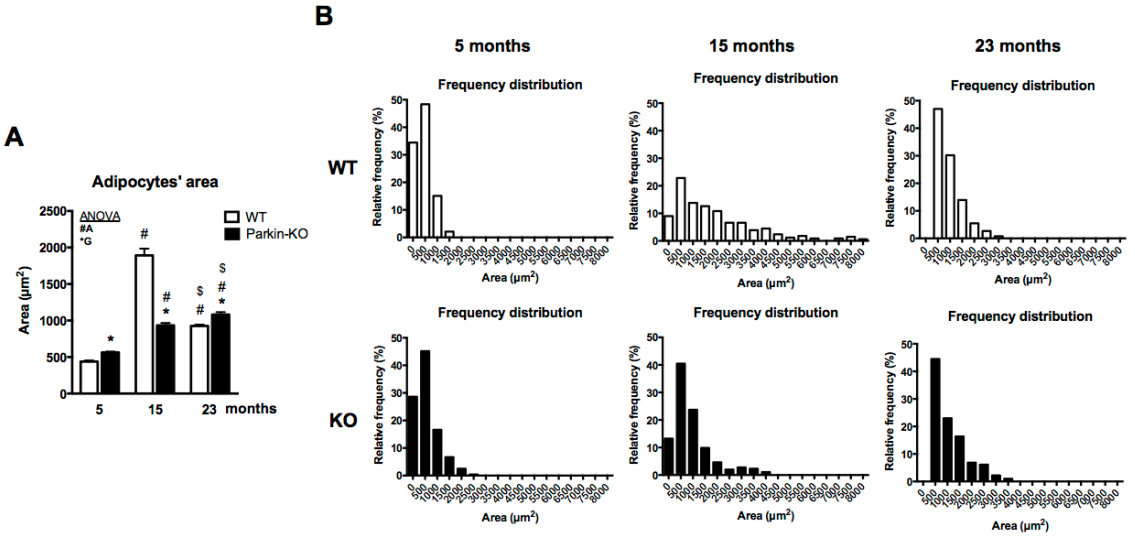

Figure 19. Adipocytes' size analysis in inguinal WAT from WT and Parkin-KO mice during aging. (A) Quantitative assessment of adipocytes' area. The bars represent means ± s.e.m. Two-way ANOVA with Tukey's *post hoc* test. (*G: genotype factor p<0.05; *p<0.05, WT vs. Parkin-KO; #A: age factor p<0.05; #p<0.05, 15 months or 23 months vs. 5 months; $p<0.05, 15 months vs. 23 months). **(B)** Adipocyte's area relative frequency distribution from histological sections of the inguinal fat depots. The bars represent frequencies of the different areas.

Figure 26 shows the pattern of gene expression for *Ucp1*, *Dio2* and *Pgc1α*, marker genes of WAT browning. In wild-type mice, the expression of the three genes was significantly down-regulated in 15-month-old mice relative to 5-month-old mice and even more intensely reduced in 23-month-old mice, in accordance with previous reports of impairment of WAT browning in aging[302]. The pattern of expression of the browning-related genes was not significantly different in iWAT from Parkin-KO mice across aging except for a somewhat higher expression in *Pgc1α* in 15 months old Parkin-KO mice.

The expression of the adipokine leptin (*Lep*) was strongly induced in iWAT from 15-month-old mice, consistently with increased adiposity and circulating leptin levels (Figure 26). Leptin genetic expression in iWAT declined thereafter in 23-month-old mice. Parkin-KO mice had lower expression of leptin in iWAT, especially at 15 months of age. For the adipokine adiponectin (*AdipoQ*), there was a significant trend to age-associated decline with no significant effects of the Parkin-KO genotype (Figure 26).

No relevant changes were found for the distinct genes encoding enzymes (*Mcad*, *Acaca*, *Fas*, *Scd1*) or transcription factors (*Srebp*, *Pparγ*) related to lipid metabolism and lipid accumulation, either in relation to age or to Parkin-KO genotype (Figure 26).

Expression of genes corresponding to Type I pro-inflammatory immune cell phenotype in iWAT (*Tnfa*, *Ccl2*, *Nos2*), showed a significant trend to be up-regulated in association with aging, whereas no effect of Parkin-KO genotype was found (Figure 26). Expression of marker gens of Type II, non-inflammatory, phenotype followed distinct trends in relation to aging. Whereas expression of *Mrc1* was reduced in 23-month-old mice and overall decreased in association with aging in accordance with ANOVA, expression of *Clec10a* was up-regulated in iWAT from 23-month-old mice. Neither Type I, nor Type II cytokine pathway's gene expression was altered in Parkin-KO mice relative to wild-type mice (Figure 26).

The expression of *Cat*, an indicator of oxidative stress, was also up-regulated in association with aging, again with no changes due to the Parkin-KO genotype (Figure 26). Hspa5 expression, indicator of ER stress, trended to be significantly reduced in association with aging. No significant effects of the Parkin-KO genotype were detected (Figure 26).

No relevant changes in the expression of genes related to autophagy was found in iWAT in relation to aging or Parkin gene deletion, apart from a trend to increased *Atg7* expression in iWAT from 15-month-old Parkin-KO mice (Figure 26).

Thermogenic activity

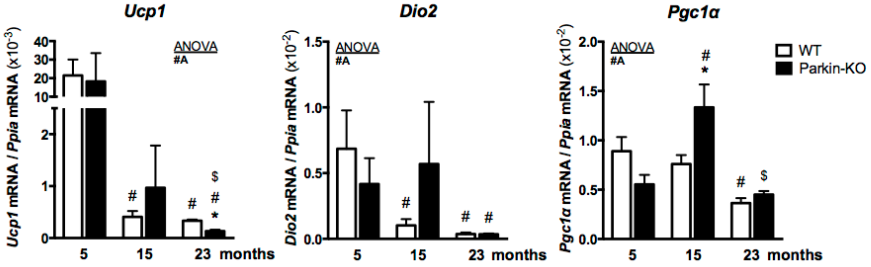

Adipokines

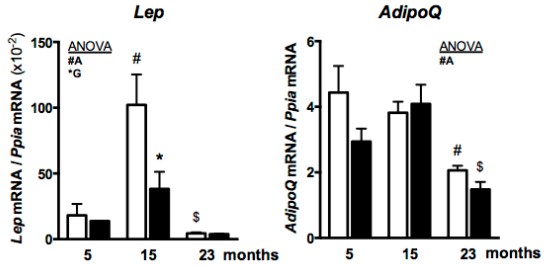

Lipid metabolism

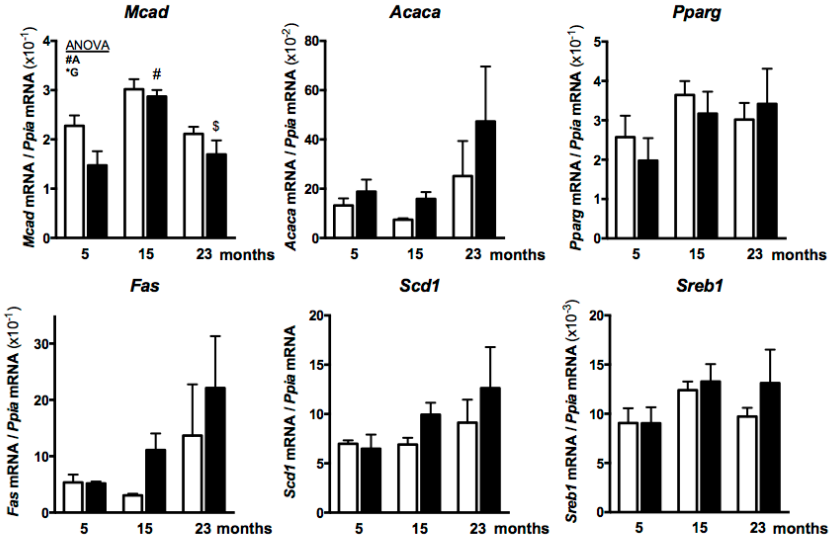

Type I cytokines

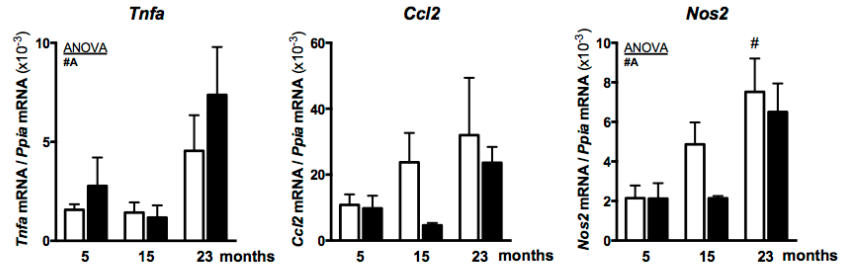

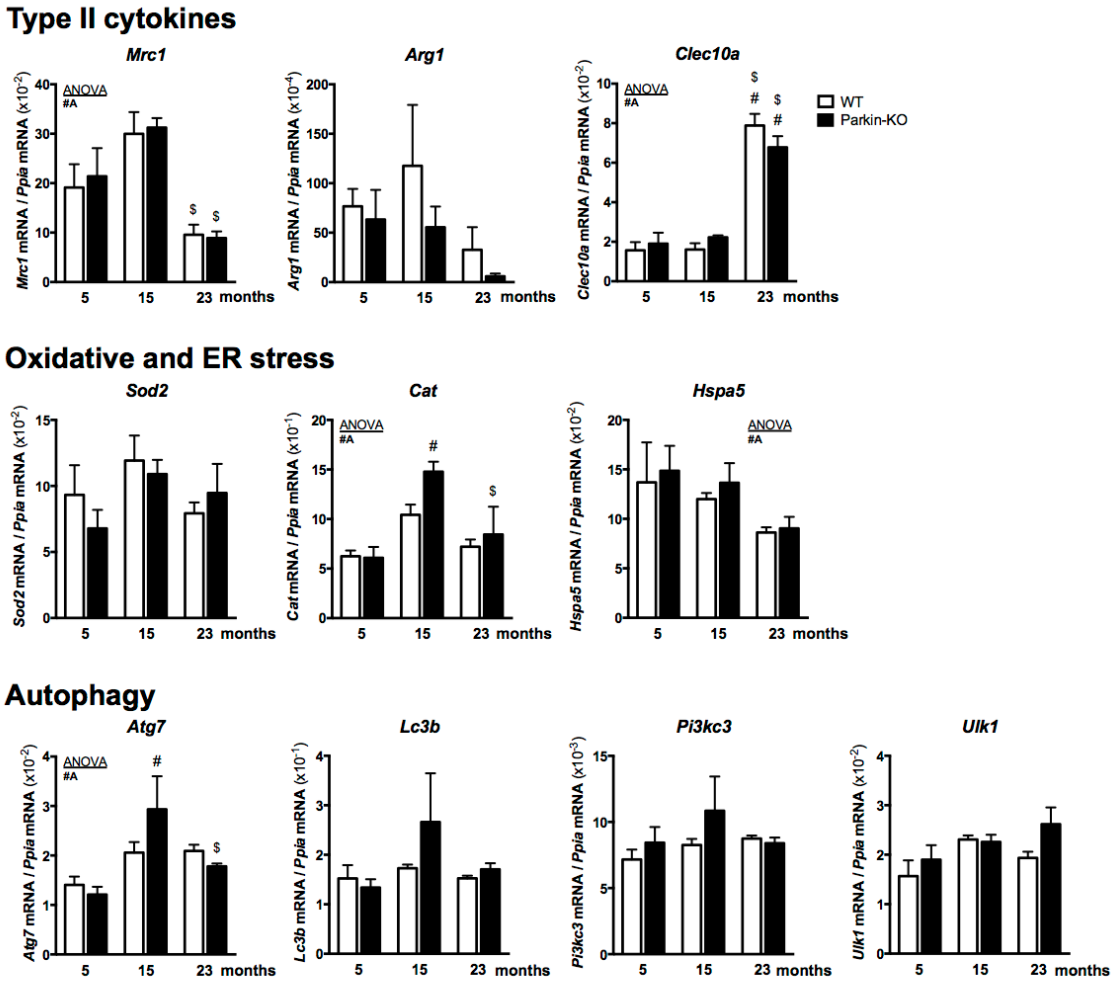

Figure 20. mRNA relative expression levels of genes related to different key metabolic pathways in inguinal white adipose tissue from WT and Parkin-KO mice at 5, 15 and 23 months old (n=8). The bars represent means ± s.e.m. Two-way ANOVA with Tukey's post hoc test. (*G: genotype factor p<0.05; *p<0.05, WT vs. Parkin-KO; #A: age factor p<0.05; #p<0.05, 15 months or 23 months vs. 5 months; $p<0.05, 15 months vs. 23 months).

The relative TH abundance was lower in iWAT from 15-month-old mice relative to 5-month-old mice (Figure 27). Although somewhat higher, it remained lower in 23-month-old mice relative to young, 5-month-old, mice. No such trend was found in Parkin-KO mice and TH levels were somewhat higher in iWAT from Parkin-KO mice in 15-month-old and 23-month-old mice.

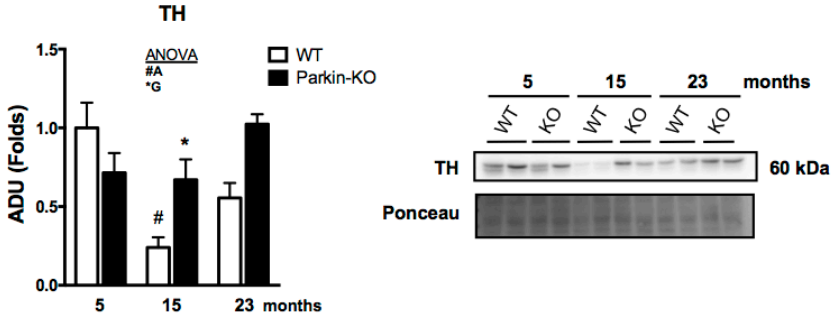

Figure 21. Tyrosine hydroxylase expression in iWAT from WT and Parkin-KO mice during aging. Quantification (left) and representative immunoblot (right) for tyrosine hydroxylase (TH) in iWAT from WT and Parkin-KO mice at 5, 15 and 23 months old. Ponceau staining was used as the loading control (n=3). The bars represent means ± s.e.m. Two-way ANOVA with Tukey's post hoc test (*G: genotype factor p<0.05; *p<0.05, WT vs. Parkin-KO; #A: age factor p<0.05; #p<0.05, 15 months vs. 5 months).

8. Mitochondrial parameters in iWAT during aging and effects of Parkin gene deletion

The relative abundance of mtDNA in iWAT declined throughout aging in wild-type mice (Figure 28A). However, there was a trend of up-regulation of the mtDNA abundance in iWAT from Parkin-KO mice, especially at 15 months of age.

In contrast to BAT, the expression of *Cox1* mRNA (mtDNA-encoded) was increased in iWAT from 23-month-old mice relative to younger mice, with no effects of Parkin gene invalidation. A similar pattern was found for the expression of *Cox7a1* transcript (nuclear genome-encoded) (Figure 28B).

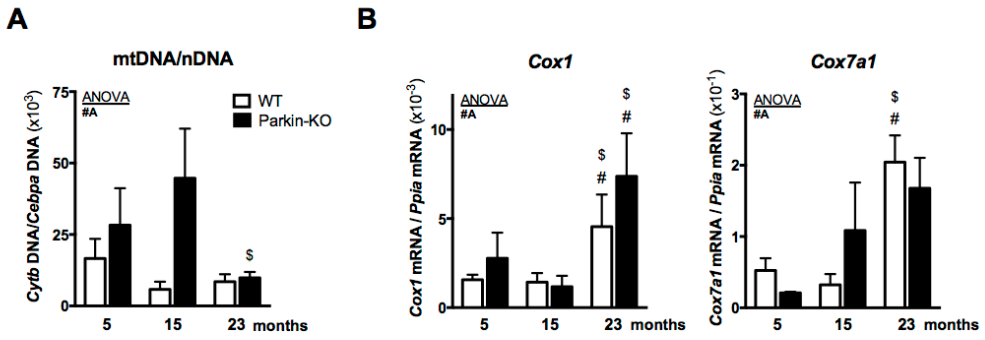

Figure 22. Mitochondrial-related parameters in inguinal white adipose tissue from WT and Parkin-KO mice during aging. (A) Mitochondrial DNA (mtDNA) content in iWAT relative to nuclear DNA (nDNA) (n=5 WT, n=6 Parkin-KO). **(B)** Relative transcript levels of gens of iWAT from WT and Parkin-KO mice at 5, 15 and 23 months old (n=8). The bars represent means ± s.e.m. Two-way ANOVA with Tukey's post hoc test. (#A: age factor $p<0.05$; #$p<0.05$, 23 months vs. 5 months; \$$p<0.05$, 15 months vs. 23 months).

9. Alterations in liver gene expression and mitochondrial parameters across aging in Parkin-KO mice

In order to determine the specificity of the changes in gene expression found in BAT and WAT adipose depots in association with aging and in response to Parkin gene ablation, a profile of gene expression was determined in liver (Figure 29).

No effects of aging or Parkin gene deletion were found for genes encoding phosphoenolpyruvate carboxykinase (*Pepck*) and glucose 6-phosphatase (*G6Pase*), enzymes of the gluconeogenesis pathway (Figure 29).

For lipid metabolism related genes, *Acaca* was significantly up-regulated in liver from 23-month-old mice, but no changes were found in relation to Parkin gene invalidation (Figure 29). The expression of the gene encoding hydroxymethyl glutaryl-CoA synthase (*Hmgcs2*), a key enzyme of ketone body synthesis from fatty acids in the liver, was significantly up-regulated in 15-month-old mice and strongly declines thereafter, in 23-month-old mice. In 15 months mice, hepatic expression of *Hmgcs2* was significantly reduced in Parkin-KO mice relative to wild-type mice (Figure 29).

The expression of genes indicative of oxidative (*Sod2* and *Cat*), ER stress (*Hspa5*), or both (*Ddit3*) were also assessed in the liver. As in BAT, most of these genes trended to be less expressed in association with aging in the liver with no significant differences in Parkin-KO mice at any age studied (Figure 29).

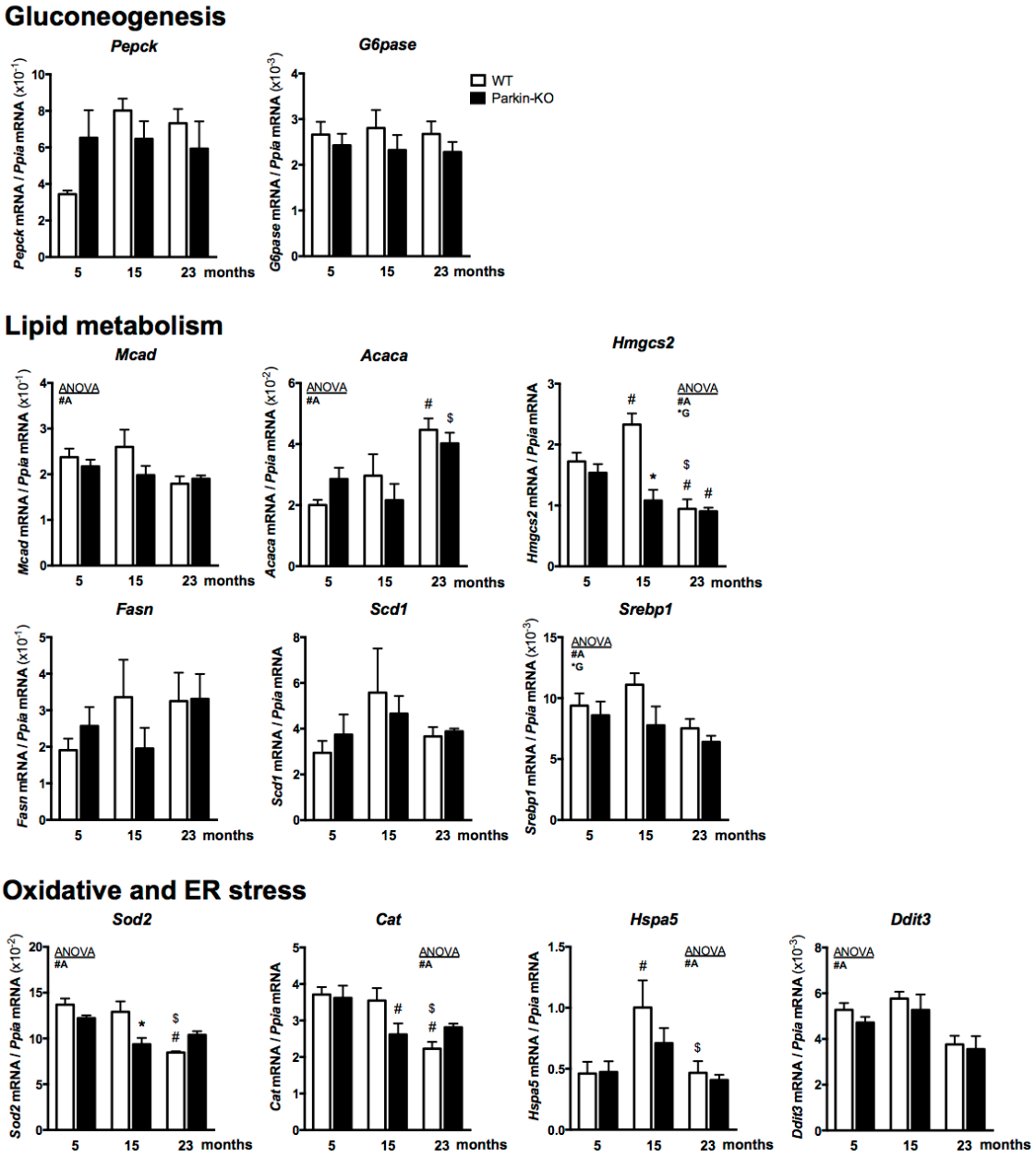

Figure 23. mRNA relative expression levels of genes related to different key metabolic pathways in liver from WT and Parkin-KO mice at 5, 15 and 23 months old (n=8). The bars represent means ± s.e.m. Two-way ANOVA with Tukey's *post hoc* test (*G: genotype factor p<0.05; *p<0.05, WT vs. Parkin-KO; #A: age factor p<0.05; #p<0.05, 15 months or 23 months vs. 5 months; $p<0.05, 15 months vs. 23 months).

Regarding mitochondrial related parameters, hepatic mitochondrial DNA abundance in wild-type mice was significantly reduced in 23-month-old mice (Figure 30A). In Parkin-KO mice, a significant decrease was found in 5 months old mice relative to the wild-type controls, but no significant changes due to genotype were found at any other aging time. The expression of the mtDNA-encoded *Cox1* transcript was reduced in liver from 23-month-old mice relative to younger mice, with no effects of Parkin gene invalidation. No changes were found for the expression of *Cox7a1*, a nuclear genome-encoded component of mitochondrial respiratory chain Complex IV (Figure 30B).

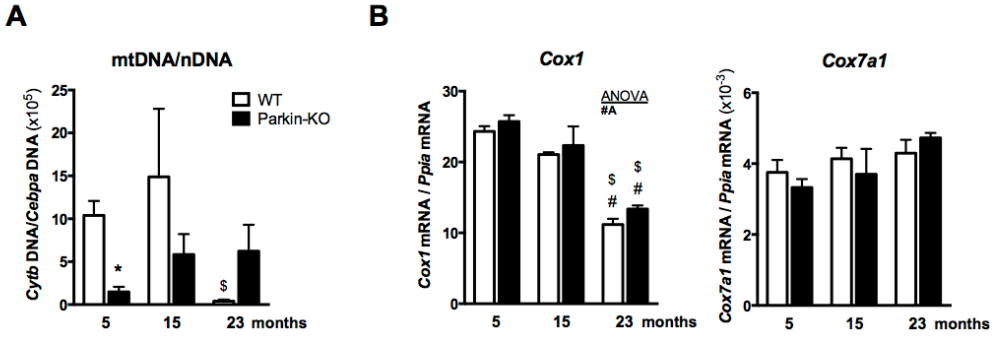

Figure 30. Mitochondrial expression parameters in liver from WT and Parkin-KO mice during aging. (A) Mitochondrial DNA (mtDNA) content in liver relative to nuclear DNA (nDNA) (n=5 WT, n=6 Parkin-KO). **(B)** Relative transcript levels of gens of liver from WT and Parkin-KO mice at 5, 15 and 23 months old (n=8). The bars represent means ± s.e.m. Two-way ANOVA with Tukey's *post hoc* test (*p<0.05, WT vs. Parkin-KO; #A: age factor p<0,05; #p<0.05, 23 months vs. 5 months; $p<0.05, 15 months vs. 23 months).

10. Evidence for altered FGF21 system in Parkin-KO mice across aging

During the characterization of changes in metabolic and hormonal parameters in our experimental model, we found a dramatic induction of plasma FGF21 levels in 15-month-old and 23-month-old mice relative to younger 5-month-old mice. Interestingly, such induction was dramatically blunted in 15-month-old Parkin-KO mice (Figure 31A).

We determined the pattern of expression of the *Fgf21* gene as well as of the genes encoding the FGF receptors *Fgfr1* and *Fgfr4* and the co-receptor *β-klotho*, mediators of the cellular actions of FGF21.

In iBAT from wild-type mice, the expression of the *Fgf21* gene was increased in 15-month-old mice and declined thereafter at 23 months of age. In Parkin-KO mice, *Fgf21* gene expression was lower, and significantly reduced in 15-month-old-mice. The expression of *Fgfr1* and *β-klotho* declined progressively with aging and a similar profile of expression occurred in Parkin-KO mice (Figure 31B).

In iWAT from wild-type mice, *Fgf21* gene expression was also dramatically induced in 15-month-old mice relative to 5-month-old mice and declined in 23-month-old mice to levels similar to those from young mice. The high expression levels of *Fgf21* in 15-month-old mice were dramatically blunted in 15-month-old Parkin-KO mice. Similarly to BAT, there was a trend of aging-associated decline in the expression of *Fgfr1* and *β-klotho* in wild-type mice, remarkable in 23-month-old, occurring similarly in Parkin-KO mice (Figure 31C).

We determined the expression levels of β-klotho, the key component of cellular responsiveness to FGF21, at protein levels in 15-month-old mice, the aging time in which changes in FGF21 were more marked in comparison with young, 5-month-old, mice. Data indicated that there was a reduction in β-klotho protein levels in iBAT and iWAT from 15-month-old relative to 5-month-old mice. However, such decrease did not occur in Parkin-KO mice and, in fact, β-klotho protein levels in BAT and iWAT were higher in 15-month-old Parkin-KO mice relative to 15-month-old wild-type mice (Figure 31D).

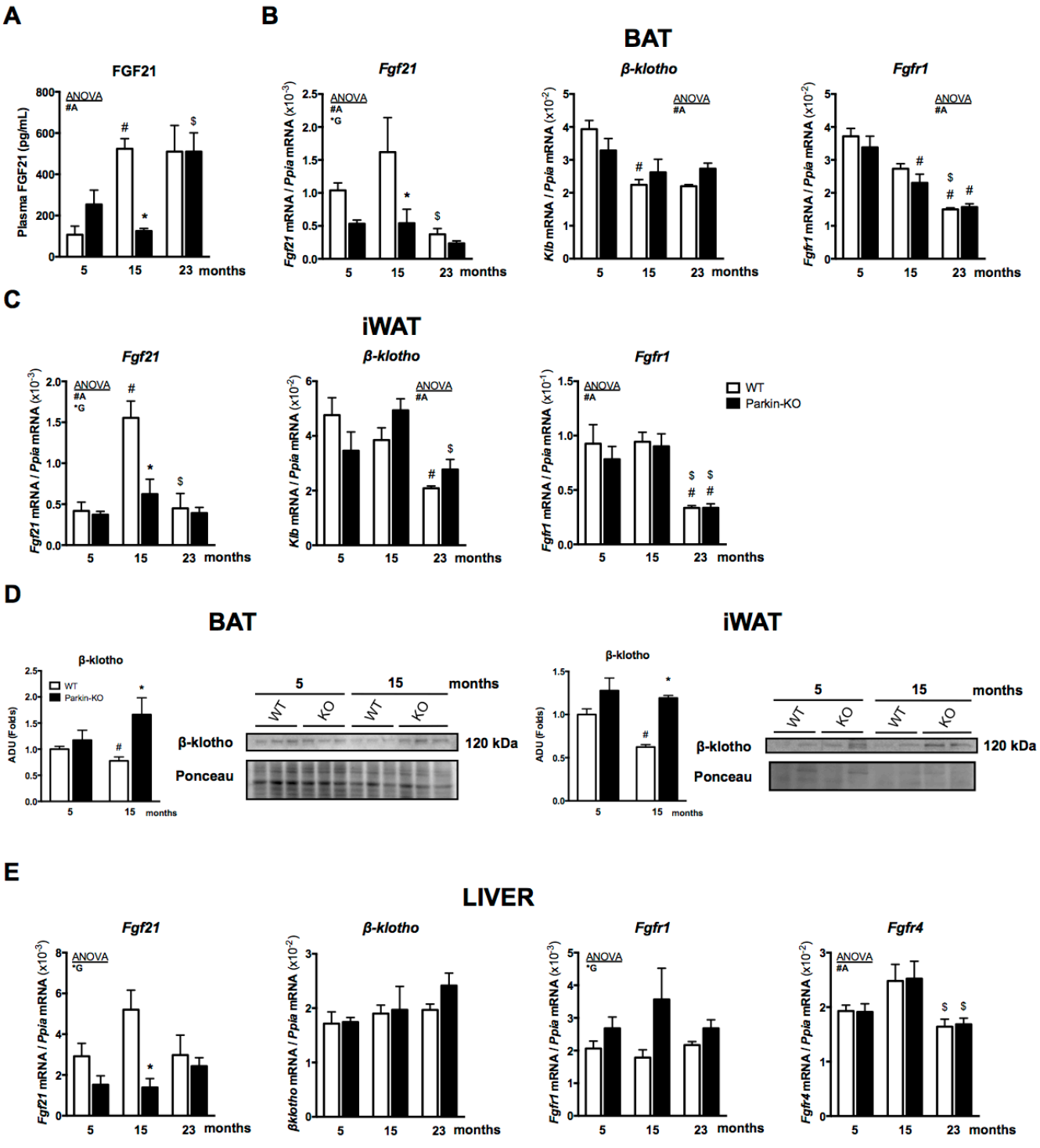

Figure 31. Characterization of FGF21 system in metabolic tissues from WT and Parkin-KO mice during aging. **(A)** FGF21 plasmatic levels in WT and Parkin-KO mice during aging. (n=6 WT, n=7 Parkin-KO). Relative transcript levels of gens of **(B)** BAT **(C)** iWAT and **(E)** liver from WT and Parkin-KO mice at 5, 15 and 23 months old (n=8). **(D)** Quantification (left) and representative immunoblot (right) for β-klotho in BAT and iWAT from WT and Parkin-KO mice at 5 and 15 months old. Ponceau staining was used as the loading control (n=3). The bars represent means ± s.e.m. Two-tailed unpaired Student's t-test or two-way ANOVA with Tukey's *post hoc* test (*G: genotype factor $p<0.05$; *$p<0.05$, WT vs. Parkin-KO; #A: age factor $p<0.05$; #$p<0.05$, 15 months or 23 months vs. 5 months; $$p<0.05$, 15 months vs. 23 months).

In wild-type mice, hepatic FGF21 expression trended to be increased in 15-month-old mice relative to 5-month-old-mice an also declined to levels similar to young mice in 23-month-old mice. No remarkable changes associated with aging or Parking gene invalidation were found for the expression of genes encoding the FGF receptors FGFR1 and FGFR4, and for β-klotho (Figure 31E).

11. GDF15 variation in Parkin-KO mice throughout aging

Considering that GDF15 is another circulating bioactive factor responsive to mitochondrial dysfunction and also involved in the control of energy metabolism, as FGF21, we evaluated GDF15 circulating levels and gene expression in our models.

During the evaluation of hormonal factors related to adiposity and energy balance we found a significant induction of plasma GDF15 levels in 15 months old mice in comparison with adult, 5 months old, mice. Interestingly, such induction was abolished in 15-month-old Parkin-KO mice. Plasmatic GDF15 levels declined thereafter at 23 months of age in wild-type mice to levels similar to adult mice (Figure 32A).

In iBAT from wild-type mice, the expression of the *Gdf15* gene was hugely increased in 15-month-old mice and declined thereafter at 23 months of age. In Parkin-KO mice, the induction in *Gdf15* gene expression at 15 months was dramatically blunted (Figure 32B).

In iWAT, *Gdf15* gene expression was down-regulated in association with aging as remarked by the ANOVA analysis. No difference was found between wild-type and Parkin-KO mice at any age (Figure 32B).

Similarly to iWAT and according to the ANOVA analysis, *Gdf15* gene expression in the liver also decreased in relation to aging. Again, no significant difference was found between wild-type and Parkin-KO mice (Figure 32B).

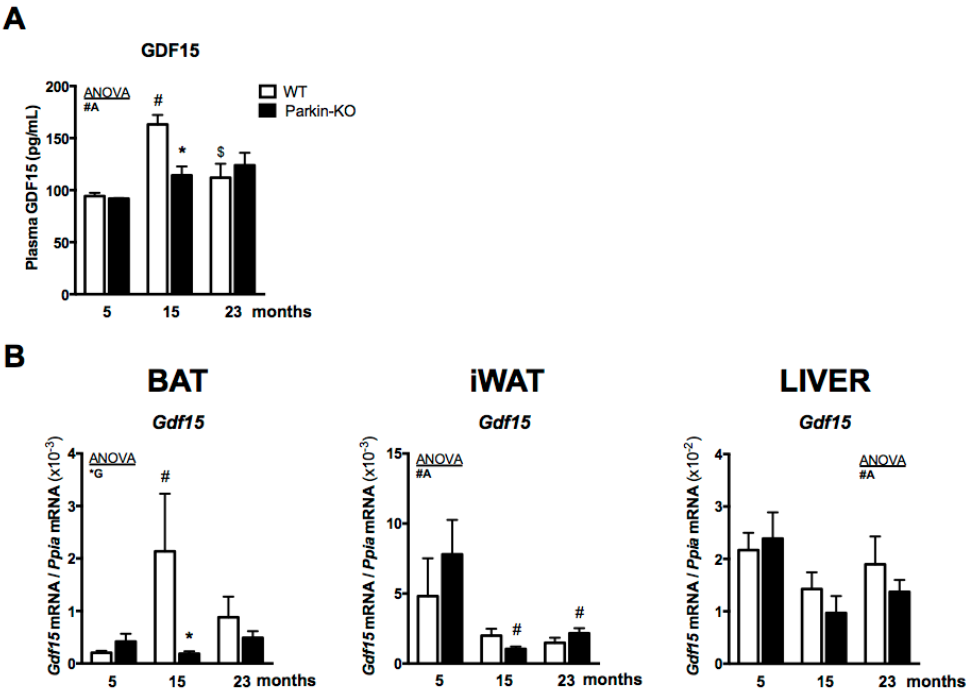

Figure 32. GDF15 circulating levels and gene expression from WT and Parkin-KO mice during aging. (A) GDF15 plasmatic levels in WT and Parkin-KO mice during aging (n=6 WT, n=7 Parkin-KO). **(B)** Relative transcript levels of *Gdf15* gene in BAT (left) iWAT (center) liver (right) from WT and Parkin-KO mice at 5, 15 and 23 months old (n=8). The bars represent means ± s.e.m. Two-way ANOVA with Tukey's *post hoc* test (*G: genotype factor p<0.05; *p<0.05, WT vs. Parkin-KO; #A: age factor p<0.05; #p<0.05, 15 months or 23 months vs. 5 months; $p<0.05, 15 months vs. 23 months).

12. Cardiac parameters during aging and effects of Parkin gene deletion

Although the focus of this thesis was oriented towards adipose tissue and metabolism-related studies, we determined some parameters in heart from our mouse models.

We observed that mice increase their relative size of heart progressively with aging (heart weight/tibia length ratio) and such increase was less intense in Parkin-KO mice (Figure 33).

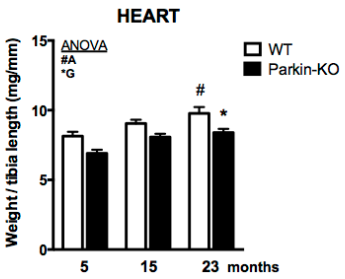

Figure 33. Heart relative weight in WT and Parkin-KO mice with advancing age (n=8). The bars represent means ± s.e.m. Two-way ANOVA with Tukey's *post hoc* test. (*G: genotype factor p<0.05; *p<0.05, WT vs. Parkin-KO; #A: age factor p<0.05; #p<0.05, 23 months vs. 5 months).

We determined the pattern of cardiac gene expression in a subset of our animal models: 5- and 15-month-old, both in WT and Parkin-KO mice. We found that the expression of the cardiac hypertrophy markers skeletal α-actin (*Acta1*) and β-myosin heavy chain (*Myhcb*) was increased in heart from aged mice relative to young ones (Figure 34). No significant differences due to the Parkin gene invalidation were observed for *Acta1*. However, *Myhcb* gene expression was significantly increased in young Parkin-KO mice relative to age-matched wild-type mice and this difference was persistent in aged mice.

The cardiac expression of several genes involved in glucose metabolism (*Glut1* and *Glut4*) was increased in association with aging similarly in WT and Parkin-KO mice whereas the cardiac expression of the lipid oxidation pathway gene *Pdk4* was not significantly altered (Figure 34).

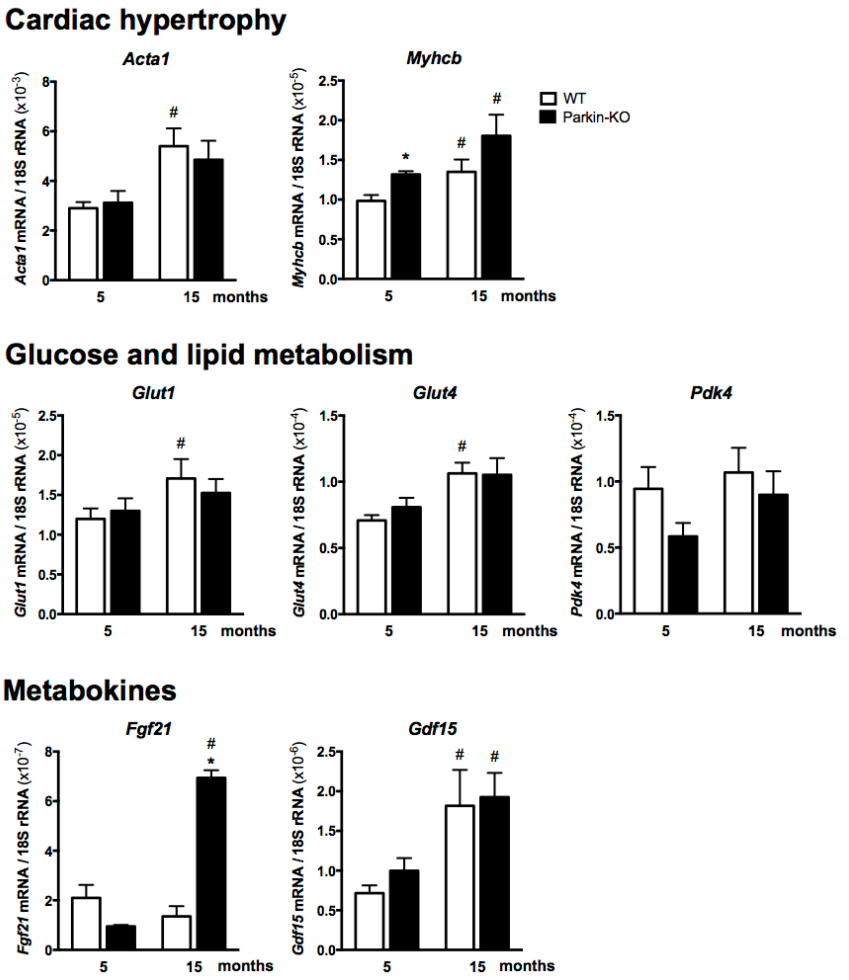

Figure 34. mRNA relative expression levels of genes related to different key metabolic pathways in heart from WT and Parkin-KO mice at 5 and 15 months old (n=8). The bars represent means ± s.e.m. Two-tailed unpaired Student's t-test (*p<0.05, WT vs. Parkin-KO; #p<0.05, 15 months vs. 5 months).

Interestingly, no changes in *Fgf21* gene expression occurred in association with aging in hearts from WT mice, but Parkin-KO mice experienced a dramatic induction of *Fgf21* mRNA levels at 15 months of age. For *Gdf15*, there was a similar intense induction of cardiac expression associated with aging, which was similar in WT and Parkin-KO mice (Figure 34).

All these data evidence that there are signs of a cardiac phenotype due to aging and Parkin loss of function, particularly in relation to FGF21, which deserves further research.

Supplemental Table 1. List of TaqMan probes used for gene expression experiments.

Gene name	Catalogue number
18S	Hs99999901_s1
Acaca	Mm01304257_m1
Acadm (Mcad)	Mm00431611_m1
Acta1	Mm00808218_g1
AdipoQ	Mm00456425_m1
Arg1	Mm00475988_m1
Atg7	Mm00512209_m1
c-Fos	Mm00487425_m1
Cat	Mm01340246_m1
Ccl2	Mm00441242_m1
Cebpa	Mm00514283_s1
Clec10a	Mm00546124_m1
Cox7a1	Mm00438296_m1
Ddit3	Mm00492097_m1
Dio2	Mm00515664_m1
Erg1	Mm00656724_m1
Fas	Mm00662319_m1
Fgf21	Mm00840165_g1
Fgfr1	Mm00438930_m1
Fgfr4	Mm00433314_m1
G6pc3 (G6pase)	Mm00450187_m1
Gdf15	Mm00442228_m1
Hmgcs2	Mm00550050_m1
Hspa5	Mm00517691_m1
Klb (β-klotho)	Mm00473122_m1
Lep (Leptin)	Mm00434759_m1
Map1lc3 (Lc3b)	Mm00782868_sH
Mrc1	Mm00485148_m1
mt-Cox1	Mm04225243_g1
mt-Cytb	Mm04225271_g1
Myh7b (Myhcb)	Mm01249950_m1
Nos2	Mm00440502_m1
Park2	Mm00450187_m1
Pck1 (Pepck)	Mm00440636_m1
Pdk4	Mm00443325_m1
Pparg	Mm00440945_m1
Ppargc1a (Pgc1α)	Mm00447183_m1
Ppia	Mm02342430_g1
Scd1	Mm00772290_m1
Slc2a1 (Glut1)	Mm00441480_m1
Slc2a4 (Glut4)	Mm00436615_m1
Sod2	Mm00449726_m1
Sreb1	Mm00550338_m1
Tnfa	Mm00443258_m1
Ucp1	Mm00494069_m1
Ulk1	Mm00437238_m1
Vps34 (Pik3c3)	Mm00619489_m1

Part 2. Human and mouse studies related to FGF21 and adipose tissue in aging

1. Mild impairment of general metabolic homeostasis with age

We studied a cohort of 28 healthy elderly individuals (≥70 years) with no overt signs of metabolic or other pathologies and compared them with a cohort of 35 young healthy controls (≤40 years) (Table 3). Of note, despite the absence of overt diabetes, our population of aged individuals showed an increase in glycemia, insulinemia and HOMA-IR relative to young individuals (Table 3), an observation previously reported and considered an indication of impaired functionality of general metabolic homeostasis and signs of insulin resistance with age[303]. There were also mild signs of systemic inflammation in association with aging, evidenced by a significant increase in the circulating levels of the cytokines TNFα and MCP-1 (Table 3).

	Control C (n=35)	**Elderly (>70)** (n=28)	*P value*
Sex (n of men (%))	23 (66,6)	14 (50)	0,193
Age (years)	38,1 ± 0,6	80,8 ± 1,1	**<0,001**
Weight (kg)	74,8 ± 5,0	70,8 ± 2,5	0,859
BMI	24,4 ± 0,6	27,4 ± 0,6	0,161
Waist-to-Hip ratio	0,86 ± 0,03	0,92 ± 0,01	0,083
Total body fat (%)	26,3 ± 2,1	37,9 ± 1,4	**0,002**
Glucose (mmol/l)	4,73 ± 0,15	5,93 ± 0,23	**0,048**
Insulin (pmol/l)	38,7 ± 8,9	123,8 ± 18,6	**0,023**
HOMA-IR	0,45 ± 0,11	1,81 ± 0,28	**0,011**
Bilirubin (mmol/l)	8,00 ± 1,32	12,69 ± 0,89	0,461
AST (U/l)	28,4 ± 2,6	22,1 ± 1,3	0,579
ALT (U/l)	40,9 ± 8,9	19,2 ± 1,5	**0,007**
Triglycerides (mmol/l)	1,07 ± 0,21	1,21 ± 0,11	0,856
Total cholesterol (mmol/l)	4,68 ± 0,31	5,08 ± 0,16	0,813
HDL cholesterol (mmol/l)	1,36 ± 0,07	1,33 ± 0,06	0,951
LDL cholesterol (mmol/l)	2,91 ± 0,32	3,17 ± 0,14	0,852
TNFα (pg/ml)	2,91 ± 0,28	4,96 ± 0,61	**0,003**
MCP-1 (pg/ml)	119,9 ± 7,0	252,1 ± 30,3	**<0,001**

Table 3. Demographic and body composition parameters and metabolic and inflammation markers. Parameters are expressed as mean ± s.e.m. unless specified. P values were calculated using Student´s t test for parametric data. Bold lettering is shown when P < 0.05; BMI, body mass index; HDL, high-density lipoprotein; LDL, low-density lipoprotein, HOMA-IR, homeostasis model assessment of insulin resistance; TNFα, tumor necrosis factor-α; AST, aspartate transaminase; ALT, alanine transaminase; MCP-1, monocyte chemoattractant protein-1.

2. Analysis of FGF21-responsive molecular machinery across aging in subcutaneous adipose tissue

We analyzed FGF21 serum levels and alterations in the expression of genes encoding components of the FGF21-responsive molecular machinery in adipose tissue from aged individuals so as to ascertain whether altered FGF21 responsiveness that develops with aging jeopardizes human health and/or accelerates metabolic disturbances associated with aging.

Serum FGF21 levels were significantly increased in elderly individuals compared with young healthy controls (Figure 35A). FGF21 levels were positively correlated with glucose levels ($r = 0.197$, $p = 0.048$), insulin levels ($r = 0.224$, $p = 0.038$), and insulin resistance, measured as HOMA-IR, ($r = 0.427$, $p = 0.005$) in the studied cohort. The levels in serum of FGF19, another endocrine FGF that originates in the intestine whose effects are also mediated by β-Klotho, were unaltered with aging (Figure 35A).

We obtained subcutaneous adipose tissue biopsies from elderly (n = 13) and young control (n = 10) individuals and analyzed several components of the FGF21-responsive molecular machinery. We found that expression of the β-Klotho gene was significantly increased in elderly individuals compared with young healthy controls (Figure 35B). Expression of the gene for FGF receptor-1 (FGFR1), the main FGF receptor that mediates FGF21 action in adipose tissue[304], was not changed (Figure 35B).

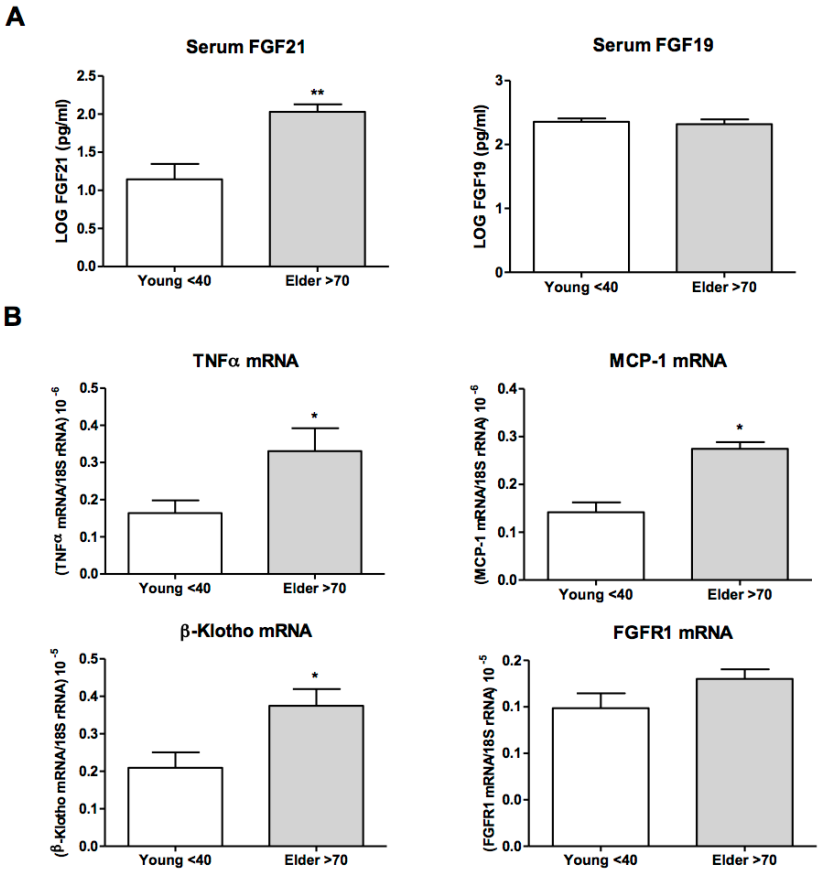

Figure 35. FGF21 serum levels and expression of genes encoding pro-inflammatory cytokines and components of the FGF21-responsive molecular machinery in adipose tissue from young and aged individuals. (A) Serum levels of FGF21 (left) and FGF19 (right) in young healthy controls (≤40) and elderly individuals (≥70). Serum levels of FGF21 and FGF19 are log-transformed. **(B)** TNFα, MCP-1, β-Klotho, and FGFR1 mRNA expression in subcutaneous adipose tissue from young healthy controls and elderly individuals. Values are expressed relative to 18S rRNA. The bars represent means ± s.e.m. Two-tailed unpaired Student's t-test (*p<0.05 and **p<0.01 for comparisons between young healthy controls and elderly individuals).

In line with gene expression results the protein levels measured by immunoblotting of β-Klotho, which determine the specific responsiveness of cells to FGF21 and FGF19, were higher in subcutaneous adipose tissue from elderly individuals compared with those from healthy young controls (Figure 36). Moreover, we found decreased ERK1/2 protein levels in elderly individuals, accompanied by an increase in the extent of ERK1/2 phosphorylation. Thus, resulting in a significantly higher ratio of phospho-ERK1/2 to total ERK1/2 protein, a marker of the extent of intracellular signaling driven by FGF21, in adipose tissue from elderly individuals than in those from young controls (Figure 36), indicating that the abnormally elevated FGF21 levels in healthy aging are not associated with repressed FGF21-responsiveness machinery in adipose tissue.

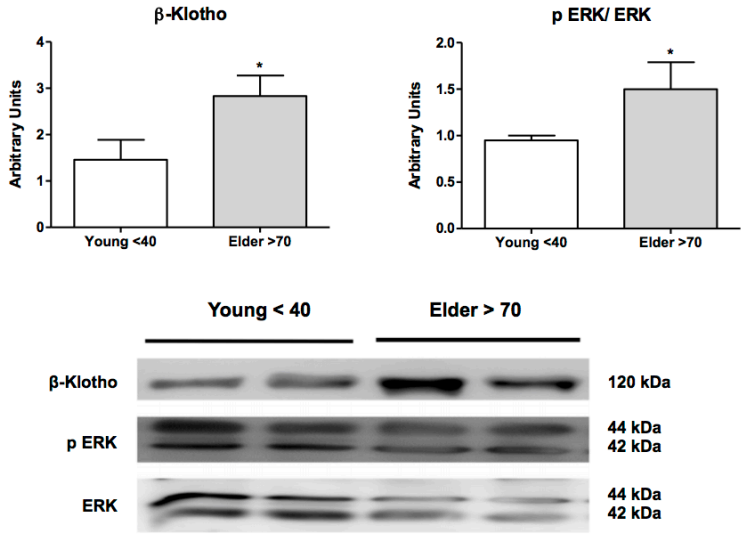

Figure 36. Immunoblotting of FGF21-responsiveness machinery components in adipose tissue from young and aged individuals. Levels of β-Klotho protein (left) and ERK1/2 phosphorylation (right) in subcutaneous adipose tissue from young healthy controls and elderly individuals. Representative immunoblot images (down). Signal intensity was determined by densitometry quantitation of protein bands in immunoblot images (six individual samples per group). Phospho-ERK1/2 levels were expressed relative to total ERK1/2. Membranes were stained with Coomassie Blue to normalize the amount of protein loaded. The bars represent means ± s.e.m. Two-tailed unpaired Student's t-test (*p<0.05 for comparisons between young healthy controls and elderly individuals).

As mentioned above, we found that plasma levels of the pro-inflammatory cytokines, TNFα and monocyte chemoattractant protein-1 (MCP-1), were significantly higher in healthy elderly individuals than in young controls (Table 3). Moreover, we found that the expression of TNFα and MCP-1 genes in adipose tissue was increased in healthy elderly individuals compared with young controls (Figure 35B). Thus, locally increased expression of TNFα in aging does not appear to lead to impaired β-Klotho expression in adipose tissue. In this context, a correlation analysis revealed a positive correlation of systemic levels of TNFα ($r = 0.376$ and $p = 0.017$) with circulating levels of FGF21 in the studied cohort.

3. Functional analysis of FGF21 effects on adipose tissue explants from aged mice

Considering that ethical and practical issues precluded the functional analysis of FGF21 effects on fresh adipose tissue from aged healthy humans, a mouse model was employed.

Aged mice (15-month-old) showed a profile of alterations relative to young (5-month-old) mice partially consistent with human data: plasma FGF21 levels were increased in relation to aging, whereas there were no signs of impaired mRNA expression of mediators of FGF21 signaling such as *Fgfr1* and *β-klotho* in subcutaneous adipose tissue, and a mild reduction in β-klotho protein levels (Figure 31, Results Part 1). The pattern of changes in mice at advanced age (23 months old) was more discordant from data in humans, evidencing a marked decline in *β-klotho* and *Fgfr1* genetic expression (Figure 31, Results Part 1). Under this scenario, we chose explants of adipose tissue from 15-month-old mice (middle-aged) and 5-month-old mice (young) and treated them with FGF21 *in vitro* to determine responsiveness. FGF21 treatment caused a significant induction in the ratio of phospho-ERK1/2 to total ERK1/2, as well as of expression of *Egr1* and *c-Fos*, early-responsive genes to FGF21[305]. The extent of FGF21 effects was not different in adipose tissue from aged and young mice (Figure 37) thus supporting unaltered responsiveness of aged adipose tissue to FGF21, as suggested by human data.

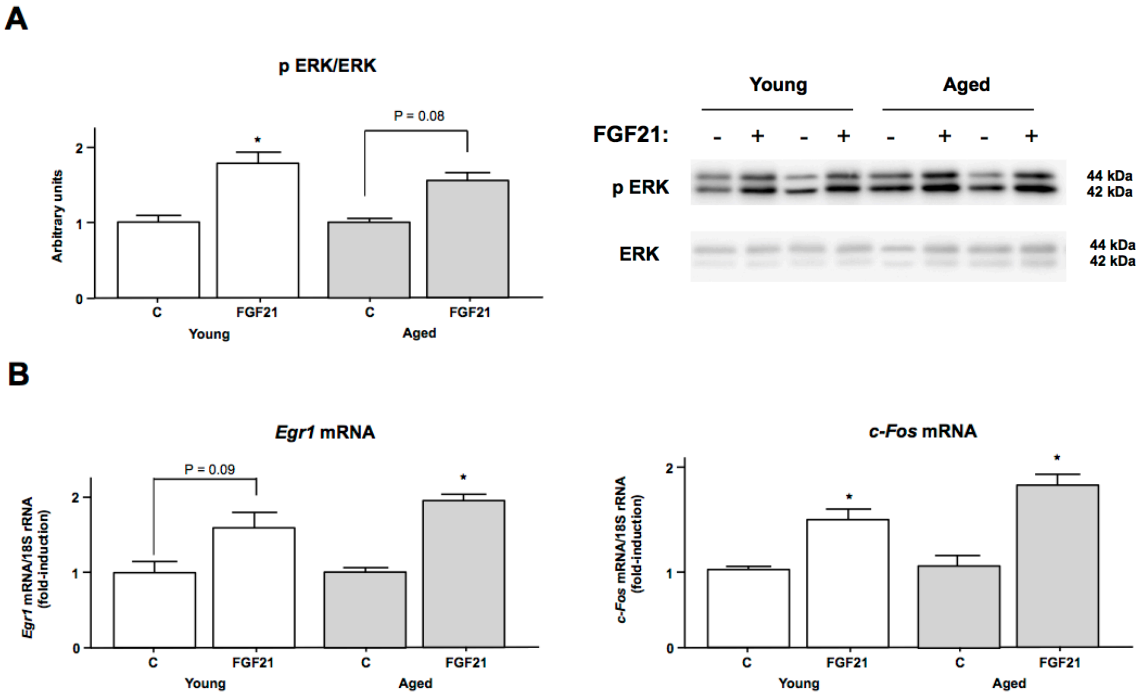

Figure 37. FGF21 *in vitro* responsiveness in adipose tissue explants from 5-month-old mice (young) and 15-month-old mice (middle-aged). (A) Levels of ERK1/2 phosphorylation and **(B)** *Egr1* mRNA, and *c-Fos* mRNA in mouse adipose tissue explants from young (5-month-old) and aged (15-month-old) mice treated with 30 nM FGF21 and non-treated controls (four mice, triplicate explant analysis per mouse). The bars represent means ± s.e.m. Two-tailed unpaired Student's t-test (*p<0.05 for comparisons FGF21-treated vs. non-treated adipose explants).

4. Separate analysis of young and elderly individuals by biological sex

Finally, considering that mouse studies were systematically performed in male mice and the human cohort study included both men and women, we checked for potential changes in circulating and gene expression parameters between men and women. Our data (Table 4) indicated no sex-associated differences in these parameters either in young or elderly individuals.

Serum levels	**Young Male (23)**	**Young female (12)**	P value male vs. female	**Elderly male (14)**	**Elderly female (14)**	P value male vs. female
FGF21 (pg/ml)	57 ± 11	46 ± 10	0,47	132 ± 23	180 ± 34	0,28
FGF19 (pg/ml)	266 ± 31	250 ± 64	0,83	495 ± 99	375 ± 114	0,44

mRNA/ 18S rRNA	**Young Male (5)**	**Young female (5)**	P value male vs. female	**Elderly male (7)**	**Elderly female (6)**	P value male vs. female
β-Klotho ($x10^{-5}$)	1,81 ± 0,64	2,59 ± 0,79	0,46	3,56 ± 0,71	4,04 ± 0,88	0,57
MCP-1 ($x10^{-5}$)	1,77 ± 0,68	1,41 ± 0,22	0,77	2,39 ± 0,37	3,01 ± 0,41	0,26
TNFα ($x10^{-6}$)	1,81 ± 0,85	1,91 ± 0,51	0,95	2,88 ± 0,70	3,61 ± 0,81	0,54
FGFR1 ($x10^{-4}$)	1,39 ± 0,57	1,71 ± 0,21	0,68	1,64 ± 0,23	1,87 ± 0,48	0,69

Table 4. Serum and mRNA levels in adipose tissue from young healthy controls and elderly individuals separated by sex. Data represent means ± s.e.m. Two-tailed unpaired Student's t-test.

5. Transcript levels of Parkin and autophagy related genes in adipose tissue from elderly individuals

In the context of our studies of aging in human adipose tissue, the expression of Parkin mRNA and other transcripts encoding components of the autophagic machinery were measured in aged and young subcutaneous adipose tissue. The expression of Parkin mRNA was unaltered in aged versus young adipose tissue (Figure 38). Genetic expression of ATG4A, ATG4D and GARBAP, whose function is related to the formation of the phagophore, was also unaltered in relation to aging, whereas the transcript levels of ULK1 and BNIP3 were significantly reduced in aged in comparison with control young adipose tissue (Figure 38). These findings indicate that, despite the assumption of impaired autophagy in aged tissues, this is only partially reflected on transcript levels in adipose tissue from elderly individuals.

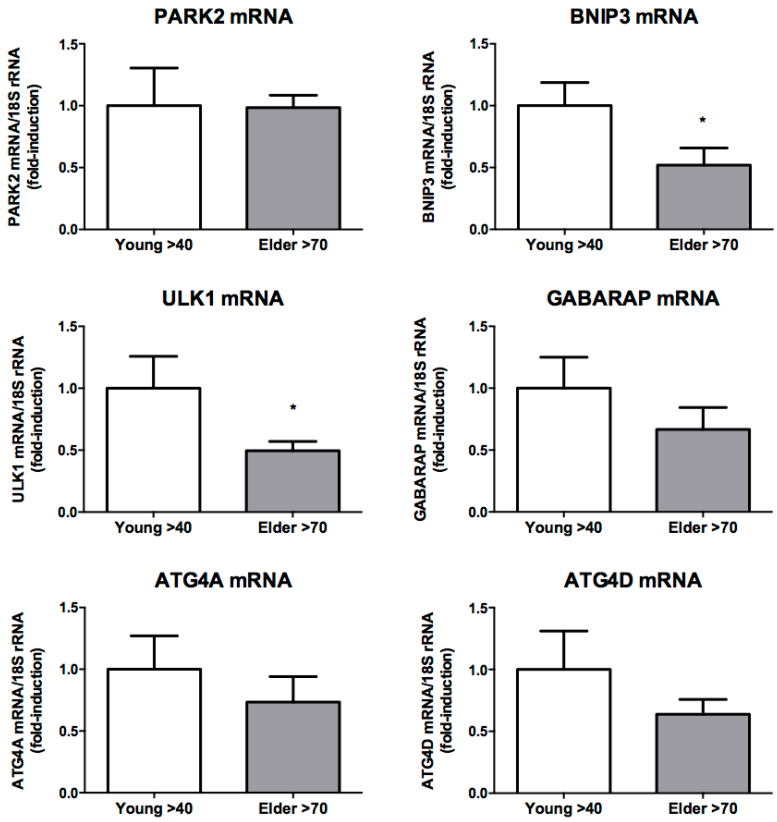

Figure 38. Expression of genes encoding autophagic machinery components in adipose tissue from young and aged individuals. Values are expressed in folds relative to 18S rRNA. The bars represent means ± s.e.m. Two-tailed unpaired Student's t-test (*p<0.05 for comparisons between young healthy controls and elderly individuals).

It will be necessary to determine whether the lack of changes in Parkin mRNA levels in adipose tissue from elderly individuals, which contrasts with findings in mice, is reflected also in unaltered (or not) Parkin protein levels. The samples limitations due to adipose tissue sample size from elderly individuals precluded this determination in the current thesis, but it would be needed in the future to ascertain whether the systematic up-regulation of Parkin in association with aging in rodent tissues is also occurring in humans.

Discussion

Aging in adipose tissues in mice

The first part of this thesis, focused in the aging of mouse models was based in establishing 3 different phases of aging of mice: adult (5-month-old), middle-aged (15-month-old) and old (23-month-old). This phases correlate to humans from around 25, 50 and 65 years old, respectively[306] (Figure 39).

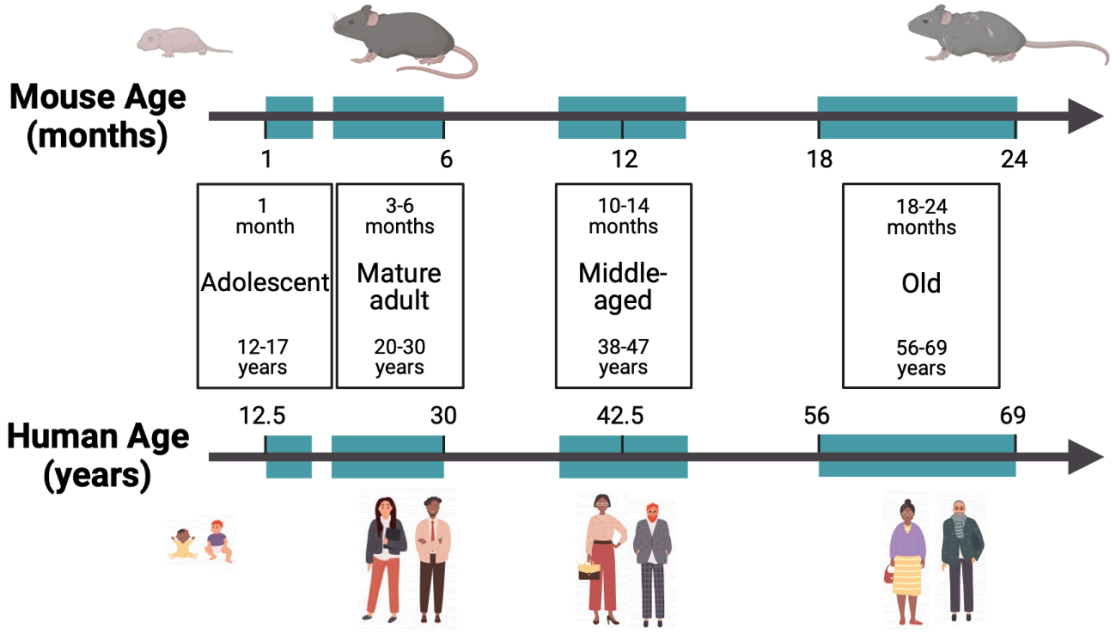

Figure 39. Life history stages in C57BL/6J mice in comparison to human beings. Adapted from https://www.jax.org/news-and-insights/jax-blog/2017/november/when-are-mice-considered-old

A middle-aged group is helpful in order to determine if an age-related change is progressive or is first expressed only in old age. In contrast, when old age is reached senescent changes can be detected in almost all biomarkers in all animals. For Parkin-KO (B6.129S4-Park2tm1Shn/J) mice and many other genotypes, such as C57BL/6J mice, the upper limit is around 24 months, when the onset of strain-specific diseases can affect biomarkers and produce misleading results. At the age of 25 months, Parkin-KO mice exhibited locomotor impairments, including hindlimb defects and neuronal loss. In addition, damaged mitochondria were found to accumulate in dopaminergic neurons. These data suggested that impairment of mitochondrial clearance might underlie the pathology of PD[275].

In our rodent model, the morphometric parameters and tissue weight in the animals studied clearly reflected the different phases of aging. There was an increase in body weight and adiposity associated with aging in 15 months old wild-type mice compared with 5 months old wild-type mice, evidenced by massive increase in the size of all adipose depots. In 23-months-old wild-type mice, body weight was lowered relative to 15-month-old mice in parallel with the regression of white adipose tissue amounts found in mice at this advanced age. These alterations in adiposity in our mouse model across aging where reminiscent to the stages of aging in humans. Typically, human's fat mass increases across aging until advanced ages[173], in which there is a relative decline in fat especially in subcutaneous fat depots[191]. The inability of subcutaneous adipocytes to act as metabolic sinks in advanced age and the subsequent accumulation of lipids within visceral fat, liver, muscle and other ectopic depots is known to be a biomarker of biological aging[191]. Overall, this scenario was represented in our rodent model. This alteration has also been strongly associated with several deleterious health outcomes such as dyslipidemia, insulin resistance and even mortality[191].

We also observed some systemic metabolic derangements in association with advancing age. Wild-type mice at 15 months of age had higher blood glucose and plasma insulin as well as reduced glucose tolerance and insulin responsiveness relative to the younger 5-month-old wild-type mice. At 23 months, the insulin resistant phenotype observed at 15 months, as happened with obesity, was reversed. These results pointed that when approaching the end of life there is a reduction in adiposity and concomitant improvement in insulin sensitivity. Our data is consistent with previous studies on the effects of age on insulin action and body composition[296-298,307,308].

Regarding leptinemia, leptin plasmatic levels and genetic expression in WAT paralleled the changes in body weight and composition with aging. There is an increase in leptin levels, together with weight gain or obesity in the middle-aged mice. These changes might be explained as overproduction of leptin due to the large amount of fat tissue. It cannot be excluded that leptin levels increase as a compensatory mechanism due to a simultaneous resistance to the peptide, as indicated by its failure to reduce food intake, to increase metabolic rate and thereby to induce weight loss. Leptin resistance is a common feature of early aging and obesity (even in the young). Later, there is a decrease in leptin levels, loss of weight and sarcopenia (corresponding to the human later elderly phase of life). Body composition rather than age is determinant for the sensitivity to central and peripheral metabolic effects of leptin as discussed elsewhere[309].

Aging has been postulated as one of the most relevant determinants of BAT activity. Furthermore, it exists the assumption of an age-related ubiquitous decline in BAT thermogenesis throughout life in humans and rodents. Even though there is an association between obesity and age, in which BAT function has a potential role, little is known about the features of age-related functionality of rodent BAT. In humans, the amount of detectable BAT measured through FDG-PET/CT to visualize BAT in live subjects declines with advancing age[310,311]. Nevertheless, the loss of BAT might not be lineal; it may rather plateau around the sixth decade of life and further decrease in the senectitude, as cold-stimulated BAT is rarely detected over the age of sixty[215]. In the present study we set out to establish the morphologic and functional changes that occur in BAT with aging in mice.

We reported an increase in iBAT depot size in association with aging in 15-month-old mice. No loss of "brown color" intensity nor major changes in cellular fat droplet were found at that aging stage, indicating that changes in size were not associated to massive "whitening" (fat accumulation) of the BAT depot. Moreover, BAT protein portion followed the same pattern of changes across aging. In 23-month-old mice iBAT mass and protein portion decreased to levels like those found in 5-month-old mice. In other studies, larger lipid droplets in the cytoplasm were observed in the brown adipocytes of advanced-aged mice, suggesting a lowered BAT activity when reaching senectitude[312,302]. We do not know whether the reasons for this discrepancy can be attributable to differences in the mouse strains and/or environmental conditions.

In our attempt to assess the impact of aging in BAT functionality, we used a CL316,243 acute treatment, a compound that activates β_3-adrenergic receptors bypassing the physiological sympathetic nervous system (SNS)-stimulated events induced by cold via central nervous system. Our data demonstrates that *in vivo*-induced thermogenic capacity in middle-aged mice is moderately altered in comparison with adult mice. There was a mild reduction in the thermogenic response in comparison with 5 months old adult mice, evidenced by a moderate lowering of BAT maximal induction and respiratory capacity in response to the treatment. This was consistent with previous observations[302,313].

Despite the increase in potentially functional BAT mass and the retained capacity to respond to thermogenic challenges in middle-aged mice, we detected a series of signs of altered function in their BAT. It was found a reduction in mRNA expression of thermogenic and respiratory chain markers in BAT in relation to aging. No relevant changes were where found regarding the transcript levels of components of the lipid metabolism or autophagy. In addition, we observed that aging led to a deviation towards a pro-inflammatory environment as evidenced by a trend to reciprocal changes in type I and type II cytokines transcript levels in the tissue. These changes were not different to those reported previously in mice aging or mice under a sustained obesogenic diet[232,302].

A reduction in mtDNA levels in BAT across aging was also detected in our study, similarly to what is observed in the adipose tissue and other tissues of mice with obesity or insulin resistance[314,315]. Besides, we found alterations in the characteristic parallel arrangement in mitochondria in electron microscopies of BAT in association with aging. In this way, the protein expression of some mitochondrial OXPHOS components tended to be reduced in middle-aged mice. Nevertheless, these changes did not seem to have an impact in mitochondrial complexes enzymatic activity, when assessed *in vitro*.

Remarkably, we reported a diminution in BAT tyrosine hydroxylase levels, indicative of reduced SNS innervation, which suggest that the local sensitivity to the SNS may be impaired within aged BAT in a similar way to what is reported in obesity[316].

In summary, in this study, we were able to observe some parameters indicative of altered BAT function in middle-aged mice. However, these changes did not result in a massive loss of basal thermogenesis and thermogenic response to β_3-adrenergic receptor stimulation in the BAT at this specific aging stage.

In the BAT of 23-month-old mice, modeling advanced aging, we were surprised to find that some parameters, such as BAT mass, were reverted in comparison to middle-aged mice, reaching values like those found in adult, 5-month-old, mice. In contrast, other parameters continued to decline and eventually were even worse (e.g., thermogenic, OXPHOS, lipid metabolism and pro-inflammatory gene markers or mitochondrial cristae distribution).

Concerning WAT, in our mice subcutaneous adipose tissue, we reported some profound changes in relation to advancing age. Mainly, we first found an enlargement of the iWAT depot in 15-month-old mice in comparison with adult, 5-month-old mice and further reduction in 23-month-old mice. At 15 months old, we observed in middle-aged mice a phenotype reminiscent of obesity: increased adipocyte size, leptin and pro-inflammatory cytokines transcript levels. This is consistent with previous research[317].

The age-associated obesity in middle-aged mice is accompanied by a collapse in the basal thermogenesis indicators like thermogenic marker genes, reduced tyrosine hydroxylase, indicative of SNS innervation and noradrenaline output into the tissue, reduced levels of mtDNA and reduced expression of adiponectin. This is also supported by previous evidence in which the consensus concerning beige adipocytes is that there is a progressive bias towards a white adipocyte phenotype, which impedes browning also in older humans[216,315,318]. In a similar way, the inductive ability of beige adipocytes in WAT declines with increasing age in mice when they are treated with CL316,243 for a week. This reduction is argued to be partly because of fewer progenitor cells associated with aging[302].

One long-standing question has been to what extent alterations in BAT decline account for systemic derangements associated with aging. In this regard, our data evidencing mild reduction in BAT activity in middle-aged animals would not support a massive effect. This raises the question whether mice are fully appropriate models for human aging studies, considering the awareness of a more dramatic decline in BAT activity in elderly individuals. It is true that, in the last stage of aging, mice are considerably more susceptible to cold than are comparably middle-aged pre-senescent mice[319], which could be related to the shrinkage in brown and beige adipose depots. It seems that many forms of BAT, if not all, potentially suffer a transition towards a WAT phenotype with advancing age both in rodents and humans. These facts may also be determinant to explain why the elder population worsens their tolerance to cold and their ability to control body temperature.

FGF21 system and adipose tissue in aging: mouse and human studies

We found a dramatic induction of plasma FGF21 levels in 15-month-old and 23-month-old mice relative to younger 5-month-old mice. This age associated induction in plasmatic FGF21 levels was accompanied, at 15 months old mice, by an increase in the expression of the *Fgf21* gene in BAT (1.5-fold), iWAT (3-fold), and liver (1.5-fold). Parallel to these events, we detected in adipose tissues, especially BAT, a trend of aging-associated decline in the expression of *Fgfr1* and *β-klotho*, mediators of the cellular actions of FGF21. The age-associated decrease in β-klotho was also translated to protein levels in these adipose depots. Those changes were not replicated in the liver, the main production site of FGF21 in standard physiological conditions. At 23 months old, although the plasmatic levels of FGF21 continued to be highly induced in comparison with adult mice, we did not observe changes in the transcript levels of *Fgf21* in adipose tissues or liver in relation to 5 months old mice. Yet, in advanced aging adipose tissues the decrease in genes encoding the FGF21 receptors were remarkably lowered.

These results highlight the importance of changes in the FGF21 endocrine system in aging. Furthermore, they might be related to an incipient state of resistance to FGF21 in adipose depots at 15 months old that would lead to the worsened situation found at 23 months old advanced-age mice. The high hormone levels did not seem to be effective in the maintenance of glycemia either to protect these mice from obesity. This possibility concurs with previous research arguing that the down-regulation of β-klotho protein in many metabolic disorders related to aging lead to an increase in FGF21 resistance e.g., in adipose tissue of high-fat-diet induced obesity in non-human primates[320], in the hearts of obese rats[321], in mouse non-alcoholic fatty liver disease[322] and in the pancreatic islets of mice modeling diabetes[323]. Moreover, the expression of β-klotho protein is crucial to sensitize FGF21 signaling in the adipose tissues of male mice to prevent obesity and promote thermogenesis[324,325]. Nevertheless, in the case of aging the reduction of β-klotho expression might also be a negative feedback mechanism to combat against chronic activation of FGF21 signaling. This might generate the above-mentioned FGF21 resistance, a phenomenon observed in many chronic inflammatory conditions.

There is rising evidence that FGF21 can alleviate many metabolic disorders common in aging, such as atherosclerosis, cardiovascular diseases, and metabolic pathologies[326-329]. The functions of FGF21 promote the maintenance of healthspan and thus increase life expectancy. Interestingly, there are clear indications that the overexpression of FGF21 can protect against age-related changes, e.g., delay thymic involution[330], and even extend the lifespan of mice[228,331]. FGF21 is not only coordinator of multi-organ energy metabolism, but it is also a stress hormone which can elicit adaptive stress responses, e.g., to combat oxidative stress[327]. Mitochondrial stress as well as ER stress triggers an integrated stress response pathway to alleviate and counteract the controversial effects of these stressors. In fact, increased level of serum FGF21 was established as a feasible diagnostic biomarker for deficiencies in mitochondrial respiration in skeletal muscles[332]. In our model, FGF21 expression and its secretion may be induced as a stress hormone by dysfunctions of mitochondria and reduced mitochondrial respiration in aged metabolic tissues, such as adipose tissues and liver. However, as discussed above, the chronic metabolic and stress-related disorders provoke FGF21 resistance, which might jeopardize the healthy aging process.

We performed a functional analysis on fresh iWAT explants from mice in order to determine the responsiveness of aged adipose tissue to FGF21. *In vitro*, acute FGF21 treatment was able to induce its downstream responsive machinery, such as P-ERK/ERK ratio and the expression of the early-responsive genes *Egr1* and *c-Fos*. The magnitude of FGF21 effects was unaltered between middle-aged and adult mice. This suggests that in the incipient stage of aging there is not a concomitant impairment of responsiveness of subcutaneous adipose tissue to FGF21. Given that the genetic expression of the FGF21 receptors system is highly reduced in an advanced stage of aging, it cannot be excluded that the same study performed in iWAT explants from 23-month-old mice might have resulted in a different outcome. It is worth mentioning that there are limitations in the *in vitro* model (i.e., relying only in short-term cellular events responsive to FGF21). Thus, conclusions from that *in vitro* experiment indicative of unaltered responsiveness to FGF21 should be taken with caution.

The importance of FGF21 system in aging led us to study this pathway specifically in a human clinical setting, especially on the basis of availability of a unique cohort of healthy young and elderly patients who agreed to provide serum and adipose tissue biopsies (Part 2). The increase in serum FGF21 levels in elderly individuals in relation to young controls was in line with previous reports describing an increase in FGF21 levels with aging[229]. However, the inverse relationship observed between FGF21 and FGF19 in obesity and diabetes[333] -upregulation of FGF21 and downregulation of FGF19- did not occur in healthy elderly individuals, despite the significant increase in FGF21. Even if healthy elderly individuals suffered local (adipose tissue) and systemic inflammation, β-Klotho expression was not impaired by pro-inflammatory signals in our clinical setting. In addition, and contrary to expectations, expression of β-Klotho and markers of FGF21 action in this FGF21-target tissue actually increased.

Our findings also confirmed that healthy human aging is associated with increased FGF21, despite the appearance of mild signs of distorted glucose homeostasis and increased inflammation associated with healthy aging; in fact, it is likely that these metabolic stressors are involved in the increase in FGF21. Thus, either FGF21 resistance *per se* does not occur during human aging or tissues other than subcutaneous fat are the actual source of such resistance. As shown above, even in middle-aged mice we could not see marked signs of impaired FGF21 action in white adipose tissue. Identification of the brain as a target of FGF21[334] highlights the possibility of a resistance to FGF21 in the brain as a particularly relevant concept in further aging research. In either case, these results are distinct to the situation that prevails in obesity, diabetes, and lipodystrophy[333,335]. As a result, further intervention-based studies, although difficult to undertake, would be required to fully determine systemic and tissue-specific sensitivity to FGF21 in human aging.

FGF21 is a representative metabokine that is responsive to mitochondrial diseases just as GDF15. Their expression is stimulated through key components of the integrated stress response and they have been well-documented as modulators to improve numerous metabolic processes or diseases[153]. The physiological role of GDF15 also has an overlapping functional spectrum with FGF21, especially in terms of energy metabolism. We assessed the changes in GDF15 plasma levels and its genetic expression during aging.

A similar pattern to FGF21 levels alterations is also observed for GDF15 changes throughout aging in mice. There was an increase in plasmatic GDF15 levels in middle-aged controls, which might be also attributable to an induction of the integrated stress response pathway in metabolic organs at that age. The age-associated increase in GDF15 plasma levels was paralleled by an induction in the transcript levels of this factor in tissues such as BAT and heart but not in liver and WAT. At 23 months of age the levels of GDF15 in plasma and BAT were reduced to a similar level to that found in 5-month-old mice.

GDF15 has been reported as a protein elevated in serum in response to mitochondrial stress and dysfunction[336], as occurring in primary mitochondrial diseases with genetic origin[337,338]. Although GDF15 serum levels are known to increase in metabolic stress-mediated inflammation[153], its role in aging remained largely unclear. Recently, it was found that GDF15 production in response to mitochondrial stress is a homeostatic mechanism protecting from aging-induced systemic inflammation and metabolic syndromes in humans and mice[339]. This discovery is very coherent with our findings in the 15-month-old mouse model in which we reported an incipient mitochondrial dysfunction. Nevertheless, the relative contribution of GDF15 expression in BAT and WAT to changes in systemic GDF15 levels across aging and also in other pathophysiological conditions is unknown.

Effects of Parkin invalidation on adipose tissues and FGF21 system in aging

Parkin deficient mice were initially generated in order to mimic the human early-onset parkinsonism, in which mutations in Parkin gene caused the pathology. Nevertheless, germline deletion of Parkin in mice resulted in relatively subtle neurological effects, as these animals do not develop intense early onset Parkinson's disease. Instead, as it was stated above, those mice only started to show symptoms compatible with the disease at very advanced ages or when they were subjected to further disruptive stimuli, like when they are crossed with the proofreading-deficient mitochondrial polymerase mice[340]. These facts suggested that there might be separated programs for basal and stress-induced mitophagy. Definitely, these mice ended up being useful tools to ascertain the physiological role of Parkin, especially after evidence in cell models (often not mammals) of a relevant role of Parkin in mitophagy in distinct cell types, including brown adipocytes[287].

Previous experience in our laboratory contributed to demonstrate the importance of Parkin in adiposity. Not only was it corroborated that Parkin is involved in adipogenesis, as young Parkin-KO mice were resistant to metabolic complications upon a high fat diet, but it was also proven that Parkin controls BAT plasticity in response and after thermogenic stimuli[287].

Before the writing of the present thesis, background research postulated that aging was related to a ubiquitous decline in BAT thermogenesis throughout life in humans and rodents[216]. Besides, autophagy is found to be reduced with advancing age[264] and, in a similar way, the activity of mitophagy was found to decrease during aging in some species and/or tissues[265]. In this PhD thesis one of our goals has been to explore the role of Parkin and potential Parkin-mediated autophagy in the aging of brown and white adipose tissues using male Parkin-KO mice as a model.

Before considering the role of Parkin in the metabolism of adipose tissues, we first assessed how is the behavior of Parkin expression in these metabolic tissues in association with aging. Surprisingly, we found an up-regulation in Parkin transcript and protein levels in relation to aging in adipose tissues that was not previously reported. At a first glance, this would be apparently in contrast with evidence of reduced mitophagy in other tissues that contribute to aging phenotypes. For instance, decreased mitophagy was observed in the hippocampal dentate gyrus in 21-month-old mice compared to 3-month-old mice[265]. Defective mitophagy is also observed in skeletal muscle satellite cells isolated from elderly humans and mice[341]. By contrast, similarly to our observations in adipose tissues, scattered reports indicate that other tissues exhibit increased expression of Parkin protein in association with aging, such as cerebral vessels[342], heart, liver and brain tissues[343]. Finally, it is reported that in obesity, an age-associated condition, the PINK1-Parkin pathway was increased in adipose tissue, playing a protective role against metabolic stress[307].

Since mammalian cells contain many mitochondria that are heterogeneous (i.e., distinct levels of membrane potential, respiratory activity, and oxidative damage), they may have needed to additionally evolve towards signaling through diverse mitophagic pathways that establish selectivity toward dysfunctional mitochondria versus healthy mitochondria, raising the possibility that age-related changes in mitophagy vary in some cell types and/or tissues. So, it is expectable the existence of cell-specific mitophagic pathways in order to ensure a healthy mitochondrial network in each cell-type. Maybe, our finding on the age-associated increase in Parkin levels in adipose tissues could also be attributed to a compensatory mechanism to respond to a decline in mitophagy elicited by other actors different from Parkin. In fact, our current observation that the presence of autophagosomes is observed similarly in BAT from Parkin-KO mice and wild-type mice would be consistent with the existence of mechanisms of autophagy not requiring Parkin as an actor.

In relation to the age-associated increase in adiposity, we observed a protection against this phenotype in Parkin-KO mice in comparison to wild-type controls in all the age stages studied. This reduced adiposity in Parkin-KO mice is correlated with decreased body weight and is consistent with other studies using these mice, and even flies as a model[273,285,344,345]. We found also that the changes in adiposity were not exclusively attributable to a decline in food intake in aged Parkin-KO mice in comparison with control, age-matched, wild-type mice. We estimated the metabolic energy efficiency and we could see how Parkin-KO mice showed also a reduction in this parameter in relation to aged controls, revealing that energy expenditure-related processes are also involved in mediating in the differences found in body weight and adiposity between aged wild-type and Parkin-KO mice. Another piece of evidence supporting this notion is that we observed a slight increase in basal oxygen consumption in middle-aged Parkin-KO mice, an estimate of energy expenditure, in comparison to wild-type mice at 15 months of age.

There are previous indications that Parkin may be involved in lipid usage as metabolic fuel based on reports of reduced fat uptake in Parkin defective cell cultures of fibroblasts, adipocytes and transformed B cells[285]. Our findings of a balanced respiratory quotient slightly deviated towards carbohydrates in 15-month-old Parkin-KO mice together with the impaired reduction in that parameter in response to β_3-adrenergic stimulus suggest alterations in the metabolic flexibility of lipid versus carbohydrate metabolism in the absence of Parkin, but further research will be needed to ascertain the mechanistic role of Parkin in the specific lipid metabolic pathways in adipocytes and, in general, in the organism.

Regarding BAT function, although reduced mass was apparent in Parkin-KO iBAT depots, especially in 15-month-old animals, no major changes in cellular fat droplet accumulation or protein portion were found in comparison to wild-type mice with advancing age. In the *in vivo* determination of iBAT thermogenic activity in response to CL316,243 injection, we found that the local increase in skin temperature at the interscapular region of mice was mildly reduced in 15-month-old Parkin-KO mice relative to age-matched wild type mice. This phenomenon is consistent with an even more intense reduction in transcript levels of thermogenic markers in Parkin-KO mice BAT during aging. Moreover, we detected changes reflecting altered function in Parkin-KO mice BAT with advancing age, as we did in the aging of wild-type mice. For instance, it was found a similar bias towards a pro-inflammatory environment and reduced SNS innervation as control animals in relation to aging. Furthermore, we also detected alterations in the mitochondrial cristae arrangement in electron microscopies of BAT in association with age in Parkin-KO mice, as well as the decreased protein expression of some mitochondrial OXPHOS components. However, these changes in Parkin-KO mice did not seem to reverberate in mitochondrial complexes enzymatic activity when assessed *in vitro*. These findings support a scenario in which the lack of Parkin in BAT from Parkin-KO mice do not result in an enhanced BAT-mediated energy expenditure, they even show an opposite trend indeed. Thus, BAT activity does not seem to conduct the protection of Parkin-KO mice against aging-associated adiposity.

We had only very mild signs that browning of WAT could be involved in protection against obesity in 15-month-old Parkin-KO mice. Minor trends of enhanced thermogenic gene expression (i.e., only PGC1α significant induction) do not allow hypothesizing a massive browning of WAT eliciting enhanced energy expenditure in middle-aged mice lacking Parkin. We were surprised to find increased levels of tyrosine hydroxylase in WAT from 15-month-old Parkin-KO mice that would be indicative of enhanced SNS innervation. However, in our optical microscopy analysis we only found smaller white adipocytes in middle-aged Parkin-KO mice that are likely to be consequence of reduced fat accretion. In addition, we did not find appearance of multilocular adipocytes that would have been indicative of browning. Perhaps at that stage of aging, when adipocyte precursors appear to be reduced in adipose depots, as mentioned above, even a SNS-mediated stimulus, as may be occurring in Parkin-KO mice, cannot achieve an overt enhancement of the browning of WAT.

Across our study of adipose tissue abnormalities in Parkin-KO mice, one of the most striking findings was the huge increase in mtDNA levels in adipose tissues of Parkin-KO mice in all the aging stages analyzed in our study. This induction in mtDNA levels can be interpreted as a defect in the degradation of mitochondria and an accumulation of these organelles in Parkin-KO mice, validating the KO model given the importance of Parkin in the clearance of defective mitochondria. Nevertheless, the extra copies of mtDNA did not seem to be translated into more functional proteins, as no marked changes were observed in the analyzed mtDNA-encoded transcripts, protein levels or enzymatic activities.

As a matter of fact, our data of enhanced mtDNA levels do not ensure the integrity of those mtDNA molecules and their functionality, as it cannot be discarded to reflect augmented fragments or dysfunctional mtDNA just not adequately eliminated due to the lack of Parkin. Additionally, mtDNA has been postulated as a potent immune system modulator. It can be released into the cytosol or the circulation to stimulate innate immunity response pathways, although the secretion mechanisms are not fully understood yet[346]. Again, although plausible, this is not reflected in a local increase in inflammation between Parkin-KO and wild-type control mice. It should be corroborated if mtDNA levels are also induced in serum in both genotypes to check whether or not Parkin is involved in the release of this element.

Major differences appeared also when analyzing parameters related to FGF21 system and GDF15 in Parkin-KO mice in comparison with wild-type control mice. Even though FGF21 and GDF15 circulating levels were up-regulated in 15-month-old control mice, we did not report such an increase of those mitochondrial stress-related metabokines in middle-aged mice lacking Parkin. The abolition of the induction in 15-month-old Parkin-KO mice in FGF21 and GDF15 circulating and transcript expression levels in the adipose tissues and liver might be tightly related to the prevention of obesity occurring in those animals, as FGF21 and GDF15 levels are known to correlate with obesity and nutritional overload[305,347,348]. As middle-aged Parkin-KO accumulates less fat in their bodies, they produce less FGF21 and GDF15. In the current experimental setting, neither mtDNA alterations in adipose tissues nor mitochondrial-related parameters had an impact into augmenting the transcript levels of marker genes related to oxidative and ER stress. These data suggest that integrated stress response did not seem to be activated by FGF21 and/or GDF15 in middle-aged mice when Parkin was absent.

At 23 months, Parkin-KO mice show an important induction in FGF21 and slight tendency to increase GDF15 circulating levels. In addition, we also reported reduced expression of FGF receptors system in adipose tissues in those animals. Nevertheless, *Fgf21* and *Gdf15* gene expression is not markedly induced in their adipose tissues or even the liver, suggesting that other tissues may play a role in the circulating induction of these stress-related hormones in those mice at that stage of aging. This is coherent as we reported indeed a reduction in the majority of oxidative or ER-stress genetic markers in the studied metabolic tissues. Thus, indicating that the integrated stress response pathway is not heavily induced by the mitochondrial changes in adipose tissues and liver from advanced age Parkin-KO mice similarly to what we observe in age-matched wild-type mice.

Conclusions

1. Aging in mice is characterized by:
   - a first period at middle aging (15 months old) characterized by increased body weight and adiposity, concurrent with hyperleptinemia along with hyperglycemia, hyperinsulinemia, reduced glucose tolerance and insulin. This is associated with signs of pro-inflammatory status in adipose tissues, reminiscent of obesity.
   - a final subsequent period of advanced aging (23 months old) in which adiposity is reduced, metabolic parameters are not worsened any more.

2. Aging results in alterations indicative of reduced BAT function in aged mice, although there is no evidence of a massive loss of basal and β_3-adrenergic receptor-mediated stimulation in middle-aged mice. Subcutaneous WAT also show signs of reduced browning in aged mice.

3. Concerning FGF21:
   - FGF21 levels and expression are increased in adipose tissues and liver from middle-aged mice, concomitantly with increased adiposity.
   - responsiveness of adipose tissue explants from middle-aged mice to FGF21 is unaltered.
   - expression of actors of cellular responsiveness to FGF21 are markedly reduced in adipose tissues in advanced aging.

   Therefore, it appears that in middle aging either FGF21 resistance does not occur or tissues other than subcutaneous fat are the actual targets of such resistance. Advanced aging is more likely to be associated with FGF21 resistance.

4. Serum FGF21 levels are increased in elderly humans in parallel with a mild deterioration of glucose homeostasis and increased inflammation, which might contribute by themselves to the increase in FGF21 in healthy aging. However, components of the FGF21-responsiveness machinery are up-regulated in elderly's subcutaneous adipose tissue.

5. Parkin transcript and protein levels are up-regulated throughout aging in adipose tissues from mice.

6. Middle-aged Parkin-KO mice develop less adiposity, which may be attributable to reduced food intake plus signs of enhanced energy expenditure. Abnormally high BAT activity does not appear to account for the protection of Parkin-KO mice against aging-associated adiposity.

7. Mitochondrial DNA levels are massively increased in BAT (and WAT) from aged Parkin-KO mice at all the aging stages analyzed in our study, but this does not result in marked changes in mtDNA-encoded transcripts, protein levels or mitochondrial oxidative enzymatic activities in BAT.

8. Lack of Parkin results in a protection against the middle age-associated increase in FGF21 levels and FGF21 expression in adipose tissues and liver, which may be secondary to reduced adiposity.

9. GDF15 levels and expression in BAT follow a pattern of changes in middle aging and in response to the lack of Parkin remarkably similar to FGF21.

Bibliography

1. WHO “Facts about overweight and obesity” *World Health Organization*, 1 Apr. 2020, https://www.who.int/news-room/fact-sheets/detail/obesity-and-overweight
2. Zafrir, B. "Brown adipose tissue: research milestones of a potential player in human energy balance and obesity." *Hormone and Metabolic Research* 45.11 (2013): 774-785.
3. Bays, Harold E. "Adiposopathy: is “sick fat” a cardiovascular disease?" *Journal of the American College of Cardiology* 57.25 (2011): 2461-2473.
4. Tamara, Alice, and Dicky L. Tahapary. "Obesity as a predictor for a poor prognosis of COVID-19: A systematic review." *Diabetes & Metabolic Syndrome: Clinical Research & Reviews* 14.4 (2020): 655-659.
5. Adan, Roger AH. "Mechanisms underlying current and future anti-obesity drugs." *Trends in neurosciences* 36.2 (2013): 133-140.
6. Rosen, Evan D., and Bruce M. Spiegelman. "What we talk about when we talk about fat." *Cell* 156.1-2 (2014): 20-44.
7. Ottaviani, Enzo, Davide Malagoli, and Claudio Franceschi. "The evolution of the adipose tissue: a neglected enigma." *General and comparative endocrinology* 174.1 (2011): 1-4.
8. Cinti, Saverio. "The adipose organ." Adipose tissue and adipokines in health and disease (2007): 3-19.
9. Dani, Christian, and Nathalie Billon. "Adipocyte precursors: developmental origins, self-renewal, and plasticity." *Adipose Tissue Biology*. Springer, New York, NY, 2012. 1-16.
10. Giralt, Marta, and Francesc Villarroya. "White, brown, beige/brite: different adipose cells for different functions?" *Endocrinology* 154.9 (2013): 2992-3000.
11. Hardouin, Pierre, Tareck Rharass, and Stéphanie Lucas. "Bone marrow adipose tissue: to be or not to be a typical adipose tissue?" *Frontiers in endocrinology* 7 (2016): 85.
12. Giordano, Antonio, et al. "White, brown and pink adipocytes: the extraordinary plasticity of the adipose organ." *Eur J Endocrinol* 170.5 (2014): R159-71.
13. Wu, Jun, et al. "Beige adipocytes are a distinct type of thermogenic fat cell in mouse and human." *Cell* 150.2 (2012): 366-376.
14. Peirce, Vivian, Stefania Carobbio, and Antonio Vidal-Puig. "The different shades of fat." *Nature* 510.7503 (2014): 76-83.
15. Walden, Tomas B., et al. "Recruited vs. nonrecruited molecular signatures of brown,“brite,” and white adipose tissues." *American journal of physiology-endocrinology and metabolism* 302.1 (2012): E19-E31.
16. Scheller, Erica L., et al. "Bone marrow adipocytes resist lipolysis and remodeling in response to β-adrenergic stimulation." *Bone* 118 (2019): 32-41.
17. Ambrosi, Thomas H., and Tim J. Schulz. "The emerging role of bone marrow adipose tissue in bone health and dysfunction." *Journal of Molecular Medicine* 95.12 (2017): 1291-1301.
18. Suchacki, Karla J., and William P. Cawthorn. "Molecular interaction of bone marrow adipose tissue with energy metabolism." *Current molecular biology reports* 4.2 (2018): 41-49.

19. Cinti, Saverio. "Anatomy of the adipose organ." *Eating and Weight Disorders-Studies on Anorexia, Bulimia and Obesity* 5.3 (2000): 132-142.
20. Gesta, Stephane, et al. "Evidence for a role of developmental genes in the origin of obesity and body fat distribution." *Proceedings of the National Academy of Sciences* 103.17 (2006): 6676-6681.
21. Medrikova, D., et al. "Sex differences during the course of diet-induced obesity in mice: adipose tissue expandability and glycemic control." *International journal of obesity* 36.2 (2012): 262-272.
22. Fuente-Martín, Esther, et al. "Sex differences in adipose tissue: it is not only a question of quantity and distribution." *Adipocyte* 2.3 (2013): 128-134.
23. Arner, P. "Obesity and the adipocyte. Regional adipocity in man." *J Endocrinol* 155 (1997): 191-192.
24. Sacks, Harold, and Michael E. Symonds. "Anatomical locations of human brown adipose tissue: functional relevance and implications in obesity and type 2 diabetes." *Diabetes* 62.6 (2013): 1783-1790.
25. Hany, Thomas F., et al. "Brown adipose tissue: a factor to consider in symmetrical tracer uptake in the neck and upper chest region." *European journal of nuclear medicine and molecular imaging* 29.10 (2002): 1393-1398.
26. Nedergaard, Jan, Tore Bengtsson, and Barbara Cannon. "Unexpected evidence for active brown adipose tissue in adult humans." *American Journal of Physiology-Endocrinology and Metabolism* (2007): 444-452.
27. Cypess, Aaron M., et al. "Identification and importance of brown adipose tissue in adult humans." *New England journal of medicine* 360.15 (2009): 1509-1517.
28. van Marken Lichtenbelt, Wouter D., et al. "Cold-activated brown adipose tissue in healthy men." *New England Journal of Medicine* 360.15 (2009): 1500-1508.
29. Virtanen, Kirsi A., et al. "Functional brown adipose tissue in healthy adults." *New England Journal of Medicine* 360.15 (2009): 1518-1525.
30. Cypess, Aaron M., et al. "Anatomical localization, gene expression profiling and functional characterization of adult human neck brown fat." *Nature medicine* 19.5 (2013): 635-639.
31. Sharp, Louis Z., et al. "Human BAT possesses molecular signatures that resemble beige/brite cells." PloS one 7.11 (2012): e49452.
32. Saito, Masayuki, et al. "High incidence of metabolically active brown adipose tissue in healthy adult humans: effects of cold exposure and adiposity." *Diabetes* 58.7 (2009): 1526-1531.
33. Symonds, Michael E., et al. "Thermal imaging to assess age-related changes of skin temperature within the supraclavicular region co-locating with brown adipose tissue in healthy children." *The Journal of pediatrics* 161.5 (2012): 892-898.
34. Cristancho, Ana G., and Mitchell A. Lazar. "Forming functional fat: a growing understanding of adipocyte differentiation." *Nature reviews Molecular cell biology* 12.11 (2011): 722-734.
35. Cannon, Barbara, and J. A. N. Nedergaard. "Brown adipose tissue: function and physiological significance." *Physiological reviews* 84 (2004): 277-359.

36. Symonds, Michael E., Mark Pope, and Helen Budge. "The ontogeny of brown adipose tissue." *Annual review of nutrition 35* (2015): 295-320.
37. Sanchez-Gurmaches, Joan, et al. "PTEN loss in the Myf5 lineage redistributes body fat and reveals subsets of white adipocytes that arise from Myf5 precursors." *Cell metabolism* 16.3 (2012): 348-362.
38. Sanchez-Gurmaches, Joan, and David A. Guertin. "Adipocytes arise from multiple lineages that are heterogeneously and dynamically distributed." *Nature communications* 5.1 (2014): 1-13.
39. Lefterova, Martina I., and Mitchell A. Lazar. "New developments in adipogenesis." *Trends in Endocrinology & Metabolism* 20.3 (2009): 107-114.
40. Takada, Ichiro, Alexander P. Kouzmenko, and Shigeaki Kato. "Wnt and PPARγ signaling in osteoblastogenesis and adipogenesis." *Nature Reviews Rheumatology* 5.8 (2009): 442-447.
41. Zamani, Nader, and Chester W. Brown. "Emerging roles for the transforming growth factor-β superfamily in regulating adiposity and energy expenditure." *Endocrine reviews* 32.3 (2011): 387-403.
42. Skillington, Jeremy, Lisa Choy, and Rik Derynck. "Bone morphogenetic protein and retinoic acid signaling cooperate to induce osteoblast differentiation of preadipocytes." *The Journal of cell biology* 159.1 (2002): 135-146.
43. Sottile, Virginie, and Klaus Seuwen. "Bone morphogenetic protein-2 stimulates adipogenic differentiation of mesenchymal precursor cells in synergy with BRL 49653 (rosiglitazone)." *FEBS letters* 475.3 (2000): 201-204.
44. Kuo, Mario Meng-Chiang, et al. "BMP-9 as a potent brown adipogenic inducer with anti-obesity capacity." *Biomaterials* 35.10 (2014): 3172-3179.
45. Tseng, Yu-Hua, et al. "New role of bone morphogenetic protein 7 in brown adipogenesis and energy expenditure." *Nature* 454.7207 (2008): 1000-1004.
46. Zhang, Jiang-Wen, et al. "Role of CREB in transcriptional regulation of CCAAT/enhancer-binding protein β gene during adipogenesis." *Journal of biological chemistry* 279.6 (2004): 4471-4478.
47. Tanaka, Takashi, et al. "Defective adipocyte differentiation in mice lacking the C/EBPβ and/or C/EBPδ gene." *The EMBO journal* 16.24 (1997): 7432-7443.
48. Tang, Qi-Qun, Jiang-Wen Zhang, and M. Daniel Lane. "Sequential gene promoter interactions of C/EBPβ, C/EBPα, and PPARγ during adipogenesis." *Biochemical and biophysical research communications* 319.1 (2004): 235-239.
49. Wu, Zhidan, et al. "Cross-regulation of C/EBPα and PPARγ controls the transcriptional pathway of adipogenesis and insulin sensitivity." *Molecular cell* 3.2 (1999): 151-158.
50. Tontonoz, Peter, and Bruce M. Spiegelman. "Fat and beyond: the diverse biology of PPARγ." *Annu. Rev. Biochem.* 77 (2008): 289-312.
51. Guan, Hong-Ping, et al. "Corepressors selectively control the transcriptional activity of PPARγ in adipocytes." *Genes & development* 19.4 (2005): 453-461.
52. Kiskinis, Evangelos, et al. "RIP140 represses the “brown-in-white” adipocyte program including a futile cycle of triacyclglycerol breakdown and synthesis." *Molecular endocrinology* 28.3 (2014): 344-356.

53. Hallberg, Magnus, et al. "A functional interaction between RIP140 and PGC-1α regulates the expression of the lipid droplet protein CIDEA." *Molecular and cellular biology* 28.22 (2008): 6785-6795.
54. Klemm, Dwight J., et al. "Insulin-induced adipocyte differentiation: activation of CREB rescues adipogenesis from the arrest caused by inhibition of prenylation." *Journal of Biological Chemistry* 276.30 (2001): 28430-28435.
55. Student, A. Kaiden, Robert Y. Hsu, and M. Daniel Lane. "Induction of fatty acid synthetase synthesis in differentiating 3T3-L1 preadipocytes." *Journal of Biological Chemistry* 255.10 (1980): 4745-4750.
56. Carmona, M. Carmen, et al. "Mitochondrial biogenesis and thyroid status maturation in brown fat require CCAAT/enhancer-binding protein α." *Journal of Biological Chemistry* 277.24 (2002): 21489-21498.
57. Seale, Patrick, et al. "Transcriptional control of brown fat determination by PRDM16." *Cell metabolism* 6.1 (2007): 38-54.
58. Ishibashi, Jeff, and Patrick Seale. "Functions of Prdm16 in thermogenic fat cells." *Temperature* 2.1 (2015): 65-72.
59. Seale, Patrick, et al. "PRDM16 controls a brown fat/skeletal muscle switch." *Nature* 454.7207 (2008): 961-967.
60. Harms, Matthew J., et al. "Prdm16 is required for the maintenance of brown adipocyte identity and function in adult mice." *Cell metabolism* 19.4 (2014): 593-604.
61. Kajimura, Shingo, et al. "Initiation of myoblast to brown fat switch by a PRDM16–C/EBP-β transcriptional complex." *Nature* 460.7259 (2009): 1154-1158.
62. Barbera, M. José, et al. "Peroxisome proliferator-activated receptor α activates transcription of the brown fat uncoupling protein-1 gene: a link between regulation of the thermogenic and lipid oxidation pathways in the brown fat cell." *Journal of Biological Chemistry* 276.2 (2001): 1486-1493.
63. Hondares, Elayne, et al. "Thiazolidinediones and rexinoids induce peroxisome proliferator-activated receptor-coactivator (PGC)-1α gene transcription: an autoregulatory loop controls PGC-1α expression in adipocytes via peroxisome proliferator-activated receptor-γ coactivation." *Endocrinology* 147.6 (2006): 2829-2838.
64. Villarroya, Francesc, Roser Iglesias, and Marta Giralt. "PPARs in the control of uncoupling proteins gene expression." *PPAR research* 2007 (2007): 74364.
65. Puigserver, Pere, et al. "A cold-inducible coactivator of nuclear receptors linked to adaptive thermogenesis." *Cell* 92.6 (1998): 829-839.
66. Ruas, Jorge L., et al. "A PGC-1α isoform induced by resistance training regulates skeletal muscle hypertrophy." *Cell* 151.6 (2012): 1319-1331.
67. Uldry, Marc, et al. "Complementary action of the PGC-1 coactivators in mitochondrial biogenesis and brown fat differentiation." *Cell metabolism* 3.5 (2006): 333-341.

68. Scime, Anthony, et al. "Rb and p107 regulate preadipocyte differentiation into white versus brown fat through repression of PGC-1α." *Cell metabolism* 2.5 (2005): 283-295.
69. Cao, Wenhong, et al. "p38 mitogen-activated protein kinase is the central regulator of cyclic AMP-dependent transcription of the brown fat uncoupling protein 1 gene." *Molecular and cellular biology* 24.7 (2004): 3057-3067.
70. Cao, Wenhong, et al. "β-Adrenergic activation of p38 MAP kinase in adipocytes: cAMP induction of the uncoupling protein 1 (UCP1) gene requires p38 MAP kinase." *Journal of Biological Chemistry* 276.29 (2001): 27077-27082.
71. Giralt, Albert, et al. "Peroxisome proliferator-activated receptor-γ coactivator-1α controls transcription of the Sirt3 gene, an essential component of the thermogenic brown adipocyte phenotype." *Journal of Biological Chemistry* 286.19 (2011): 16958-16966.
72. Bouillaud, Frederic, et al. "Acquirement of brown fat cell features by human white adipocytes." *Journal of Biological Chemistry* 278.35 (2003): 33370-33376.
73. Wulf, Anne, et al. "T3-mediated expression of PGC-1α via a far upstream located thyroid hormone response element." *Molecular and cellular endocrinology* 287.1-2 (2008): 90-95.
74. Young, P., J. R. S. Arch, and Margaret Ashwell. "Brown adipose tissue in the parametrial fat pad of the mouse." *FEBS letters* 167.1 (1984): 10-14.
75. Cinti, Saverio. "Reversible physiological transdifferentiation in the adipose organ." *Proceedings of the Nutrition Society* 68.4 (2009): 340-349.
76. Wang, Qiong A., et al. "Tracking adipogenesis during white adipose tissue development, expansion and regeneration." *Nature medicine* 19.10 (2013): 1338-1344.
77. Wang, Wenshan, and Patrick Seale. "Control of brown and beige fat development." *Nature reviews Molecular cell biology* 17.11 (2016): 691.
78. Harms, Matthew, and Patrick Seale. "Brown and beige fat: development, function and therapeutic potential." *Nature medicine* 19.10 (2013): 1252-1263.
79. Elabd, Christian, et al. "Human multipotent adipose‐derived stem cells differentiate into functional brown adipocytes." Stem cells 27.11 (2009): 2753-2760.
80. Gburcik, Valentina, et al. "An essential role for Tbx15 in the differentiation of brown and “brite” but not white adipocytes." *American Journal of Physiology-Endocrinology and Metabolism* 303.8 (2012): E1053-E1060.
81. Shao, Mengle, et al. "Zfp423 maintains white adipocyte identity through suppression of the beige cell thermogenic gene program." *Cell metabolism* 23.6 (2016): 1167-1184.
82. Zafrir, B. "Brown adipose tissue: research milestones of a potential player in human energy balance and obesity." *Hormone and Metabolic Research* 45.11 (2013): 774-785.
83. Goldberg, Ira J., Robert H. Eckel, and Nada A. Abumrad. "Regulation of fatty acid uptake into tissues: lipoprotein lipase-and CD36-mediated pathways." *Journal of lipid research* 50 (2009): S86-S90.

84. Strable, Maggie S., and James M. Ntambi. "Genetic control of de novo lipogenesis: role in diet-induced obesity." *Critical reviews in biochemistry and molecular biology* 45.3 (2010): 199-214.
85. Brasaemle, Dawn L. "Thematic review series: adipocyte biology. The perilipin family of structural lipid droplet proteins: stabilization of lipid droplets and control of lipolysis." *Journal of lipid research* 48.12 (2007): 2547-2559.
86. Kersten, Sander. "Mechanisms of nutritional and hormonal regulation of lipogenesis." *EMBO reports* 2.4 (2001): 282-286.
87. Frühbeck, Gema, et al. "Regulation of adipocyte lipolysis." *Nutrition research reviews* 27.1 (2014): 63-93.
88. Sztalryd, Carole, et al. "Perilipin A is essential for the translocation of hormone-sensitive lipase during lipolytic activation." *The Journal of cell biology* 161.6 (2003): 1093-1103.
89. Zechner, Rudolf, et al. "FAT SIGNALS-lipases and lipolysis in lipid metabolism and signaling." *Cell metabolism* 15.3 (2012): 279-291.
90. Friedman, Jeffrey M., and Jeffrey L. Halaas. "Leptin and the regulation of body weight in mammals." *Nature* 395.6704 (1998): 763-770.
91. Hu, Erding, Peng Liang, and Bruce M. Spiegelman. "AdipoQ is a novel adipose-specific gene dysregulated in obesity." *Journal of biological chemistry* 271.18 (1996): 10697-10703.
92. Steinberg, Gregory R., et al. "Endurance training partially reverses dietary-induced leptin resistance in rodent skeletal muscle." *American Journal of Physiology-Endocrinology And Metabolism* 286 (2004): E57-63.
93. Qiao, Liping, et al. "Adiponectin reduces thermogenesis by inhibiting brown adipose tissue activation in mice." *Diabetologia* 57.5 (2014): 1027-1036.
94. Kadowaki, Takashi, et al. "Adiponectin and adiponectin receptors in insulin resistance, diabetes, and the metabolic syndrome." *The Journal of clinical investigation* 116.7 (2006): 1784-1792.
95. Li, Shanshan, et al. "Adiponectin levels and risk of type 2 diabetes: a systematic review and meta-analysis." *Jama* 302.2 (2009): 179-188.
96. Rajala, Michael W., et al. "Regulation of resistin expression and circulating levels in obesity, diabetes, and fasting." *Diabetes* 53.7 (2004): 1671-1679.
97. Hotamisligil, Gokhan S., Narinder S. Shargill, and Bruce M. Spiegelman. "Adipose expression of tumor necrosis factor-alpha: direct role in obesity-linked insulin resistance." *Science* 259.5091 (1993): 87-91.
98. Ouchi, Noriyuki, et al. "Adipokines in inflammation and metabolic disease." *Nature reviews immunology* 11.2 (2011): 85-97.
99. Piquer-Garcia, Irene, et al. "A role for Oncostatin M in the impairment of glucose homeostasis in obesity." *The Journal of Clinical Endocrinology & Metabolism* 105.3 (2020): e337-e348.
100. Rasmussen, Andrew Theodore. "The so-called hibernating gland." *Journal of Morphology* 38.1 (1923): 147-205.

101. Morrison, Shaun F., Christopher J. Madden, and Domenico Tupone. "Central neural regulation of brown adipose tissue thermogenesis and energy expenditure." *Cell metabolism* 19.5 (2014): 741-756.
102. Townsend, Kristy L., and Yu-Hua Tseng. "Brown fat fuel utilization and thermogenesis." *Trends in Endocrinology & Metabolism* 25.4 (2014): 168-177.
103. Rothwell, Nancy J., and Michael J. Stock. "A role for brown adipose tissue in diet-induced thermogenesis." *Nature* 281.5726 (1979): 31-35.
104. Lee, Paul, Michael M. Swarbrick, and Ken KY Ho. "Brown adipose tissue in adult humans: a metabolic renaissance." *Endocrine reviews* 34.3 (2013): 413-438.
105. Nicholls, David G., Vibeke SM Bernson, and Gillian M. Heaton. "The identification of the component in the inner membrane of brown adipose tissue mitochondria responsible for regulating energy dissipation." *Effectors of Thermogenesis* (1978): 89-93.
106. Golozoubova, Valeria, et al. "Only UCP1 can mediate adaptive nonshivering thermogenesis in the cold." *The FASEB Journal* 15.11 (2001): 2048-2050.
107. Krauss, Stefan, Chen-Yu Zhang, and Bradford B. Lowell. "The mitochondrial uncoupling-protein homologues." *Nature reviews Molecular cell biology* 6.3 (2005): 248-261.
108. Feldmann, Helena M., et al. "UCP1 ablation induces obesity and abolishes diet-induced thermogenesis in mice exempt from thermal stress by living at thermoneutrality." *Cell metabolism* 9.2 (2009): 203-209.
109. Cannon, Barbara, and Jan Nedergaard. "Nonshivering thermogenesis and its adequate measurement in metabolic studies." *Journal of Experimental Biology* 214.2 (2011): 242-253.
110. Haman, François. "Shivering in the cold: from mechanisms of fuel selection to survival." *Journal of Applied Physiology* 100.5 (2006): 1702-1708.
111. Nguyen, Khoa D., et al. "Alternatively activated macrophages produce catecholamines to sustain adaptive thermogenesis." *Nature* 480.7375 (2011): 104-108.
112. Collins, Sheila. "β-Adrenoceptor signaling networks in adipocytes for recruiting stored fat and energy expenditure." *Frontiers in endocrinology* 2 (2012): 102.
113. Thonberg, Håkan, et al. "As the proliferation promoter noradrenaline induces expression of ICER (induced cAMP early repressor) in proliferative brown adipocytes, ICER may not be a universal tumour suppressor." *Biochemical Journal* 354.1 (2001): 169-177.
114. Thonberg, Håkan, et al. "A novel pathway for adrenergic stimulation of cAMP-response-element-binding protein (CREB) phosphorylation: mediation via α1-adrenoceptors and protein kinase C activation." *Biochemical Journal* 364.1 (2002): 73-79.
115. Giralt, Marta, Montserrat Cairó, and Francesc Villarroya. "Hormonal and nutritional signalling in the control of brown and beige adipose tissue activation and recruitment." *Best Practice & Research Clinical Endocrinology & Metabolism* 30.4 (2016): 515-525.

116. Bianco, Antonio C., and J. Enrique Silva. "Optimal response of key enzymes and uncoupling protein to cold in BAT depends on local T3 generation." *American Journal of Physiology-Endocrinology And Metabolism* 253.3 (1987): E255-E263.
117. Silva, J. E., and P. R. Larsen. "Adrenergic activation of triiodothyronine production in brown adipose tissue." *Nature* 305.5936 (1983): 712-713.
118. Villarroya, Francesc, and Antonio Vidal-Puig. "Beyond the sympathetic tone: the new brown fat activators." *Cell metabolism* 17.5 (2013): 638-643.
119. Hondares, Elayne, et al. "Thermogenic activation induces FGF21 expression and release in brown adipose tissue." *Journal of Biological Chemistry* 286.15 (2011): 12983-12990.
120. Hondares, Elayne, et al. "Hepatic FGF21 expression is induced at birth via PPARα in response to milk intake and contributes to thermogenic activation of neonatal brown fat." *Cell metabolism* 11.3 (2010): 206-212.
121. Kleiner, Sandra, et al. "FGF21 regulates PGC-1α and browning of white adipose tissues in adaptive thermogenesis." *Genes & development* 26.3 (2012): 271-281.
122. Douris, Nicholas, et al. "Central fibroblast growth factor 21 browns white fat via sympathetic action in male mice." *Endocrinology* 156.7 (2015): 2470-2481.
123. Giralt, Marta, Aleix Gavaldà-Navarro, and Francesc Villarroya. "Fibroblast growth factor-21, energy balance and obesity." *Molecular and cellular endocrinology* 418 (2015): 66-73.
124. Gaich, Gregory, et al. "The effects of LY2405319, an FGF21 analog, in obese human subjects with type 2 diabetes." *Cell metabolism* 18.3 (2013): 333-340.
125. Talukdar, Saswata, et al. "A long-acting FGF21 molecule, PF-05231023, decreases body weight and improves lipid profile in non-human primates and type 2 diabetic subjects." *Cell metabolism* 23.3 (2016): 427-440.
126. Broeders, Evie PM, et al. "The bile acid chenodeoxycholic acid increases human brown adipose tissue activity." *Cell metabolism* 22.3 (2015): 418-426.
127. Fu, Ling, et al. "Fibroblast growth factor 19 increases metabolic rate and reverses dietary and leptin-deficient diabetes." Endocrinology 145.6 (2004): 2594-2603.
128. Antonellis, Patrick J., et al. "The anti-obesity effect of FGF19 does not require UCP1-dependent thermogenesis." *Molecular metabolism* 30 (2019): 131-139.
129. Morón-Ros, Samantha, et al. "FGF15/19 is required for adipose tissue plasticity in response to thermogenic adaptations." *Molecular metabolism* 43 (2021): 101113.
130. Beiroa, Daniel, et al. "GLP-1 agonism stimulates brown adipose tissue thermogenesis and browning through hypothalamic AMPK." *Diabetes* 63.10 (2014): 3346-3358.
131. Lee, Paul, et al. "Irisin and FGF21 are cold-induced endocrine activators of brown fat function in humans." *Cell metabolism* 19.2 (2014): 302-309.

132. Roberts, Lee D., et al. "β-Aminoisobutyric acid induces browning of white fat and hepatic β-oxidation and is inversely correlated with cardiometabolic risk factors." *Cell metabolism* 19.1 (2014): 96-108.
133. Jeremic, Nevena, Pankaj Chaturvedi, and Suresh C. Tyagi. "Browning of white fat: novel insight into factors, mechanisms, and therapeutics." *Journal of cellular physiology* 232.1 (2017): 61-68.
134. Bordicchia, Marica, et al. "Cardiac natriuretic peptides act via p38 MAPK to induce the brown fat thermogenic program in mouse and human adipocytes." *The Journal of clinical investigation* 122.3 (2012): 1022-1036.
135. Villarroya, F., M. Giralt, and R. Iglesias. "Retinoids and adipose tissues: metabolism, cell differentiation and gene expression." *International journal of obesity* 23.1 (1999): 1-6.
136. Bonet, M. L., et al. "Opposite effects of feeding a vitamin A-deficient diet and retinoic acid treatment on brown adipose tissue uncoupling protein 1 (UCP1), UCP2 and leptin expression." *Journal of endocrinology* 166.3 (2000): 511-517.
137. Méndez‐Lara, Karen Alejandra, et al. "Nicotinamide Protects Against Diet-Induced Body Weight Gain, Increases Energy Expenditure and Induces White Adipose Tissue Beiging." *Molecular Nutrition & Food Research* (2021): 2100111.
138. Flachs, P., M. Rossmeisl, and J. Kopecky. "The effect of n-3 fatty acids on glucose homeostasis and insulin sensitivity." *Physiological research* 63 (2014): S93.
139. Oudart, H., et al. "Brown fat thermogenesis in rats fed high-fat diets enriched with n-3 polyunsaturated fatty acids." *International journal of obesity* 21.11 (1997): 955-962.
140. Quesada-López, Tania, et al. "The lipid sensor GPR120 promotes brown fat activation and FGF21 release from adipocytes." *Nature communications* 7.1 (2016): 1-17.
141. Andrade, João Marcus Oliveira, et al. "Resveratrol increases brown adipose tissue thermogenesis markers by increasing SIRT1 and energy expenditure and decreasing fat accumulation in adipose tissue of mice fed a standard diet." *European journal of nutrition* 53.7 (2014): 1503-1510.
142. Wang, Songbo, et al. "Resveratrol induces brown-like adipocyte formation in white fat through activation of AMP-activated protein kinase (AMPK) α1." *International journal of obesity* 39.6 (2015): 967-976.
143. de Ligt, Marlies, Silvie Timmers, and Patrick Schrauwen. "Resveratrol and obesity: can resveratrol relieve metabolic disturbances?" *Biochimica et biophysica acta (BBA)-Molecular basis of disease* 1852.6 (2015): 1137-1144.
144. Yoneshiro, Takeshi, and Masayuki Saito. "Transient receptor potential activated brown fat thermogenesis as a target of food ingredients for obesity management." *Current Opinion in Clinical Nutrition & Metabolic Care* 16.6 (2013): 625-631.
145. Seoane-Collazo, Patricia, et al. "Hypothalamic-autonomic control of energy homeostasis." Endocrine 50.2 (2015): 276-291.

146. Villarroya, Francesc, et al. "Brown adipose tissue as a secretory organ." *Nature Reviews Endocrinology* 13.1 (2017): 26.
147. Villarroya, Joan, et al. "New insights into the secretory functions of brown adipose tissue." *Journal of Endocrinology* 243.2 (2019): R19-R27.
148. Gavaldà-Navarro, Aleix, et al. "The endocrine role of brown adipose tissue: An update on actors and actions." *Reviews in Endocrine and Metabolic Disorders* (2021): 1-11.
149. Villarroya, Francesc, et al. "Toward an understanding of how immune cells control brown and beige adipobiology." Cell metabolism 27.5 (2018): 954-961.
150. Cereijo, Rubén, et al. "CXCL14, a brown adipokine that mediates brown-fat-to-macrophage communication in thermogenic adaptation." *Cell metabolism* 28.5 (2018): 750-763.
151. Campderrós, Laura, et al. "Brown adipocytes secrete GDF15 in response to thermogenic activation." *Obesity* 27.10 (2019): 1606-1616.
152. Johnen, Heiko, et al. "Tumor-induced anorexia and weight loss are mediated by the TGF-β superfamily cytokine MIC-1." *Nature medicine* 13.11 (2007): 1333-1340.
153. Kang, Seul Gi, et al. "Differential roles of GDF15 and FGF21 in systemic metabolic adaptation to the mitochondrial integrated stress response." *Iscience* 24.3 (2021): 102181.
154. Nisoli, Enzo, et al. "Expression of nerve growth factor in brown adipose tissue: implications for thermogenesis and obesity." *Endocrinology* 137.2 (1996): 495-503.
155. Rosell, Meritxell, et al. " Brown and white adipose tissues: intrinsic differences in gene expression and response to cold exposure in mice." *American Journal of Physiology-Endocrinology and Metabolism* 306.8 (2014): E945-E964.
156. Zeng, Xing, et al. "Innervation of thermogenic adipose tissue via a calsyntenin 3β–S100b axis." *Nature* 569.7755 (2019): 229-235.
157. Wang, Guo-Xiao, et al. "The brown fat–enriched secreted factor Nrg4 preserves metabolic homeostasis through attenuation of hepatic lipogenesis." *Nature medicine* 20.12 (2014): 1436.
158. Whittle, Andrew J., et al. "BMP8B increases brown adipose tissue thermogenesis through both central and peripheral actions." *Cell* 149.4 (2012): 871-885.
159. Pellegrinelli, Vanessa, et al. "Adipocyte-secreted BMP8b mediates adrenergic-induced remodeling of the neuro-vascular network in adipose tissue." *Nature communications* 9.1 (2018): 1-18.
160. Peyrou, Marion, et al. "The kallikrein-kinin pathway as a mechanism for auto-control of brown adipose tissue activity." Nature communications 11.1 (2020): 1-16.
161. Shan, Tizhong, et al. "Myostatin knockout drives browning of white adipose tissue through activating the AMPK-PGC1α-Fndc5 pathway in muscle." *The FASEB Journal* 27.5 (2013): 1981-1989.

162. Kong, Xingxing, et al. "Brown adipose tissue controls skeletal muscle function via the secretion of myostatin." *Cell metabolism* 28.4 (2018): 631-643.
163. Planavila, Anna, et al. "Fibroblast growth factor 21 protects against cardiac hypertrophy in mice." *Nature communications* 4.1 (2013): 1-12.
164. Ruan, Cheng-Chao, et al. "A2A receptor activation attenuates hypertensive cardiac remodeling via promoting brown adipose tissue-derived FGF21." *Cell metabolism* 28.3 (2018): 476-489.
165. Thoonen, Robrecht, et al. "Functional brown adipose tissue limits cardiomyocyte injury and adverse remodeling in catecholamine-induced cardiomyopathy." *Journal of molecular and cellular cardiology* 84 (2015): 202-211.
166. Keipert, Susanne, et al. "Genetic disruption of uncoupling protein 1 in mice renders brown adipose tissue a significant source of FGF21 secretion." *Molecular metabolism* 4.7 (2015): 537-542.
167. WHO “WHO delivers advice and support for older people during COVID-19” *World Health Organization*, 3 Apr. 2020, www.who.int/news-room/feature-stories/detail/who-delivers-advice-and-support-for-older-people-during-covid-19
168. CDC “Older Adults: At greater risk of requiring hospitalization or dying if diagnosed with COVID-19” *Centers for Disease Control and Prevention*, 19 Feb. 2021, www.cdc.gov/coronavirus/2019-ncov/need-extra-precautions/older-adults.html
169. Ahima, Rexford S. "Connecting obesity, aging and diabetes." *Nature medicine* 15.9 (2009): 996-997.
170. Minamino, Tohru, et al. "A crucial role for adipose tissue p53 in the regulation of insulin resistance." *Nature medicine* 15.9 (2009): 1082-1087.
171. Gong, Huan, et al. "Age-dependent tissue expression patterns of Sirt1 in senescence-accelerated mice." *Molecular medicine reports* 10.6 (2014): 3296-3302.
172. Barzilai, Nir, et al. "Metformin as a tool to target aging." *Cell metabolism* 23.6 (2016): 1060-1065.
173. Hales, Craig M., et al. "Trends in obesity and severe obesity prevalence in US youth and adults by sex and age, 2007-2008 to 2015-2016." *Jama* 319.16 (2018): 1723-1725.
174. Flegal, Katherine M., et al. "Trends in obesity among adults in the United States, 2005 to 2014." *Jama* 315.21 (2016): 2284-2291.
175. Kirkman, M. Sue, et al. "Diabetes in older adults." *Diabetes care* 35.12 (2012): 2650-2664.
176. Haffner, Steven M. "Pre-diabetes, insulin resistance, inflammation and CVD risk." *Diabetes research and clinical practice* 61 (2003): S9-S18.
177. Armani, Andrea, et al. "Molecular mechanisms underlying metabolic syndrome: the expanding role of the adipocyte." *The FASEB Journal* 31.10 (2017): 4240-4255.
178. Stout, Michael B., et al. "Physiological aging: links among adipose tissue dysfunction, diabetes, and frailty." Physiology 32.1 (2017): 9-19.

179. Frank, Aaron P., et al. "Determinants of body fat distribution in humans may provide insight about obesity-related health risks." *Journal of lipid research* 60.10 (2019): 1710-1719.
180. Moreau, Kerrie L. "Intersection between gonadal function and vascular aging in women." *Journal of Applied Physiology* 125.12 (2018): 1881-1887.
181. Fried, Linda P., et al. "Frailty in older adults: evidence for a phenotype." *The Journals of Gerontology Series A: Biological Sciences and Medical Sciences* 56.3 (2001): M146-M157.
182. Visser, Marjolein, et al. "Muscle mass, muscle strength, and muscle fat infiltration as predictors of incident mobility limitations in well-functioning older persons." *The Journals of Gerontology Series A: Biological Sciences and Medical Sciences* 60.3 (2005): 324-333.
183. Kruglikov, Ilja L., and Philipp E. Scherer. "Skin aging: are adipocytes the next target?" *Aging (Albany NY)* 8.7 (2016): 1457.
184. Kirkland, James L., et al. "Adipogenesis and aging: does aging make fat go MAD?" *Experimental gerontology* 37.6 (2002): 757-767.
185. Martin-Ruiz, Carmen, et al. "Stochastic variation in telomere shortening rate causes heterogeneity of human fibroblast replicative life span." *Journal of Biological Chemistry* 279.17 (2004): 17826-17833.
186. Tchkonia, Tamara, et al. "Cellular senescence and the senescent secretory phenotype: therapeutic opportunities." *The Journal of clinical investigation* 123.3 (2013): 966-972.
187. Guo, Wen, et al. "Aging results in paradoxical susceptibility of fat cell progenitors to lipotoxicity." *American Journal of Physiology-Endocrinology and Metabolism* 292.4 (2007): E1041-E1051.
188. Mack, Isabelle, et al. "Functional analyses reveal the greater potency of preadipocytes compared with adipocytes as endothelial cell activator under normoxia, hypoxia, and TNF α exposure." *American Journal of Physiology-Endocrinology and Metabolism* 297.3 (2009): E735-E748.
189. Franceschi, Claudio, et al. "Inflamm-aging: an evolutionary perspective on immunosenescence." *Annals of the New York Academy of Sciences* 908.1 (2000): 244-254.
190. Zhu, Y. I., et al. "The Achilles' heel of senescent cells: from transcriptome to senolytic drugs." *Aging cell* 14.4 (2015): 644-658.
191. Kuk, Jennifer L., et al. "Age-related changes in total and regional fat distribution." *Ageing research reviews* 8.4 (2009): 339-348.
192. Isakson, Petter, et al. "Impaired preadipocyte differentiation in human abdominal obesity: role of Wnt, tumor necrosis factor-α, and inflammation." *Diabetes* 58.7 (2009): 1550-1557.
193. Martin, George M., and Junko Oshima. "Lessons from human progeroid syndromes." *Nature* 408.6809 (2000): 263-266.
194. Schosserer, Markus, et al. "Age-induced changes in white, brite, and brown adipose depots: a mini-review." *Gerontology* 64.3 (2018): 229-236.

195. Mennes, Elise, et al. "Aging-associated reductions in lipolytic and mitochondrial proteins in mouse adipose tissue are not rescued by metformin treatment." Journals of *Gerontology Series A: Biomedical Sciences and Medical Sciences* 69.9 (2014): 1060-1068.
196. Hallgren, P., et al. "Influence of age, fat cell weight, and obesity on O2 consumption of human adipose tissue." *American Journal of Physiology-Endocrinology and Metabolism* 256.4 (1989): E467-E474.
197. Soro-Arnaiz, Ines, et al. "Role of mitochondrial complex IV in age-dependent obesity." Cell reports 16.11 (2016): 2991-3002.
198. Mancuso, Peter, and Benjamin Bouchard. "The impact of aging on adipose function and adipokine synthesis." *Frontiers in endocrinology* 10 (2019): 137.
199. Roszkowska‐Gancarz, Malgorzata, et al. "Age-related changes of leptin and leptin receptor variants in healthy elderly and long-lived adults." *Geriatrics & gerontology international* 15.3 (2015): 365-371.
200. Scarpace, Philip J., et al. "Impaired leptin responsiveness in aged rats." *Diabetes* 49.3 (2000): 431-435.
201. Gencer, Baris, et al. "Association between resistin levels and cardiovascular disease events in older adults: the health, aging and body composition study." *Atherosclerosis* 245 (2016): 181-186.
202. Ohmori, Reiko, et al. "Associations between serum resistin levels and insulin resistance, inflammation, and coronary artery disease." *Journal of the American College of Cardiology* 46.2 (2005): 379-380.
203. Wu, Dayong, et al. "Aging up-regulates expression of inflammatory mediators in mouse adipose tissue." *The Journal of Immunology* 179.7 (2007): 4829-4839.
204. Lumeng, Carey N., et al. "Aging is associated with an increase in T cells and inflammatory macrophages in visceral adipose tissue." *The Journal of Immunology* 187.12 (2011): 6208-6216.
205. Obata, Yoshinari, et al. "Relationship between serum adiponectin levels and age in healthy subjects and patients with type 2 diabetes." *Clinical endocrinology* 79.2 (2013): 204-210.
206. Rieth, Nathalie, et al. "Effects of short-term corticoid ingestion on food intake and adipokines in healthy recreationally trained men." *European journal of applied physiology* 105.2 (2009): 309-313.
207. Cawthorn, William P., et al. "Bone marrow adipose tissue is an endocrine organ that contributes to increased circulating adiponectin during caloric restriction." *Cell metabolism* 20.2 (2014): 368-375.
208. Sull, Jae Woong, et al. "Serum adiponectin is associated with smoking status in healthy Korean men." *Endocrine journal* 56.1 (2009): 73-78.
209. Hotta, Kikuko, et al. "Plasma concentrations of a novel, adipose-specific protein, adiponectin, in type 2 diabetic patients." *Arteriosclerosis, thrombosis, and vascular biology* 20.6 (2000): 1595-1599.

210. Kizer, Jorge R., et al. "Change in circulating adiponectin in advanced old age: determinants and impact on physical function and mortality. The Cardiovascular Health Study All Stars Study." *Journals of Gerontology Series A: Biomedical Sciences and Medical Sciences* 65.11 (2010): 1208-1214.
211. Ponrartana, Skorn, Houchun H. Hu, and Vicente Gilsanz. "On the relevance of brown adipose tissue in children." *Annals of the New York Academy of Sciences* 1302.1 (2013): 24-29.
212. Gilsanz, Vicente, et al. "Functional brown adipose tissue is related to muscle volume in children and adolescents." *The Journal of pediatrics* 158.5 (2011): 722-726.
213. Rogers, Nicole H. "Brown adipose tissue during puberty and with aging." *Annals of medicine* 47.2 (2015): 142-149.
214. Persichetti, Agnese, et al. "Prevalence, mass, and glucose-uptake activity of 18 F-FDG-detected brown adipose tissue in humans living in a temperate zone of Italy." *PloS one* 8.5 (2013): e63391.
215. Pfannenberg, Christina, et al. "Impact of age on the relationships of brown adipose tissue with sex and adiposity in humans." *Diabetes* 59.7 (2010): 1789-1793.
216. Berry, Daniel C., et al. "Cellular aging contributes to failure of cold-induced beige adipocyte formation in old mice and humans." *Cell metabolism* 25.1 (2017): 166-181.
217. Bahler, Lonneke, et al. "Differences in sympathetic nervous stimulation of brown adipose tissue between the young and old, and the lean and obese." *Journal of Nuclear Medicine* 57.3 (2016): 372-377.
218. Wilson-Fritch, Leanne, et al. "Mitochondrial remodeling in adipose tissue associated with obesity and treatment with rosiglitazone." *The Journal of clinical investigation* 114.9 (2004): 1281-1289.
219. Fabbiano, Salvatore, et al. "Caloric restriction leads to browning of white adipose tissue through type 2 immune signaling." *Cell metabolism* 24.3 (2016): 434-446.
220. Cedikova, Miroslava, et al. "Mitochondria in white, brown, and beige adipocytes." *Stem cells international* 2016 (2016).
221. Wu, Jun, et al. "Beige adipocytes are a distinct type of thermogenic fat cell in mouse and human." *Cell* 150.2 (2012): 366-376.
222. Becerril, Sara, et al. "Role of PRDM16 in the activation of brown fat programming. Relevance to the development of obesity." *Histol Histopathol* 28 (2013): 1411-1425.
223. Khanh, Vuong Cat, et al. "Aging impairs beige adipocyte differentiation of mesenchymal stem cells via the reduced expression of Sirtuin 1." *Biochemical and biophysical research communications* 500.3 (2018): 682-690.
224. Valle, Adamo, et al. "The serum levels of 17β-estradiol, progesterone and triiodothyronine correlate with brown adipose tissue thermogenic parameters during aging." *Cellular Physiology and Biochemistry* 22.1-4 (2008): 337-346.

225. Soumano, Korian, et al. "Glucocorticoids inhibit the transcriptional response of the uncoupling protein-1 gene to adrenergic stimulation in a brown adipose cell line." *Molecular and cellular endocrinology* 165.1-2 (2000): 7-15.
226. Lee, Joo-Young, et al. "Triiodothyronine induces UCP-1 expression and mitochondrial biogenesis in human adipocytes." *American Journal of Physiology-Cell Physiology* 302.2 (2012): C463-C472.
227. Lin, Ligen, et al. "The suppression of ghrelin signaling mitigates age-associated thermogenic impairment." *Aging (Albany NY)* 6.12 (2014): 1019.
228. Zhang, Yuan, et al. "The starvation hormone, fibroblast growth factor-21, extends lifespan in mice." *eLife* 1 (2012): e00065.
229. Hanks, Lynae J., et al. "Circulating levels of fibroblast growth factor-21 increase with age independently of body composition indices among healthy individuals." *Journal of clinical & translational endocrinology* 2.2 (2015): 77-82.
230. Sanchis-Gomar, Fabian, et al. "A preliminary candidate approach identifies the combination of chemerin, fetuin-A, and fibroblast growth factors 19 and 21 as a potential biomarker panel of successful aging." *Age* 37.3 (2015): 1-8.
231. Taniguchi, Hirokazu, et al. "Endurance exercise reduces hepatic fat content and serum fibroblast growth factor 21 levels in elderly men." *The Journal of Clinical Endocrinology* 101.1 (2016): 191-198.
232. Villarroya, F., et al. "Inflammation of brown/beige adipose tissues in obesity and metabolic disease." *Journal of Internal Medicine* 284.5 (2018): 492-504.
233. Zoico, Elena, et al. "Brown and beige adipose tissue and aging." *Frontiers in endocrinology* 10 (2019): 368.
234. Uchiyama, Yasuo, et al. “Autophagy–physiology and pathophysiology.” *Histochemistry and cell biology* 129.4 (2008): 407-420.
235. Cuervo, Ana Maria, and Esther Wong. “Chaperone-mediated autophagy: roles in disease and aging.” *Cell research* 24.1 (2014): 92-104.
236. Bento, Carla F., et al. “Mammalian autophagy: how does it work?” *Annual review of biochemistry* 85 (2016): 685-713.
237. Gatica, Damián, Vikramjit Lahiri, and Daniel J. Klionsky. “Cargo recognition and degradation by selective autophagy.” *Nature cell biology* 20.3 (2018): 233-242.
238. Feng, Yuchen, et al. “The machinery of macroautophagy.” *Cell research* 24.1 (2014): 24-41.
239. Zhang, Yong, et al. "Adipose-specific deletion of autophagy-related gene 7 (atg7) in mice reveals a role in adipogenesis." *Proceedings of the National Academy of Sciences* 106.47 (2009): 19860-19865.
240. Baerga, Rebecca, et al. "Targeted deletion of autophagy-related 5 (atg5) impairs adipogenesis in a cellular model and in mice." *Autophagy* 5.8 (2009): 1118-1130.
241. Guo, Liang, et al. "Transactivation of Atg4b by C/EBPβ promotes autophagy to facilitate adipogenesis." *Molecular and cellular biology* 33.16 (2013): 3180-3190.

242. Martinez-Lopez, Nuria, et al. "Autophagy in Myf5+ progenitors regulates energy and glucose homeostasis through control of brown fat and skeletal muscle development." *EMBO reports* 14.9 (2013): 795-803.
243. Singh, Rajat, et al. "Autophagy regulates adipose mass and differentiation in mice." *The Journal of clinical investigation* 119.11 (2009): 3329-3339.
244. Armani, Andrea, et al. "Mineralocorticoid receptor antagonism induces browning of white adipose tissue through impairment of autophagy and prevents adipocyte dysfunction in high-fat-diet-fed mice." *The FASEB Journal* 28.8 (2014): 3745-3757.
245. Spinelli, Jessica B., and Marcia C. Haigis. “The multifaceted contributions of mitochondria to cellular metabolism.” *Nature cell biology* 20.7 (2018): 745-754.
246. Mehta, Manan M., Samuel E. Weinberg, and Navdeep S. Chandel. “Mitochondrial control of immunity: beyond ATP.” *Nature Reviews Immunology* 17.10 (2017): 608.
247. Kalkavan, Halime, and Douglas R. Green. “MOMP, cell suicide as a BCL-2 family business.” *Cell Death & Differentiation* 25.1 (2018): 46-55.
248. Lisowski, Pawel, et al. “Mitochondria and the dynamic control of stem cell homeostasis.” *EMBO reports* 19.5 (2018): e45432.
249. Wong, Hoi-Shan, et al. “Production of superoxide and hydrogen peroxide from specific mitochondrial sites under different 154ioenergetics conditions.” *Journal of Biological Chemistry* 292.41 (2017): 16804-16809.
250. Scheibye-Knudsen, Morten, et al. “Protecting the mitochondrial powerhouse.” *Trends in cell biology* 25.3 (2015): 158-170.
251. Eisner, Verónica, Martin Picard, and György Hajnóczky. “Mitochondrial dynamics in adaptive and maladaptive cellular stress responses.” *Nature cell biology* 20.7 (2018): 755-765.
252. Onishi, Mashun, et al. “Molecular mechanisms and physiological functions of mitophagy.” *The EMBO Journal* 40.3 (2021): e104705.
253. Kitada, Tohru, et al. “Mutations in the parkin gene cause autosomal recessive juvenile parkinsonism.” *Nature* 392.6676 (1998): 605-608.
254. Valente, Enza Maria, et al. “Hereditary early-onset Parkinson’s disease caused by mutations in PINK1.” Science 304.5674 (2004): 1158-1160.
255. Narendra, Derek, et al. “Parkin is recruited selectively to impaired mitochondria and promotes their autophagy.” *The Journal of cell biology* 183.5 (2008): 795-803.
256. Sarraf, Shireen A., et al. “Landscape of the PARKIN-dependent ubiquitylome in response to mitochondrial depolarization.” *Nature* 496.7445 (2013): 372-376.
257. Bayne, Andrew N., and Jean-François Trempe. “Mechanisms of PINK1, ubiquitin and Parkin interactions in mitochondrial quality control and beyond.” *Cellular and Molecular Life Sciences* 76.23 (2019): 4589-4611.
258. Nguyen, Thanh N., Benjamin S. Padman, and Michael Lazarou. “Deciphering the molecular signals of PINK1/Parkin mitophagy.” *Trends in cell biology* 26.10 (2016): 733-744.

259. Tanaka, Keiji. “The PINK1–Parkin axis: an overview.” *Neuroscience research* 159 (2020): 9-15.
260. Cornelissen, Tom, et al. “Deficiency of parkin and PINK1 impairs age-dependent mitophagy in Drosophila.” *Elife* 7 (2018): e35878.
261. Lee, Juliette J., et al. “Basal mitophagy is widespread in Drosophila but minimally affected by loss of Pink1 or parkin.” *Journal of Cell Biology* 217.5 (2018): 1613-1622.
262. Gispert, Suzana, et al. “Parkinson phenotype in aged PINK1-deficient mice is accompanied by progressive mitochondrial dysfunction in absence of neurodegeneration.” *PloS one* 4.6 (2009): e5777.
263. Perez, Francisco A., and Richard D. Palmiter. “Parkin-deficient mice are not a robust model of parkinsonism.” *Proceedings of the National Academy of Sciences* 102.6 (2005): 2174-2179.
264. Hansen, Malene, David C. Rubinsztein, and David W. Walker. “Autophagy as a promoter of longevity: insights from model organisms.” *Nature reviews Molecular cell biology* 19.9 (2018): 579-593.
265. Sun, Nuo, et al. “Measuring in vivo mitophagy.” *Molecular cell* 60.4 (2015): 685-696.
266. Kujoth, Gregory C., et al. “Mitochondrial DNA mutations, oxidative stress, and apoptosis in mammalian aging.” *Science* 309.5733 (2005): 481-484.
267. Greene, Jessica C., et al. “Mitochondrial pathology and apoptotic muscle degeneration in Drosophila parkin mutants.” *Proceedings of the National Academy of Sciences* 100.7 (2003): 4078-4083.
268. Rana, Anil, Michael Rera, and David W. Walker. “Parkin overexpression during aging reduces proteotoxicity, alters mitochondrial dynamics, and extends lifespan.” *Proceedings of the National Academy of Sciences* 110.21 (2013): 8638-8643.
269. Yang, Yufeng, et al. “Mitochondrial pathology and muscle and dopaminergic neuron degeneration caused by inactivation of Drosophila Pink1 is rescued by Parkin.” *Proceedings of the National Academy of Sciences* 103.28 (2006): 10793-10798.
270. Palikaras, Konstantinos, Eirini Lionaki, and Nektarios Tavernarakis. “Coordination of mitophagy and mitochondrial biogenesis during ageing in C. elegans.” *Nature* 521.7553 (2015): 525-528.
271. Dorn, Gerald W. “Mitochondrial pruning by Nix and Bnip3: an essential function for cardiac-expressed death factors.” *Journal of cardiovascular translational research* 3.4 (2010): 374-383.
272. Dorn II, Gerald W. “Parkin-dependent mitophagy in the heart.” *Journal of molecular and cellular cardiology* 95 (2016): 42-49.
273. Kubli, Dieter A., et al. “Parkin protein deficiency exacerbates cardiac injury and reduces survival following myocardial infarction.” *Journal of Biological Chemistry* 288.2 (2013): 915-926.

274. Lionaki, Eirini, et al. "Mitochondria, autophagy and age-associated neurodegenerative diseases: New insights into a complex interplay." *Biochimica et Biophysica Acta (BBA)-Bioenergetics* 1847.11 (2015): 1412-142
275. Noda, Sachiko, et al. "Loss of Parkin contributes to mitochondrial turnover and dopaminergic neuronal loss in aged mice." *Neurobiology of disease* 136 (2020): 104717.
276. Solano, Rosa M., et al. "Glial dysfunction in parkin null mice: effects of aging." *Journal of Neuroscience* 28.3 (2008): 598-611.
277. Scarffe, Leslie A., et al. "Parkin and PINK1: much more than mitophagy." *Trends in neurosciences* 37.6 (2014): 315-324.
278. Bernardini, J. P., M. Lazarou, and Grant Dewson. "Parkin and mitophagy in cancer." *Oncogene* 36.10 (2017): 1315-1327.
279. Stevens, Daniel A., et al. "Parkin loss leads to PARIS-dependent declines in mitochondrial mass and respiration." *Proceedings of the National Academy of Sciences* 112.37 (2015): 11696-11701.
280. Kuroda, Yukiko, et al. "Parkin enhances mitochondrial biogenesis in proliferating cells." *Human molecular genetics* 15.6 (2006): 883-895.
281. Zhang, Cen, et al. "Parkin, a p53 target gene, mediates the role of p53 in glucose metabolism and the Warburg effect." *Proceedings of the National Academy of Sciences* 108.39 (2011): 16259-16264.
282. Palacino, James J., et al. “Mitochondrial dysfunction and oxidative damage in parkin-deficient mice.” *Journal of Biological Chemistry* 279.18 (2004): 18614-18622.
283. Liu, Kun, et al. "Parkin regulates the activity of pyruvate kinase M2." *Journal of Biological Chemistry* 291.19 (2016): 10307-10317.
284. Jin, Hyun-Seok, et al. "The PARK2 gene is involved in the maintenance of pancreatic β-cell functions related to insulin production and secretion." *Molecular and cellular endocrinology* 382.1 (2014): 178-189.
285. Kim, Kye-Young, et al. "Parkin is a lipid-responsive regulator of fat uptake in mice and mutant human cells." *The Journal of clinical investigation* 121.9 (2011).
286. Costa, Diana K., et al. "Reduced intestinal lipid absorption and body weight-independent improvements in insulin sensitivity in high-fat diet-fed Park2 knockout mice." *American Journal of Physiology-Endocrinology and Metabolism* 311.1 (2016): E105-E116.
287. Cairó, Montserrat, et al. "Parkin controls brown adipose tissue plasticity in response to adaptive thermogenesis." *EMBO reports* 20.5 (2019): e46832.
288. Cairó, Montserrat, et al. "Thermogenic activation represses autophagy in brown adipose tissue." *International journal of obesity* 40.10 (2016): 1591-1599.
289. Taylor, David, and Roberta A. Gottlieb. "Parkin-mediated mitophagy is downregulated in browning of white adipose tissue." *Obesity* 25.4 (2017): 704-712.

290. Lu, Xiaodan, et al. "Mitophagy controls beige adipocyte maintenance through a Parkin-dependent and UCP1-independent mechanism." *Science signaling* 11.527 (2018).
291. Goldberg, Matthew S., et al. "Parkin-deficient mice exhibit nigrostriatal deficits but not loss of dopaminergic neurons." *Journal of Biological Chemistry* 278.44 (2003): 43628-43635.
292. Guallar, Jordi P., et al. "Differential gene expression indicates that 'buffalo hump'is a distinct adipose tissue disturbance in HIV-1-associated lipodystrophy." *Aids* 22.5 (2008): 575-584.
293. Schindelin, Johannes, et al. "Fiji: an open-source platform for biological-image analysis." *Nature methods* 9.7 (2012): 676-682.
294. Galarraga, Miguel, et al. "Adiposoft: automated software for the analysis of white adipose tissue cellularity in histological sections." *Journal of lipid research* 53.12 (2012): 2791-2796.
295. Domingo, Pere, et al. "Circulating fibroblast growth factor 23 (FGF23) levels are associated with metabolic disturbances and fat distribution but not cardiovascular risk in HIV-infected patients." *Journal of Antimicrobial Chemotherapy* 70.6 (2015): 1825-1832.
296. Oh, Yoon Sin, et al. "Increase of calcium sensing receptor expression is related to compensatory insulin secretion during aging in mice." *PloS one* 11.7 (2016): e0159689.
297. Bodogai, Monica, et al. "Commensal bacteria contribute to insulin resistance in aging by activating innate B1a cells." *Science translational medicine* 10.467 (2018).
298. Dongil, Pilar, et al. "PAS kinase deficiency reduces aging effects in mice." *Aging (Albany NY)* 12.3 (2020): 2275.
299. Danysz, Wojciech, et al. "Browning of white adipose tissue induced by the β3 agonist CL-316,243 after local and systemic treatment-PK-PD relationship." *Biochimica et Biophysica Acta (BBA)-Molecular Basis of Disease* 1864.9 (2018): 2972-2982.
300. Crane, Justin D., et al. "A standardized infrared imaging technique that specifically detects UCP1-mediated thermogenesis in vivo." *Molecular metabolism* 3.4 (2014): 490-494.
301. Bartness, T. J., C. H. Vaughan, and C. K. Song. "Sympathetic and sensory innervation of brown adipose tissue." *International journal of obesity* 34.1 (2010): S36-S42.
302. Shin, Woongchul, et al. "Impaired adrenergic agonis-dependent beige adipocyte induction in aged mice." *Obesity* 25.2 (2017): 417-423.
303. Barzilai, Nir, et al. "The critical role of metabolic pathways in aging." *Diabetes* 61.6 (2012): 1315-1322.
304. Kurosu, Hiroshi, et al. "Tissue-specific expression of βKlotho and fibroblast growth factor (FGF) receptor isoforms determines metabolic activity of FGF19 and FGF21." *Journal of Biological Chemistry* 282.37 (2007): 26687-26695.

305. Chui, Patricia C., et al. "Obesity is a fibroblast growth factor 21 (FGF21)-resistant state." *Diabetes* 59.11 (2010): 2781-2789.
306. Flurkey, Kevin, Joanne M. Currer, and D. E. Harrison. "Mouse models in aging research." *The mouse in biomedical research*. Academic Press, 2007. 637-672.
307. Cui, Chen, et al. "PINK1-Parkin alleviates metabolic stress induced by obesity in adipose tissue and in 3T3-L1 preadipocytes." *Biochemical and biophysical research communications* 498.3 (2018): 445-452.
308. Reynolds, Thomas H., et al. "The impact of age and sex on body composition and glucose sensitivity in C57BL/6J mice." *Physiological reports* 7.3 (2019).
309. Balaskó, Márta, et al. "Leptin and aging: Review and questions with particular emphasis on its role in the central regulation of energy balance." *Journal of chemical neuroanatomy* 61 (2014): 248-255.
310. Cohade, Christian, Karen A. Mourtzikos, and Richard L. Wahl. ""“USA-Fat”: prevalence is related to ambient outdoor temperature-evaluation with 18F-FDG PET/CT." *Journal of Nuclear Medicine* 44.8 (2003): 1267-1270.
311. Yoneshiro, Takeshi, et al. "Age-related decrease in cold-activated brown adipose tissue and accumulation of body fat in healthy humans." *Obesity* 19.9 (2011): 1755-1760.
312. Sellayah, Dyan, and Devanjan Sikder. "Orexin restores aging-related brown adipose tissue dysfunction in male mice." *Endocrinology* 155.2 (2014): 485-501.
313. Rajakumari, Sona, and Simran Srivastava. "Aging and β3-adrenergic stimulation alter mitochondrial lipidome of adipose tissue." *Biochimica et Biophysica Acta (BBA)-Molecular and Cell Biology of Lipids* 1866.7 (2021): 158922.
314. Kazachkova, Nadiya, et al. "Mitochondrial DNA damage patterns and aging: revising the evidences for humans and mice." *Aging and disease* 4.6 (2013): 337.
315. Lee, Jae Ho, et al. "The role of adipose tissue mitochondria: regulation of mitochondrial function for the treatment of metabolic diseases." *International journal of molecular sciences* 20.19 (2019): 4924.
316. Seals, Douglas R., and Christopher Bell. "Chronic sympathetic activation: consequence and cause of age-associated obesity?." *Diabetes* 53.2 (2004): 276-284.
317. Weisberg, Stuart P., et al. "Obesity is associated with macrophage accumulation in adipose tissue." *The Journal of clinical investigation* 112.12 (2003): 1796-1808.
318. Larabee, Chelsea M., Oliver C. Neely, and Ana I. Domingos. "Obesity: a neuroimmunometabolic perspective." *Nature Reviews Endocrinology* 16.1 (2020): 30-43.
319. McDonald, Roger B., and Barbara A. Horwitz. "Brown adipose tissue thermogenesis during aging and senescence." *Journal of bioenergetics and biomembranes* 31.5 (1999): 507-516.

320. Nygaard, Eva B., et al. "Increased fibroblast growth factor 21 expression in high-fat diet-sensitive non-human primates (*Macaca mulatta*)." *International journal of obesity* 38.2 (2014): 183-191.
321. Patel, Vanlata, et al. "Novel insights into the cardio-protective effects of FGF21 in lean and obese rat hearts." *PloS one* 9.2 (2014): e87102.
322. Rusli, Fenni, et al. "Fibroblast growth factor 21 reflects liver fat accumulation and dysregulation of signalling pathways in the liver of C57BL/6J mice." *Scientific reports* 6.1 (2016): 1-16.
323. So, Wing Yan, et al. "High glucose represses β-klotho expression and impairs fibroblast growth factor 21 action in mouse pancreatic islets: involvement of peroxisome proliferator–activated receptor γ signaling." *Diabetes* 62.11 (2013): 3751-3759.
324. Samms, Ricardo J., et al. "Overexpression of β-klotho in adipose tissue sensitizes male mice to endogenous FGF21 and provides protection from diet-induced obesity." *Endocrinology* 157.4 (2016): 1467-1480.
325. Moure, Ricardo, et al. "Levels of β-klotho determine the thermogenic responsiveness of adipose tissues: involvement of the autocrine action of FGF21." *American Journal of Physiology-Endocrinology and Metabolism* 320.4 (2021): E822-E834.
326. Kim, Kook Hwan, and Myung-Shik Lee. "FGF21 as a mediator of adaptive responses to stress and metabolic benefits of anti-diabetic drugs." *J Endocrinol* 226.1 (2015): R1-R16.
327. Planavila, Anna, et al. "Fibroblast growth factor 21 protects the heart from oxidative stress." *Cardiovascular research* 106.1 (2015): 19-31.
328. Jin, Leigang, Zhuofeng Lin, and Aimin Xu. "Fibroblast growth factor 21 protects against atherosclerosis via fine-tuning the multiorgan crosstalk." *Diabetes & metabolism journal* 40.1 (2016): 22.
329. Zarei, Mohammad, et al. "Targeting FGF21 for the treatment of nonalcoholic steatohepatitis." *Trends in pharmacological sciences* 41.3 (2020): 199-208.
330. Youm, Yun-Hee, et al. "Prolongevity hormone FGF21 protects against immune senescence by delaying age-related thymic involution." *Proceedings of the National Academy of Sciences* 113.4 (2016): 1026-1031.
331. Inagaki, Takeshi, et al. "Inhibition of growth hormone signaling by the fasting-induced hormone FGF21." *Cell metabolism* 8.1 (2008): 77-83.
332. Suomalainen, Anu, et al. "FGF-21 as a biomarker for muscle-manifesting mitochondrial respiratory chain deficiencies: a diagnostic study." *The Lancet Neurology* 10.9 (2011): 806-818.
333. Gallego-Escuredo, J. M., et al. "Opposite alterations in FGF21 and FGF19 levels and disturbed expression of the receptor machinery for endocrine FGFs in obese patients." *International journal of obesity* 39.1 (2015): 121-129.
334. Kuroda, Mariko, et al. "Peripherally derived FGF21 promotes remyelination in the central nervous system." *The Journal of clinical investigation* 127.9 (2017): 3496-3509.

335. Gallego-Escuredo, José M., et al. "Reduced levels of serum FGF19 and impaired expression of receptors for endocrine FGFs in adipose tissue from HIV-infected patients." *Journal of Acquired Immune Deficiency Syndromes* 61.5 (2012): 527-534.
336. Fujita, Yasunori, et al. "Secreted growth differentiation factor 15 as a potential biomarker for mitochondrial dysfunctions in aging and age-related disorders." *Geriatrics & gerontology international* 16 (2016): 17-29.
337. Montero, Raquel, et al. "GDF-15 is elevated in children with mitochondrial diseases and is induced by mitochondrial dysfunction." *PloS one* 11.2 (2016): e0148709.
338. Dominguez-Gonzalez, Cristina, et al. "Growth Differentiation Factor 15 is a potential biomarker of therapeutic response for TK2 deficient myopathy." *Scientific reports* 10.1 (2020): 1-13.
339. Moon, Ji Sun, et al. "Growth differentiation factor 15 protects against the aging-mediated systemic inflammatory response in humans and mice." *Aging cell* 19.8 (2020): e13195.
340. Pickrell, Alicia M., et al. "Endogenous Parkin preserves dopaminergic substantia nigral neurons following mitochondrial DNA mutagenic stress." *Neuron* 87.2 (2015): 371-381.
341. García-Prat, Laura, et al. "Autophagy maintains stemness by preventing senescence." *Nature* 529.7584 (2016): 37-42.
342. Tyrrell, Daniel J., et al. "Aging Impairs Mitochondrial Function and Mitophagy and Elevates Interleukin 6 Within the Cerebral Vasculature." *Journal of the American Heart Association* 9.23 (2020): e017820.
343. Liang, Wenjing, et al. "Aging is associated with a decline in Atg9b‐mediated autophagosome formation and appearance of enlarged mitochondria in the heart." *Aging cell* 19.8 (2020): e13187.
344. Fujiwara, Mikio, et al. "Parkin as a tumor suppressor gene for hepatocellular carcinoma." *Oncogene* 27.46 (2008): 6002-6011.
345. Pesah, Yakov, et al. "Drosophila parkin mutants have decreased mass and cell size and increased sensitivity to oxygen radical stress." *Development* 131.9 (2004): 2183-2194.
346. Jang, Ji Yong, et al. "The role of mitochondria in aging." *The Journal of clinical investigation* 128.9 (2018): 3662-3670.
347. Salminen, Antero, Kai Kaarniranta, and Anu Kauppinen. "Regulation of longevity by FGF21: Interaction between energy metabolism and stress responses." *Ageing research reviews* 37 (2017): 79-93.
348. Patel, Satish, et al. "GDF15 provides an endocrine signal of nutritional stress in mice and humans." *Cell metabolism* 29.3 (2019): 707-718.

Appendix

Aging is associated with increased FGF21 levels but unaltered FGF21 responsiveness in adipose tissue

Journal: Aging Cell. 2018 Oct; 17(5): e12822. **PMID:** 30043445 **IF:** 7.346

Abstract:
Fibroblast growth factor 21 (FGF21) has been proposed to be an antiaging hormone on the basis of experimental studies in rodent models. However, circulating FGF21 levels are increased with aging in rodents and humans. Moreover, despite the metabolic health-promoting effects of FGF21, the levels of this hormone are increased under conditions such as obesity and diabetes, an apparent incongruity that has been attributed to altered tissue responsiveness to FGF21. Here, we investigated serum FGF21 levels and expression of genes encoding components of the FGF21‐response molecular machinery in adipose tissue from healthy elderly individuals (≥70 years old) and young controls. Serum FGF21 levels were increased in elderly individuals and were positively correlated with insulinemia and HOMA-IR, indices of mildly deteriorated glucose homeostasis. Levels of β-Klotho, the coreceptor required for cellular responsiveness to FGF21, were increased in subcutaneous adipose tissue from elderly individuals relative to those from young controls, whereas FGF receptor-1 levels were unaltered. Moreover, total ERK1/2 protein levels were decreased in elderly individuals in association with an increase in the ERK1/2 phosphorylation ratio relative to young controls. Adipose explants from aged and young mice respond similarly to FGF21 "ex vivo". Thus, in contrast to what is observed in obesity and diabetes, high levels of FGF21 in healthy aging are not associated with repressed FGF21-responsiveness machinery in adipose tissue. The lack of evidence for impaired FGF21 responsiveness in adipose tissue establishes a distinction between alterations in the FGF21 endocrine system in aging and chronic metabolic pathologies.